



Comparison of heart valve flow dynamics assessment between echocardiography and pulse duplication

L Thompson-Jooste

Dissertation submitted in fulfilment of the requirements of the degree

**Master of Health Sciences in Clinical Technology
(M_HSCT)**

Department of Health Sciences
Faculty of Health and Environmental Sciences
Central University of Technology
Bloemfontein, South Africa

Supervisors

Prof FE Smit MB ChB, FC (cardio) SA, PhD, FACC; University of the Free State
Dr L Botes D Tech Biomedical Technology; Central University of Technology
Mr K Davis BEng Mechanical Engineering, University of Stellenbosch

October 2017

DECLARATION OF INDEPENDENT WORK

I, Liezl Thompson-Jooste, do hereby declare that this dissertation:

Comparison of heart valve flow dynamics assessment between echocardiography and pulse duplication

submitted to the Central University of Technology for the degree ***Master in Health Sciences
Clinical Technology*** is my own independent work and that it has not been submitted to any institution by me or any other person in fulfilment of the requirements for the attainment of any qualification.

Principal Investigator:

Signed:



Date: 2017/11/10

TABLE OF CONTENTS

	Page
.....	
ACKNOWLEDGEMENTS.....	VI
LIST OF ABBREVIATIONS	VII
IMPORTANT DEFINITIONS.....	XI
LIST OF FIGURES	XIII
LIST OF TABLES.....	XV
SUMMARY	XVI
CHAPTER 1 INTRODUCTION	1
1.1 BACKGROUND.....	1
1.2 AIM.....	3
1.3 OBJECTIVES	3
CHAPTER 2 LITERATURE REVIEW.....	4
2.1 INTRODUCTION.....	4
2.2 PROSTHETIC HEART VALVES	5
2.2.1 History of prosthetic heart valve development.....	7
2.2.2 Medtronic-Hall tilting disc valve (mechanical valve)	9
2.2.3 Carbomedics bi-leaflet valve (mechanical valve).....	11
2.2.4 Carpentier-Edwards bioprosthesis (tissue valve)	14
2.2.5 The University of Cape Town (UCT) valve.....	15
2.3 HYDRODYNAMIC TESTING OF HEART VALVES.....	19
2.4 PULSE DUPLICATION	20
2.4.1 The history of pulse duplication	20

2.4.2 The purpose and function of the pulse duplicator system.....	22
2.4.3 The mechanical components of the pulse duplicator system	24
2.4.4 Performing pulse duplication analysis	29
2.4.5 Pros and cons associated with pulse duplication	33
2.5 ECHOCARDIOGRAPHY	33
2.5.1 The history of echocardiography	34
2.5.2 The purpose and function of echocardiography	35
2.5.3 Prosthetic valvular geometry determined by echocardiography.....	38
2.5.4 Echocardiography and pulse duplication.....	42
CHAPTER 3 METHODOLOGY.....	43
3.1 STUDY LOCATION AND MATERIAL	43
3.2 STUDY DESIGN AND LAYOUT	44
3.3 HYDRODYNAMIC EVALUATION OF PROSTHETIC HEART VALVES	46
3.3.1 Pulse duplication.....	46
3.3.2 Echocardiography	53
CHAPTER 4 RESULTS	57
4.1 Introduction	57
4.2 PULSE DUPLICATION RESULTS OF THE FIVE (5) PROSTHETIC HEART VALVES	57
4.2.1 Pressure drop.....	59
4.2.2 Effective orifice area (EOA).....	60
4.2.3 Regurgitation fraction (RF)	61
4.2.4 Closing volume.....	62
4.2.5 Leakage volume	63
4.3 ECHOCARDIOGRAPHIC RESULTS OF THE FIVE (5) PROSTHETIC HEART VALVES.....	64
4.3.1 Pressure drop.....	64
4.3.2 Percentage difference: pressure drop	65

4.3.3 Effective orifice area (EOA)	67
4.3.4 Percentage difference of EOA.....	68
4.4 DISCUSSION.....	69
4.4.1 Introduction	69
4.4.2 Pulse duplication.....	69
4.4.3 Echocardiography	73
CHAPTER 5 CONCLUSION	75
5.1 Limitations.....	76
5.2 Recommendations	76
CHAPTER 6 REFERENCES	77

ACKNOWLEDGEMENTS

- Firstly, I would like to thank my supervisor **Dr Lezelle Botes** for her assistance and advice during my research study. In the beginning when I started with this endeavour who would have thought what would lie ahead. No one is ever sure as to how a project will pan out, and I am thankful for her guidance throughout, it was invaluable and without her support this study would not have been possible.
- **Professor Francis Smit** I wish to thank for all the input, advice and wisdom whenever I needed direction or had a question about my research. His experience and guidance have been invaluable in both this study as well as my professional career. His efforts in the establishment of a research department made my study a reality and will allow future researchers and perfusionists to engage in research activities.
- In **Dr Johan Jordaan** I had a colleague that was on a similar journey than me. I want to thank him for the insight that he gave me into the nuances of my study.
- **Mr Kyle Davis**, the input made to the calculations and towards my results is of great value, without the application of his engineering approach to the project, it would not have been possible.
- The **staff of the Research and Perfusion Department of Cardiothoracic Surgery, Universitas Academic Hospital**, I wish to thank them all for their support and help during the data collection and standing in for me if need be. Every gesture and contribution, whether big or small, have made a difference.
- When you have a family you never do anything truly alone, they are part and parcel to all your endeavours, for this I extend my appreciation to my husband, **Charl Jooste**, for his unwavering support during this journey, it means the world to me.

LIST OF ABBREVIATIONS

ACT	Activated clotting time
ANSI	American National Standards Institute
AAMI	Association for the Advancement of Medical Instrumentation
AS	Aortic valve stenosis
ASE	American Society of Echocardiography
AV	Aortic valve
AVA	Aortic valve area
AVR	Aortic valve replacement
BDC Labs Inc	BDC laboratories Incorporated
BMI	Body mass index
BPM	Beats per minute
BSI	British Standard Institution
CFD	Computational fluid dynamics
CI	Cardiac index
Ci	Confidence interval
CPB	Cardio pulmonary bypass
cps	centipoise
CSA	Cross sectional area
CT	Computed tomography
cm ²	Square centimetre
cm	Centimetre
cm/s	Centimetre per second
CO	Cardiac output
CSV	Comma-separated values
CVP	Central venous pressure
CW	Continuous wave

DAS	Data acquisition system
DVI	Doppler velocity index
DVR	Double valve replacement
Dyn/cm ²	Dyne per centimetre squared
EOA	Effective orifice area
EAE	European Association of Echocardiography
Env. Ti	Envelope time
FDA	Food and Drug Administration
FEM	Finite element method
g/l	Grams per litre
GOA	Geometric orifice area
ISO	International Organization for Standardization
L/min	Litres per minute
LVOT	Left ventricular outflow tract
m/s	Meters per second
MAP	Mean arterial pressure
MHV _s	Mechanical heart valves
mg/l	Milligrams per litre
mm/h	Millimetres per hour
mmHg	Millimetres mercury
Mmol	Millimole
Mmol/l	Millimole per litre
mPa.s	millipascal per second
MR	Magnetic resonance
MRI	Magnetic resonance imagery
OR	Odds ratio
P _{ao}	Aortic Pressure
POA	Possible orifice area
Pa	Pascal
P _{cl}	Closing pressure
P _{max}	Maximum pressure
P _{mean}	Mean pressure

Pt1/2	Pressure half time
PV	Prosthetic valve
Pv	Ventricular pressure
PTFE	polytetrafluoroethylene
pt/y	Patients per year
rQ _{rms}	Root mean square forward volumetric flow rate
RA	Right atrium
RF	Regurgitation fraction
RMS	Root Mean Square
RV	Right ventricle
RVOT	Right ventricle outflow tract
RVOT-VTI	Right ventricle outflow tract velocity time integral
sec	Second
SFDA	State Food and Drug Administration
SJM	St. Jude Medical
SOP	Standard operating procedures
SV	Stroke volume
TEE	Trans-oesophageal echocardiography
T _{cl}	Time interval of valve closure
T _L	Rest of cycle
THVs	Tissue heart valves
Tv	Total volume
TVI	Time velocity integral
TÜV	Technical Inspection Association
U/l	Units per litre
UFS	University of the Free State
UCT	University of Cape Town
v	Velocity
VC	Vena contracta
VIA	Viscoelastic impedance adapter
ViVitro Labs Inc.	ViVitro laboratories Incorporated
V _{CL}	Closing Volume

V_L	Leakage volume
V_{LVOT}	Velocity in the LVOT
V_{PV}	Velocity in the prosthetic valve
V_{max}	Maximum velocity
V_{mean}	Mean velocity
P_{max}	Maximum pressure
VR	Velocity ratio
VTI	Velocity time integral
2D	Two dimensional
3D	Three dimensional
ΔP	Delta pressure

IMPORTANT DEFINITIONS

Cardio pulmonary bypass A technique that temporarily supports the function of the heart and lungs during surgery, maintaining the circulation of blood and the oxygen content of the body (Gravlee *et al.*, 2008).

Computational Fluid Dynamics (CFD) A branch of fluid mechanics that uses numerical procedures and algorithms to solve and analyse partial differential equations that involve fluid flows. Computers are used to perform the calculations required to simulate the interaction of liquids and gases with surfaces defined by boundary conditions (Yogonathan *et al.*, 2005).

Doppler velocity index (DVI) Is a dimensionless ratio of the proximal velocity in the Left Ventricular Outflow tract (LVOT) to that of flow velocity through the prosthesis (PV): $DVI = V_{LVOT} / V_{PV}$. This parameter is used to evaluate valve obstruction, particularly when the cross-sectional area of the LVOT cannot be obtained (Pibarot *et al.*, 2009).

Effective orifice area The effective orifice area (EOA) is the minimal cross-sectional area of the flow jet downstream of a native or prosthetic heart valve. The EOA is the standard parameter used for the clinical assessment of valvular stenosis severity. It is determined either from Doppler echocardiography by using the continuity equation or from catheterization by applying the Gorlin formula (Hakki *et al.*, 1981).

Finite element method (FEM) The finite element method (FEM) is a numerical method for solving partial differential equations. It can be used for predicting how a structure reacts or deforms because of real-world forces, vibration, heat energy transfer, fluid flow, and other physical effects. Finite element analysis shows whether a product will break, wear out, or work the way it was designed (Babuška *et al.*, 2004).

Glycar valve The modified UCT valve in this dissertation will be referred to as the Glycar valve. This term replaces the terms: modified UCT valve, Frater valve; Goosen/UCT valve, Poppet valve.

Non-Newtonian fluid In a Newtonian fluid, the relation between the shear stress and the shear rate is linear, passing through the origin, the constant of proportionality being the coefficient of viscosity. In a non-Newtonian fluid, the relation between the shear stress and the shear rate is nonlinear and can even be time-dependent (time dependent viscosity). Therefore, a constant coefficient of viscosity cannot be defined (Tropea *et al.*, 2007).

<p>Pressure drop</p>	<p>In this dissertation, pressure drop will refer to the averaged pressure difference across a heart valve during the forward flow phase from an engineering perspective. The term will be used during CFD and pulse duplication analysis(https://www.ncbi.nlm.nih.gov/pmc/articles/PMC3839173/).</p>
<p>Pressure gradient</p>	<p>In this dissertation, pressure gradient will refer to the pressure difference generated across a heart valve during the forward flow phase from a clinical perspective. The term will be used in the <i>in vivo</i> and clinical situation. In this study pressure difference has the same meaning and the terms may be used interchangeably(https://www.ncbi.nlm.nih.gov/pmc/articles/PMC3839173/).</p>
<p>Pulse duplication</p>	<p>The pulse duplicator system assesses the performance of cardiovascular devices and prosthetic heart valves under simulated cardiac conditions. It simulates physiological or other complex flow variations while allowing the user to vary the peripheral resistance and compliance of the system (Kuettinga <i>et al.</i>, 2014).</p>
<p>Reynolds number</p>	<p>In fluid mechanics, the Reynolds number (Re) is a dimensionless quantity that is used to predict flow patterns in different fluid flow situations. Laminar flow occurs at low Reynolds numbers, where viscous forces are dominant, and is characterized by smooth, constant fluid motion; turbulent flow occurs at high Reynolds numbers (greater than 1000) and is dominated by inertial forces, which tend to produce chaotic eddies, vortices and other flow instabilities (Chandran, 2010).</p>
<p>Vena contracta</p>	<p>Vena contracta is the point in a fluid stream where the diameter of the stream is the least, and fluid velocity is at its maximum, such as in the case of a stream emerging from a nozzle or orifice (Falkovich, 2011).</p>

LIST OF FIGURES

Figure number	Title	Page
Figure 2.1	Different types of prosthetic heart valves	7
Figure 2.2	Timeline towards the ideal prosthetic heart valve	8
Figure 2.3	The Medtronic Hall tilting disc heart valve	10
Figure 2.4	Flow fields downstream of the tilting disc valve during forward flow phase and the leakage flow phase	11
Figure 2.5	The Carbomedics bi-leaflet valve	12
Figure 2.6	Open bi-leaflet dividing into two lateral and one central orifice region	13
Figure 2.7	Flow fields downstream of the bi-leaflet valve during forward flow phase and the leakage flow phase	13
Figure 2.8	Carpentier-Edwards tissue valve	14
Figure 2.9	Starr-Edwards Model 6000 mitral prosthesis	16
Figure 2.10	The University of Cape Town Valve	17
Figure 2.11	Schematic presentation of the re-engineered UCT valve as used in the CFD evaluation	19
Figure 2.12	The ViVitro system with a schematic representation of the heart	25
Figure 2.13	The ViVitro Labs AR series SuperPump	26
Figure 2.14	Presentation of the chambers insertion in the pulse duplicator	27
Figure 2.15	ViVitest data acquisition system (DAS)	28
Figure 2.16	Echocardiographic viewing chambers in a ViVitro pulse duplication system	34
Figure 2.17	The Doppler effect	36
Figure 2.18	Doppler pulsed wave and continuous wave Doppler echocardiography from the apical view	37
Figure 3.1	The <i>in vitro</i> evaluation of the flow dynamics of five prosthetic heart valves using pulse duplication and echocardiography	45
Figure 3.2	ViVitro pulse duplicator and data acquisition system	46
Figure 3.3	The ViVitro pulse duplicator system mimicking the human heart	47

Figure 3.4	The ventricle pressure measured for the bi-leaflet valve over time during a cardiac cycle under the five test conditions	49
Figure 3.5	The aortic pressure measured for the bi-leaflet valve over time during a cardiac cycle under the five test conditions	50
Figure 3.6	The pressure difference between the pressure generated across the valve and the pressure generated in the aorta	50
Figure 3.7	Schematic representation of the positive pressure period of an aortic forward flow interval	51
Figure 3.8	The flow wave form and regurgitant volumes for one cycle, with the volumetric change rate in relation to time	53
Figure 3.9	Echocardiography performed during pulse duplication	54
Figure 4.1	Pressure drop for each test	59
Figure 4.2	Pulse duplication EOA and CO comparison between prosthetic heart valves per test condition	60
Figure 4.3	Pulse duplication percentage regurgitation comparison between prosthetic valves per test condition	61
Figure 4.4	Pulse duplication closing volume comparison between prosthetic valves per test condition	62
Figure 4.5	Pulse duplication leakage volume comparison between prosthetic valves per test condition	63
Figure 4.6	Echocardiography measured pressure drop comparison between prosthetic valves per test condition	64
Figure 4.7	Echocardiography percentage pressure drop comparison between prosthetic valves per test condition	65
Figure 4.8	Echocardiography vs. pulse duplication pressure drop for bi-leaflet and tissue valve per test condition	66
Figure 4.9	Echocardiography EOA comparison between prosthetic valves per test condition	67
Figure 4.10	Echocardiography percentage difference in EOA comparison between prosthetic valves per test condition	68
Figure 4.11	Bi-leaflet valve internal diameter measurement	70
Figure 4.12	Echocardiographic continuous wave propagation through the five valves	74

LIST OF TABLES

Table number	Title	Page
Table 2.1	The minimal ISO 5840:2015 performance requirements for pulse duplication evaluation	31
Table 3.1	Physiological testing conditions used during pulse duplication	48
Table 4.1	Hydrodynamic pulse duplicator and echocardiographic results for the prosthetic heart valves per test condition	59

SUMMARY

INTRODUCTION

Heart valve surgery and valvular heart disease still pose a significant threat to patients worldwide. The aortic valve doesn't remain healthy and has largely been the focus of innovation and the development of replacement heart valves. Improving the ability of blood to flow through a prosthetic valve while minimizing the load on the heart is regarded as one of the performance objectives of prosthetic heart valves. In order to meet valvular performance objectives and to assess whether potential prosthetic heart valves meets hydrodynamic performance, testing simulated under *in vivo* flow conditions is necessary.

Pulse duplication is widely accepted as a valid method to determine the performance of heart valves during their development. Few specialised centres exist to perform pulse duplication tests accurately and in accordance to the required ISO and FDA standards for cardiovascular implants. Real-time patient data of prosthetic heart valves is however not obtained with pulse duplication but with echocardiography. Modern day pulse duplicators come equipped with viewing chambers that can allow for echocardiographic measurements.

Therefore, the aim of this study was to perform pulse duplication and echocardiography simultaneously on five different prosthetic heart valves using a commercial ViVitro pulse duplicator system.

METHODS

A hydrodynamic evaluation was performed on five prosthetic heart valves (i) Medtronic-Hall mechanical valve (tilting disc), (ii) Carbomedics mechanical valve (bileaflet), (iii) Glycar mechanical valve (Glycar), (iv) Edwards Perimount (tissue valve), (v) ViVitro reference (ViVitro) using pulse duplication and echocardiography. All the valves were inserted in the aortic position of the pulse duplicator and echocardiographic measurements was performed simultaneously. Each of the valves were tested at 5 different testing conditions by varying the

stroke volume and beats per minute. The study concludes with a comparison between the pulse duplicator data and the echocardiography data acquired.

RESULTS

Pulse duplication: -The Glycar valve had the largest pressure drop across the valve at the lowest CO (3.6 L/min) of 17.15 mmHg, although it increased steadily at a slower rate than the other four valves. The Glycar and tissue valve had the highest EOA of 1.885 cm² and 1.884 cm² respectively at a peak CO of 9.6 L/min. The bi-leaflet valve had the highest EOA of 2.002 cm² (CO 3.6 L/min), however the EOA deteriorated as the CO increased resulting in an EOA of 1.572 cm² at a CO of 9.6L/min. The tissue valve had the largest RF for all testing conditions, ranging from 16.3% (CO 8.0 L/min) to 25.6% (4.9 L/min) where the bi-leaflet valve had the lowest (0.72% - 3.42%).

Echocardiography: -The Glycar valve had the lowest overall pressure drop for all CO. The pulse duplicator pressure drop results were more consistent than three echocardiography results measured on the pulse duplicator. The bileaflet and Glycar valves EOA showed better consistency across the CO range than the ViVitro, tissue and tilting disk valves. The data showed that no definite correlation between all the valves exists between echocardiography and pulse duplication for EOA. However, a correlation for pressure drop between the pulse duplicator and echocardiographic data was demonstrated for both the tissue and bi-leaflet valve.

CONCLUSION

The pulse duplication results show that all five valves meet the ISO standard for the minimum EOA value of 0.85 cm² for 21mm prosthetic aortic valves. The EOA relates the ability of fluid to flow through the valve by relating the volumetric flow rate to the pressure drop. The echocardiography pressure drop results were comparable with the pulse duplication data for the bi-leaflet and tissue valve only. The results differed between 11.4% and 42.26%, which is in line with published literature where the reported difference is no more than 50%.

To conclude, no absolute comparison could be drawn between pulse duplication and echocardiographic measurements performed simultaneously on the ViVitro pulse duplication system.

CHAPTER 1

INTRODUCTION

1.1 BACKGROUND

Heart valve surgery and valvular heart disease pose unique clinical challenges compared to that of other cardiovascular diseases. The prevalence of valvular heart disease is less and its clinical end points is more indolent because the outcomes associated with prosthetic heart valves are of interest only decades later rather than acutely after intervention (Bach, 2003). According to the American Heart Association, up to 1.5 million people in the United States suffer from aortic stenosis (AS). Severe AS develops in 300,000 people worldwide, which has a one-year survival rate of approximately 50 percent, if left untreated (Spinner, 2015). Therefore, the onset of heart valve disease opened a new commercial market in the field of cardiovascular medicine.

The first prosthetic heart valve was developed in 1952 (Wieting, 1989) and since then several prosthetic heart valves (e.g. Ball valves, mechanical valves, non-tilting disc valves, tilting disc valves, bi-leaflet valves and tissue valves) were introduced and existing valves were modified, all of them aiming to produce the perfect prosthetic heart valve. The perfect prosthetic heart valve is defined in literature as a valve with a pressure gradient as low as possible, excellent hemodynamic behaviour, long term durability, low thromboembolic incidence, biocompatibility, ease of implantation, whilst stagnation, recirculation zones and shear stresses in the clearance region should be minimized in order to prevent the initiation of coagulation (Dumont *et al.*, 2005; Verdonck *et al.*, 1997).

Decades ago, when heart valves were first implanted, valvular regulatory requirements were minimal or non-existing. Today extensive *in vitro* hydrodynamic testing followed by an *in vivo* evaluation of valvular performance in animal models are compulsory to ensure short- and long-term success prior to human implantation. *In vitro* hydrodynamic testing is an evaluation of valvular performance conducted under dynamic conditions in a controlled environment (Wheatley *et al.*, 2000, Fisher *et al.*, 1986). The ISO 5840:2015 guidelines states that the *in*

vitro evaluation of an aortic valve only requires simulation of the systemic circulation, including the left atrium (LA), left ventricle (LV) and large arteries. A system capable of meeting these requirements and reproducing physiological flow characteristics, is the pulse duplication system (Fischer *et al.*, 1986).

However, pulse duplication testing is not for the faint hearted. Besides the fact that it is very expensive and that only a few testing centres exist worldwide the technical difficulty in performing these tests are extremely challenging. For this reason, more and more emphasis is placed on exploring alternative methods to replace pulse duplication without compromising the results required for valvular approval (ISO 5840:2015). One such an alternative method that can be explored is echocardiography.

An echocardiogram is an ultrasonic graphic outline of the heart's movement. The test provides images of the heart valves and chambers using high frequency sound waves. Echocardiography is used to evaluate the pumping action of the heart and is often combined with Doppler ultrasound and colour Doppler to evaluate blood flow across the heart valves (Saunders, 2009). The analysis of valve geometry is based on mathematical models constructed on the human aortic valve. Furthermore, echocardiographic machines are not as expensive as pulse duplication systems, are readily available and can measure similar valve geometry as the pulse duplicator system.

As with many engineering creations, the valvular design process is never complete. When prosthetic devices are implanted in humans, improvements are constantly made. Research and development efforts seek to recreate and simulate the human environment on the bench and in animals, but there are always lessons to be learned and improvements to be made (Spinner, 2015). Therefore, the aim of this study was to compare the valvular flow dynamics obtained via pulse duplication with the valvular flow dynamics simultaneously obtained using echocardiography of five (5) aortic prosthetic heart valves in a pulse duplication system.

1.2 AIM

The aim of this study was:

- To assess and compare the *in vitro* hydrodynamic flow characteristics of five (5) prosthetic aortic heart valves evaluated in a pulse duplication system using pulse duplication and echocardiography.

1.3 OBJECTIVES

The objectives of this study were:

- To evaluate and compare the valvular flow dynamics [mean flow rate (ml/min), mean pressure difference (mmHg), pump rate (ml/min), cardiac output (ml/min), stroke volume (ml/min), forward flow duration and effective orifice area (EOA), RMS] of five (5) aortic prosthetic heart valves using pulse duplication.
- To evaluate and compare the valvular flow dynamics [mean flow rate (ml/min), mean pressure difference (mmHg), pump rate (ml/min), cardiac output (ml/min), stroke volume (ml/min), forward flow duration and effective orifice area (EOA), RMS] of five (5) aortic prosthetic heart valves using echocardiography while performing pulse duplication.
- A comparison between pulse duplication and echocardiographic valvular flow dynamic measurements of five (5) aortic prosthetic heart valves assessed during pulse duplication.

CHAPTER 2

LITERATURE REVIEW

2.1 INTRODUCTION

The heart functions as the central pumping unit of the circulatory system relying on arteries and veins to supply blood to the body. The heart pumps approximately 5 litres of blood per minute and the cardiac valves open and close around 40 million times in a year (Bazan and Ortiz, 2011).

Inadequate operation of heart valves can lead to the development of some circulatory system diseases by seriously interfering with the blood pumping capacity. Valvular heart disease is a global health problem and results in approximately 275, 000 valve replacement procedures performed annually worldwide (Sierad *et al.*, 2010). As the world's population is aging, the incidence of prosthetic heart valve implantation and the need for prosthetic heart valves continue to increase. Since the first successful implantation of a prosthetic heart valve (1952), more than fifty different mechanical and biological valve models were designed. In the past, mostly mechanical heart valves (MHVs) was implanted due to their reliable long-term durability but currently bio-prosthetic tissue heart valves (THVs) are implanted just as frequently as mechanical heart valves due to their fluid dynamic behaviour and freedom from anticoagulant therapy (Kuan *et al.*, 2011). Yet, none of the MHVs nor the THVs is free from complications and neither the MHVs nor the THVs meet the demands of an ideal heart valve prosthesis as outlined by Harkin and Curtis (1967).

In order to manufacture the perfect valve, these valves need to be assessed for valvular flow behaviour and hydrodynamic characteristics (Dasi *et al.*, 2009; Yoganathan *et al.*, 2004; Fung *et al.*, 1997). In order to make an accurate appraisal of how effective prosthetic valves will be in corrective surgery, the motion of the prosthetic valves must be tested under circumstances comparable to those observed in the living heart. Testing under real-life conditions allows for the identification of shortcomings in the prosthetic valves and promotes intelligently directed corrective steps (Davila *et al.*, 1955). However, the assessment of the function of heart valve

prosthesis remains challenging, as prosthesis malfunction is unpredictable but not uncommon (Blauwet and Fletcher, 2014).

2.2 PROSTHETIC HEART VALVES

Heart valve disease is often the result of degenerative valve calcification, endocarditis, rheumatic fever or congenital birth defects (Rajamannan *et al.*, 2011; Marijon *et al.*, 2012; Karaci *et al.*, 2012; Knirsch and Nadal, 2011). If valve damage occurs resulting in valvular stenosis and/or regurgitation valve prolapse and surgical repair is not an option, the native valve is usually replaced with a suitable prosthetic valve.

However, prosthetic heart valves are not without complications and these complications can be divided into six main categories (Grunkemeier and Anderson, 1998):

- Structural valvular deterioration
- Non-structural dysfunction
- Valve thrombosis
- Embolism
- Bleeding
- Endocarditis

To date the ideal heart valve substitute does not exist and each of the available prosthetic valves has inherent limitations. To qualify as a successful heart valve substitute, the valve must have the following performance characteristics (ANSI/AAMI/ISO:2005):

- Allows forward flow with acceptable small mean pressure drop
- Prevents retrograde flow with acceptably small regurgitation
- Resists embolization
- Resist haemolysis
- Resist thrombus formation
- Is biocompatible
- Is compatible with *in vivo* diagnostic technique

- Is deliverable and implantable in the target population
- Remains fixed once placed
- Has an acceptable noise level
- Has reproducible function
- Maintains its functionality for a reasonable lifetime, consistent with its generic class
- Maintains its functionality and sterility for a reasonable shelf life prior to implantation

Therefore, to summarize the ideal prosthetic heart valve should be a valve that mimics the haemodynamic properties and performance of a natural heart valve, its durability should exceed the life expectancy of the patient, and there should be no need for anticoagulation or antiplatelet therapy.

Currently there are many prosthetic heart valves available which include mechanical valves (cage-ball valves, monoleaflet and bi-leaflet tilting disk valves), homografts, bio-prosthetic valves (porcine and bovine stented and stentless pericardial valves, and percutaneous bioprosthesis) (Dasi *et al.*, 2009; Pirabot and Dumesnil, 2009) and even polymeric heart valves (De Gaetano *et al.*, 2015) (Figure 2.1). Tissue-engineered valves are also being investigated as an emerging technology (Mol *et al.*, 2009; Ramaswamy *et al.*, 2010).

Based on their durability, mechanical valves are more often recommended for younger patients, although the patient will remain on anticoagulant therapy to prevent thrombotic complications (Korossis *et al.*, 2000). Anticoagulant therapy can be avoided by selecting homograft and biological prosthetic valves, however, these valves are at risk for fibrosis, calcification, degeneration and immunogenic complications contributing to valve failure (Ghanbari *et al.*, 2009).

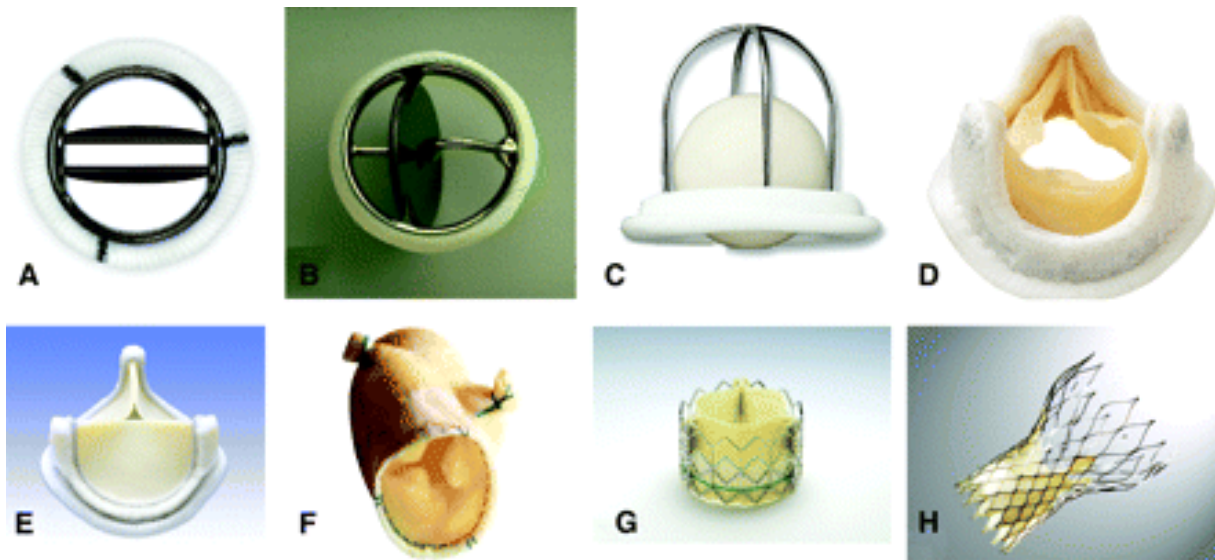


Figure 2.1: Different types of prosthetic heart valves

A. Bi-leaflet mechanical valve (St Jude); **B.** monoleaflet mechanical valve (Medtronic Hall); **C.** caged ball valve (Starr-Edwards); **D.** stented porcine bioprosthesis (Medtronic Mosaic); **E.** stented pericardial bioprosthesis (Carpentier-Edwards Magna); **F.** stentless porcine bioprosthesis (Medtronic Freestyle); **G.** percutaneous bioprosthesis expanded over a balloon (Edwards Sapien); **H.** self-expandable percutaneous bioprosthesis (CoreValve) (adapted from Pibarot *et al.*, 2009).

2.2.1 History of prosthetic heart valve development

The timeline of significant milestones in the history of prosthetic heart valve development is summarized in Figure 2.2.

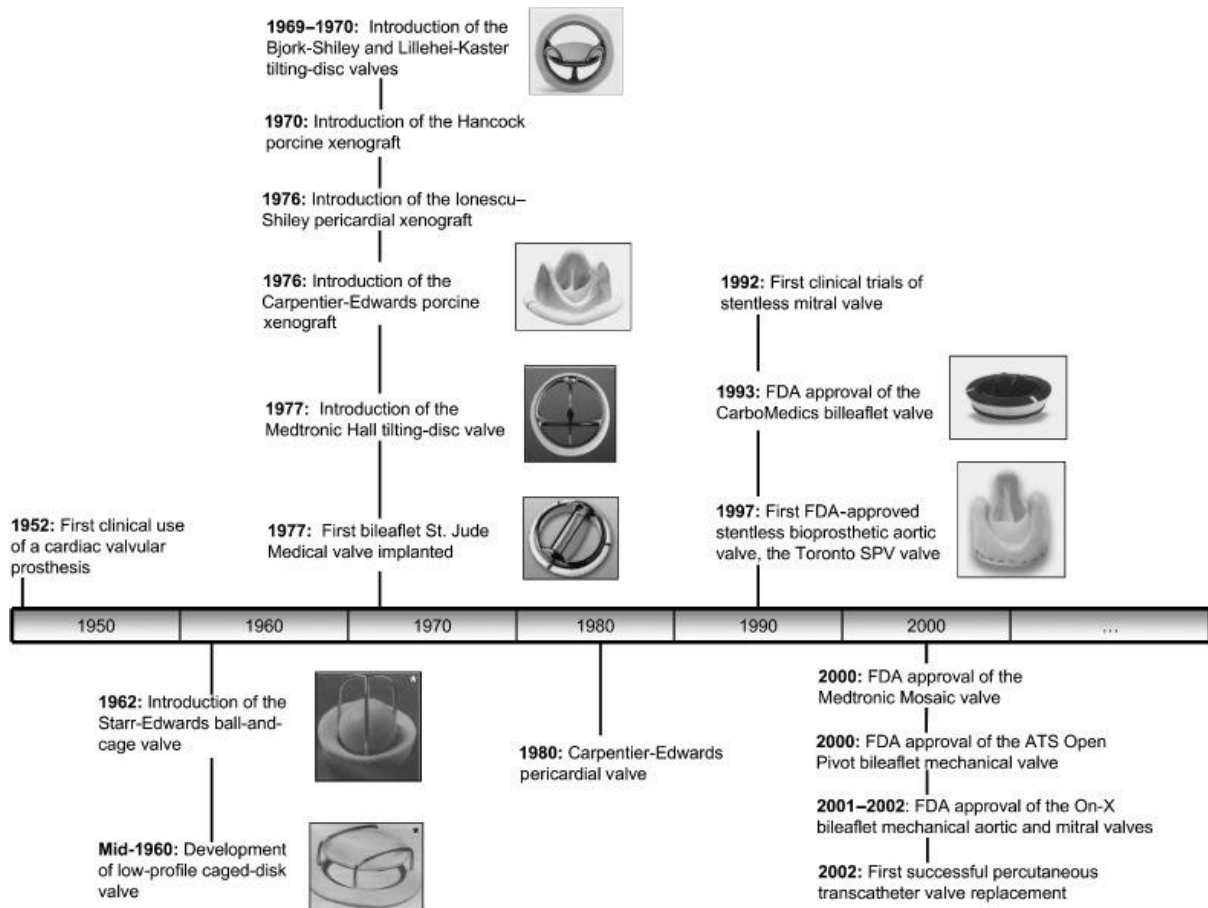


Figure 2.2: Timeline towards the ideal prosthetic heart valve (adapted from Dasi *et al.*, 2009)

Since 2002 some of the major contributions in the field of heart valve development was the trans-catheter aortic valve implantation (TAVI). According to Dr J Beckerman, TAVI will be indeed a game-changer. It is maybe not (the cardiology equivalent to) landing a man on the moon—for, that will be the day we figure out how to prevent aortic stenosis, but for the time being, TAVI will help more patients with critical aortic stenosis to live longer and fuller lives (Buntz, 2012).

The first-in-man TAVI implantation was performed in 2002, and took flight in 2004 in the hands of Edwards Lifesciences, with major improvements in devices and approaches (Cribier, 2012). This percutaneous trans-femoral aortic valve implantation is currently available too much broader patient population and more patients especially the elderly is eligible to receive this procedure (Buntz, 2012; Lichtenstein, 2006).

At the same time, the self-expanding CoreValve was launched. TAVI has an important role in non-operable and high-surgical-risk patients. More than 50,000 patients have benefited from TAVI procedures worldwide and the numbers is still increasing (Cribier, 2012).

For the purpose of this study the hydrodynamic performance of five prosthetic heart valves (Medtronic-Hall tilting disc valve, Carbomedics bi-leaflet valve, Glycar valve, Perimount tissue valve and the ViVitro reference valve) were assessed and compared using pulse duplication and echocardiography.

2.2.2 Medtronic-Hall tilting disc valve (mechanical valve)

The Hall-Kaster valve was first implanted in 1977 and was developed by Dr Karl Victor Hall in collaboration with Robert Kaster (Gott *et al.*, 2003). The valve was widely used worldwide and in 1987, after minimal engineering modifications, the manufacturing and distribution of the valve was taken over by Medtronic, hence the name change to Medtronic-Hall tilting disk valve (Butchart *et al.*, 2001). This valve is the second most frequently implanted mechanical valve only being beaten by the St Jude bi-leaflet valve (Antunes *et al.*, 1988).

This valve has a unique tilting pyrolytic disc with a small central perforation accommodating a thin metal strut that guides the disc during opening and closing (Gott *et al.*, 2003). Unique design features were incorporated to limit the valve's susceptibility to thrombosis. When compared to previous tilting disc designs, the relative size of the minor orifice was increased and the disc was made to lift out of the housing and rotate on opening, all features designed to improve washing of vulnerable points and to eliminate areas of low velocity flow (Butchart *et al.*, 2001) (Figure 2.3).

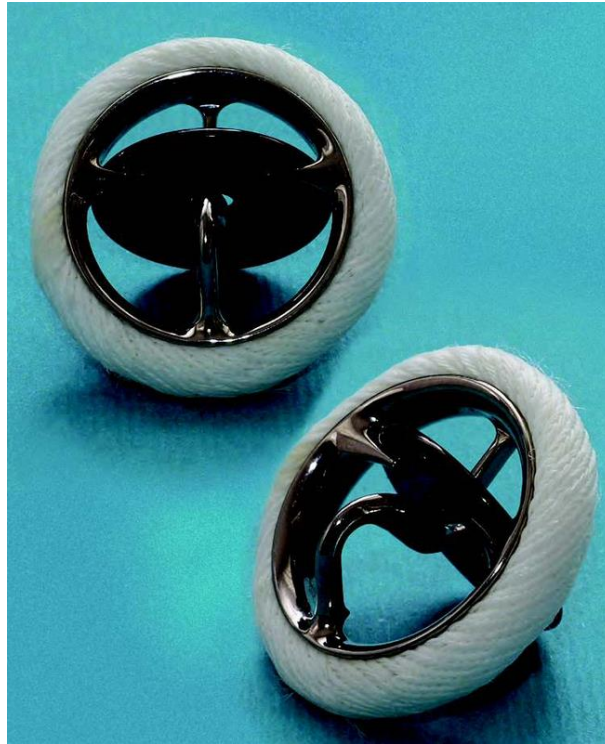


Figure 2.3: The Medtronic Hall tilting disc heart valve (adapted from http://www.cthsurgery.com/uploads/2/6/5/4/26542699/4782632_orig.png)

2.2.2.1 Haemodynamic flow characteristics of the tilting disc valve

The Medtronic-Hall valve disk has a maximum opening angle of 75 degrees for the aortic valve and 70 degrees for the mitral valve (Antunes, 2015). Resistance to flow is generated by forward flow if the disk does not open to 90 degrees, causing small eddies of stagnant flow proximal and around the valve disk leading to thrombus development (Lillehei *et al.*, 1989). The small hole in the occluder can result in a characteristic central regurgitant jet.

Blood flow through the valve will be established when the valve is open and the pyrolytic disk tilts to form a major and minor orifice (Figure 2.4). From the major orifice, a large flow jet emanates whereas a smaller jet of lesser velocity and magnitude emanates from the minor orifices. Recirculation in the wake of the disk is the result of the two jets presenting with different velocity magnitudes and a recirculation flow pattern can be seen in the sinus region. According to Chandran *et al.* (2007; 1983) high turbulent shear stresses are confined to narrow regions at the edges of the major orifice jet. At peak systole, the maximum turbulent

shear stresses measured are in the order of 1500 dyne/cm². The major orifice region has less turbulent shear stresses and are less dispersed than in the minor orifice region.

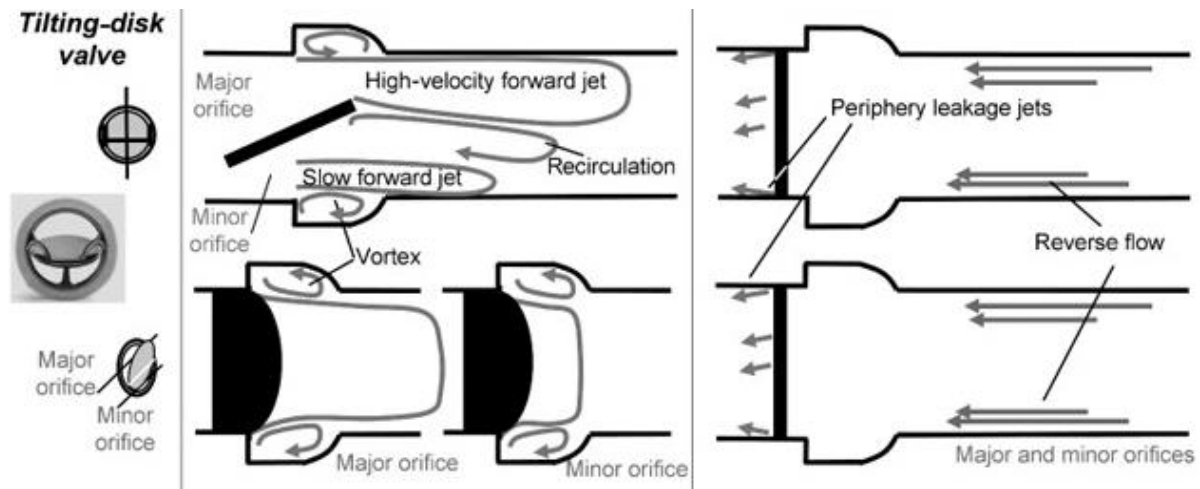


Figure 2.4: Flow fields downstream of the tilting disc valve during forward flow phase (left) and the leakage flow phase (right)(adapted from Dasi *et al.*, 2009)

When the valve closes, the tilting disc moves back and seats on the valve housing occluding the valve orifice which can create a small gap at the periphery of the disc creating a small amount of flow regurgitation. The Medtronic-Hall tilting disk valve design includes a retaining mechanism for the disc. This mechanism is created by the presence of a hole in the centre of the tilting disk, allowing for blood flow through the hole during the closed phase. The leakage through the hole may cause levels of shear stress, potentially increasing platelet activation (Zoghbi *et al.*, 2009).

2.2.3 Carbomedics bi-leaflet valve (mechanical valve)

The United States Food and Drug administration (FDA) approved the Carbomedics bi-leaflet valve (Sorin group, Austin, Texas, United States of America) in 1993 (Figure 2.5). The valve is a bi-leaflet pyrolytic carbon heart valve and differs from the St. Jude Medical prosthesis in having an inner ring composed of pyrolytic carbon rather than pyrolite-covered graphite (Chandran, 2010). This allows for a more sophisticated geometry for the pivotal recesses (Bernal *et al.*, 1998; Chambers *et al.*, 1993). The closure to the leaflets is controlled by the recesses and allow for regurgitant “washing jets” that reduces the risk of thromboembolism.

Furthermore, the leaflets are flat with relatively limited excursion, opening at 12° vertically and closing at 25° horizontally. The valve was designed to reduce regurgitation around the occlude and to aid closure when implanted at an angle. Leaflet escape is prevented by a titanium stiffening ring and helps to control pivot geometry. Leaflet orientation can be optimized by rotating the inner ring within the sewing ring at the time of implantation (Chambers *et al.*, 1993).

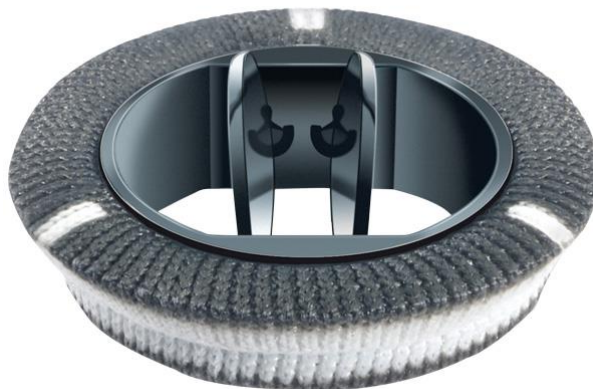


Figure 2.5: The Carbomedics bi-leaflet valve (adapted from <http://www.livanova.sorin.com/file/view-1370.action>)

Mechanical valves will always be obstructive in nature, due to the dynamic fluid interaction with the valve mechanisms. Although the design moralities may be the same, small modifications in the basic design of bi-leaflets may have a large impact on overall function.

2.2.3.1 Haemodynamic flow characteristics of the bi-leaflet mechanical valve

The leaflets are open at an angle of 75° to 90° relative to the annulus plane and divides the area available for flow into three regions; a small slit-like central orifice between the 2 open leaflets and 2 larger semi-circular orifices laterally (Pibarot *et al.*, 2009).

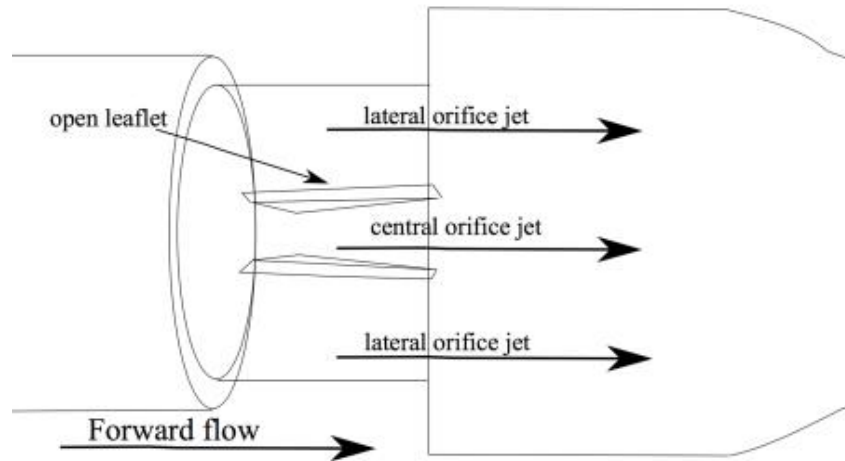


Figure 2.6: Open bi-leaflet dividing into two lateral and one central orifice region (adapted from Yun *et al.*, 2014)

Chandran *et al.* (2007) reported that measurements along the centre plane of the valve 8 mm distal to the valve annulus provides an indication that the velocity in the lateral orifices (2.2 m/s) is higher than in the central orifice (2 m/s). Furthermore, two recirculation regions are seen in the sinus region of the aortic root during both systole and diastole (Barannyk *et al.*, 2013). Flow disturbances is more evident downstream of the valve and alternating rotating vortices form in the wake of the leaflets at peak forward flow. However, these vortices disappear during the deceleration phase and is replaced by a highly chaotic flow field (Dasi *et al.*, 2007).

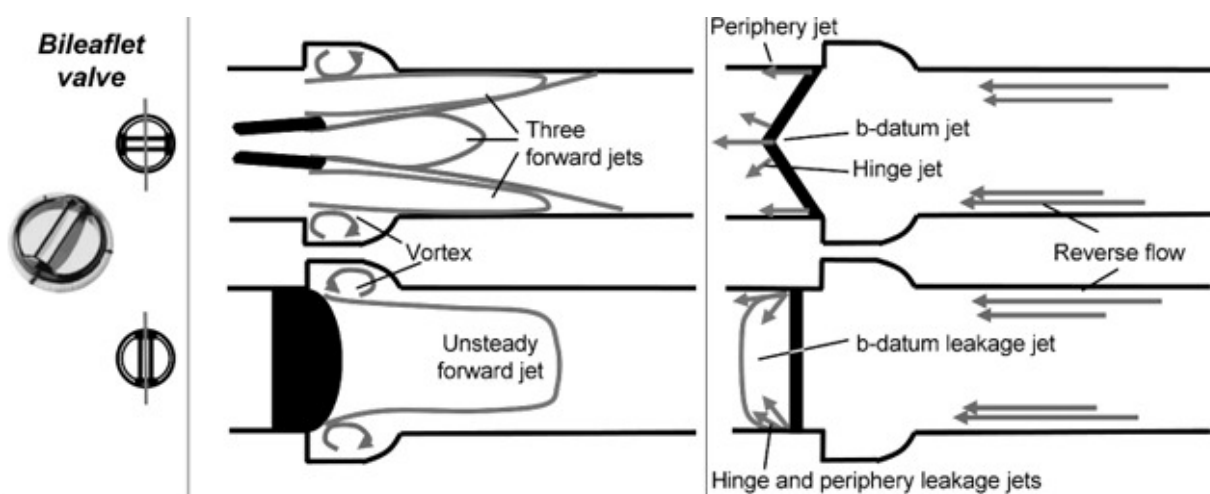


Figure 2.7: Flow fields downstream of the bi-leaflet valve during forward flow phase (left) and the leakage flow phase (right) (adapted from Dasi *et al.*, 2009)

At peak systole, the peak turbulent shear stresses measured along the centreline plane is about 1500 dyn/cm^2 downstream of the valve (Rao *et al.*, 2016).

The leaflets rotate and close the valve orifice during the leakage flow phase. The design of the bi-leaflet mechanical valve includes a degree of leakage flow through the b-datum gap (the line where the two leaflets meet one another) and the periphery gaps, but mainly appears in the gap present at the hinge region (Dasi *et al.*, 2009). Once the valve is in the closed position, the high-pressure difference across the valve causes high velocity jets emerging from the hinge. These narrow jets were originally designed to ‘wash’ the hinges of the valve, preventing areas of flow stasis and inhibiting micro-thrombus formation. However, the magnitude of this retrograde flow has been shown to be detrimental to blood cells and the shear stress generated in the three areas of leakage flow can cause the development of thrombosis (Leo *et al.*, 2006; Zilla *et al.*, 2008).

2.2.4 Carpentier-Edwards bioprosthesis (tissue valve)

The Carpentier-Edwards (Perimount) pericardial valve (Edwards Lifesciences LLC, Irvine, CA, USA) was introduced to clinical use in 1981 and was approved for commercial use in the United States in 1991. The valve is characterized by superior hemodynamic performance with improved durability compared to previous pericardial valves (Gao *et al.*, 2004).

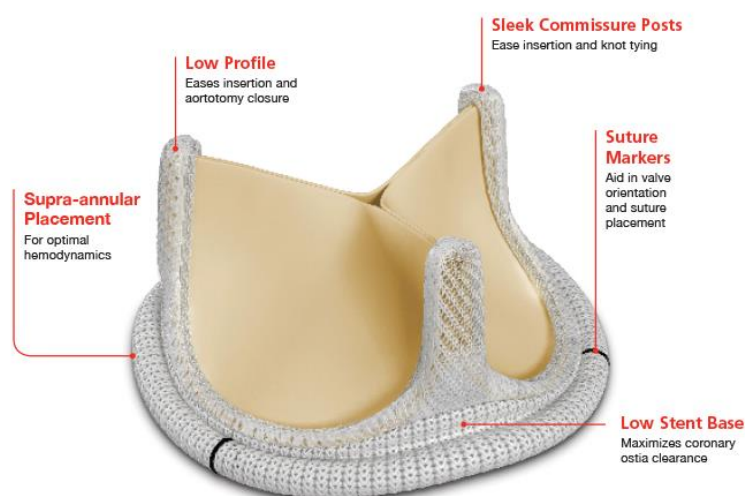


Figure 2.8: Carpentier-Edwards tissue valve (adapted from http://edwardsprod.blob.core.windows.net/media/Default/_Profiles/8ae8ae66/dd56a63e/easeofimplant-3.png?v=636268439490000000)

The valve is constructed from glutaraldehyde-tanned bovine pericardium and XenoLogiX (treatment) is used to reduce the phospholipid content and prevent calcification in these valves (Picket *et al.*, 1997). The valve is equipped with unique design features conceived to minimize cusp stress and to reduce abrasion wear. The stented orifice ring is composed of Elgiloy and embrace the commissural pericardial cusps and provides flexibility and elasticity (memory) to the valve. The valvular leaflets are constructed out of bovine pericardium and mounted on the inside of the orifice ring. The sewing ring is a molded silicone rubber that is covered with a polytetrafluoroethylene (PTFE) cloth (Butany *et al.*, 2003). This design configuration offers superior performance when compared to bioprosthesis with adjacent pericardial cusps encircling a ventral strut. The valve also demonstrates superior distortion tolerance and is less prone to incompetence (Frater *et al.*, 1992). When performing stress analysis on these valves it showed that the maximal tension is diverted from the line of the cups apposition to the free edge approximating the post apices (Pick *et al.*, 1997).

2.2.4.1 Haemodynamic flow characteristics of the pericardial tissue valve

The first bio-engineered pericardial tissue valve (Edwards valve) designed to withstand high pressures in the mitral position has a collagen structure of pericardial tissue making the valve more resilient than porcine tissue valves. Their geometric similarity to natural valves offers a large orifice in the ejection phase and facilitates a less disturbed aortic blood flow pattern (Yin *et al.*, 2006). The design of tissue valves results in transvalvular flow turbulence and improper stress distribution on the valvular leaflets. These two factors influence the long-term limitation as well as the durability of the tissue valve.

Consistent pericardial tissue thickness is crucial for co-aptation and leaflet thickness is measured and matched within 0.0254 mm to avoid leaflet stress and issues with long-term performance (Cox *et al.*, 2005).

2.2.5 The University of Cape Town (UCT) valve

The Starr-Edwards Model 6000 mitral valve was introduced in 1960 and was the first artificial valve prosthesis that enjoyed widespread clinical use (Figure 2.9). The valve design included

four Stellite struts joined at the apex, the outflow and inflow faces were metallic, has a radiolucent poppet and the sewing ring were covered by cloth (Macmanus *et al.*, 1977; Matthews, 1998). The major disadvantage of this mechanical heart valve was thromboembolic complications (Cleland and Molly, 1973).



Figure 2.9: Starr-Edwards Model 6000 mitral prosthesis (adapted from: http://americanhistory.si.edu/collections/search/object/nmah_1726277)

In 1963, Mr Carl Goosen, (Chief Cardiopulmonary Bypass Technician) and Prof Christiaan Barnard (Cardiothoracic Surgeon) at the University of Cape Town designed a mechanical heart valve based on the first-generation Starr-Edwards prosthetic valve (Model 6100) but made several modifications. They modified the valve design to reduce shear stress across the valve to improve the flow characteristics and created the UCT valve. This resulted in less contact activation of the coagulation system and platelet activation adherence to the valve (Dangas *et al.*, 2016).

The valve consists of two components; the one part is secured in the aortic root and the other is freely mobile. The fixed portion is manufactured from a single piece of stainless steel. The ring forms the seat for the mobile unit to which a rim of plastic material is attached to allow the valve to be sutured in the sub coronary position. The steel ring has two polished stainless-

steel arms, one above projecting into the aorta and one below in the left ventricular outflow area. At the end of both arms is a small ring which limit and guide the movement of the mobile portion of the valve. The mobile portion of the valve is hemispherical on the ventricular aspect and on the aortic aspect it is cone-shaped. In the Type I valve the seat was covered with closely-woven Teflon cloth (Figure 2.10a) and in the Type 2 valve the mobile portion of the valve closed on a bare stainless-steel seat (Figure 2.10b). In the Type 3 valve the stainless-steel seat was covered with Dacron-velour cloth (Figure 2.10c) (Schrire *et al.*, 1970; Frater, 1969; Barnard *et al.*, 1963).

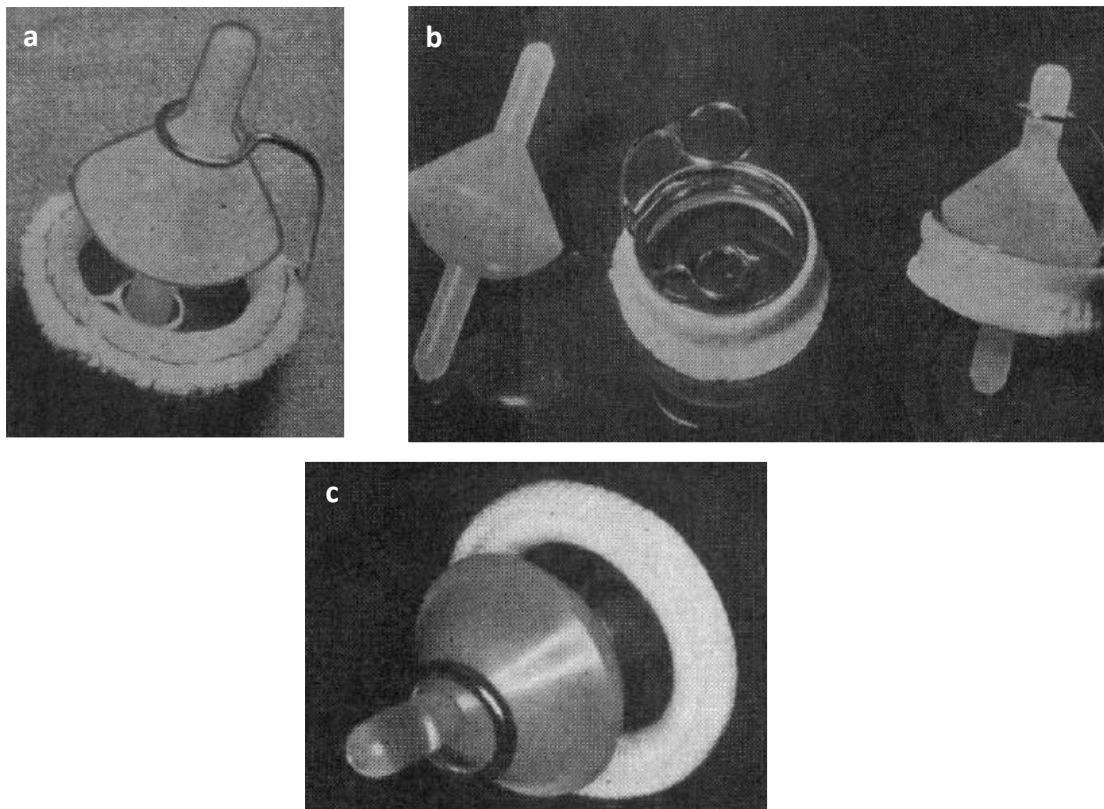


Figure 2.10: The University of Cape Town Valve. (a) Type 1 valve showing the Teflon-covered ring (b) Type 2 with bare steel ring (c) Type 3 with Dacron-velour cloth-covered seat (adapted from Schrire *et al.*, 1970)

Prof RWM Frater, (Einstein institute, New York, USA) implanted forty-five aortic UCT valves into patients and followed them for eighty-two patient years. None of the patients received any anti-coagulation therapy, and his rationale being that the flow across the valve would not activate coagulation (Pratt, 1952). One early death was reported due to coronary thrombosis; the thrombus was thought to have originated from the suture ring of the valve. One late death was reported at 4 years post-operatively due to re-operation complications to repair

valvular dehiscence. The valve salvage from this patient showed no signs of pitting, wear or fat infiltration into the poppet. The valve showed no signs of thrombosis and the cloth covering was adequately covered with Neointima. Although the valve showed yellow discoloration, no wear was found on the occlude and the thin metal struts were thrombus free (Frater, 1969).

With the introduction of the second-generation tilting disk valves with their superior flow and fluid dynamics the production and commercialization of the UCT valve was halted. However, in 2007 a case study was published by Pipilis *et al.* (2007) of an explanted aortic UCT valve from a patient in Athens, Greece. The patient (sixty years) received a UCT valve thirty-seven years ago, in Cape Town. She was admitted due to a high gradient across the UCT valve and presented with concomitant mitral valve stenosis. A valve replacement was performed and again the valve was reported to be in excellent condition with no signs of any thrombosis. The high gradient was attributed to patient prosthesis mismatch.

This sparked renewed interest in the UCT valve. Design alterations were performed incorporating modern day CFD, valve design and manufacturing technology, resulting in the development of the Glycar valve.

The following design modifications were incorporated in the new Glycar prosthetic heart valve:

- i. The leading and trailing edges are rounded incorporating aerofoil concepts.
- ii. The distal conal tapering of the Glycar valve is improved for better laminar flow.
- iii. The sharp edges at the border of the Glycar valve are removed and is rounded to decrease flow acceleration across the edges, less shear stress (shear stress must be less than 10 pascals to avoid platelet activation).
- iv. The guiding struts/arms are tapered into a teardrop shape refining fluid dynamic interaction.
- v. The housing is rounded on the inner surface and extended to simulate aerofoil principals.
- vi. The housing is machined from a solid stainless-steel block, eliminating welding of the struts to the housing, eliminating metal fatigue.

- vii. In the closed position, the Glycar valve-seats flush to the housing. Retrograde blood-flow, follows a laminar flow pattern across the conical shape into the sinuses.

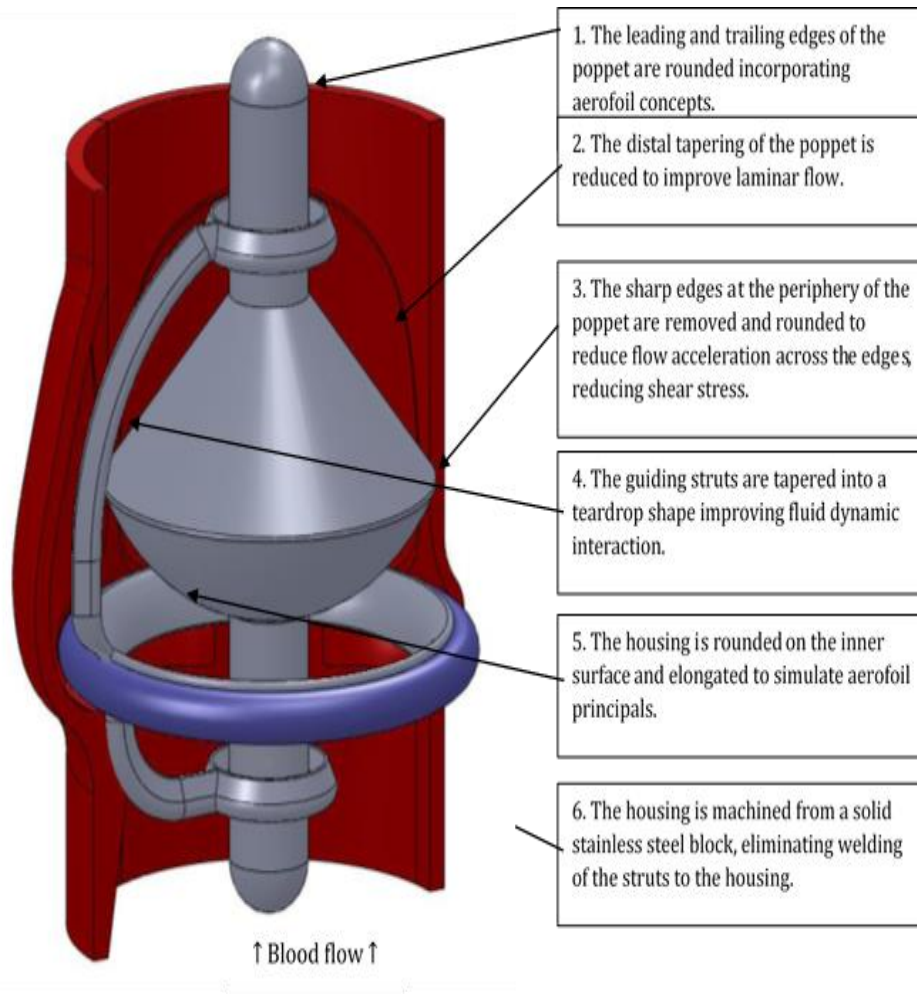


Figure 2.11: Schematic presentation of the re-engineered UCT valve as used in the CFD evaluation

2.2.5.1 Haemodynamic flow characteristics of the Glycar valve

The haemodynamic flow characteristics of the Glycar valve have not been published before, but some aspects have been studied in a recent PhD completed at the UFS (Jordaan JC, 2017).

2.3 HYDRODYNAMIC TESTING OF HEART VALVES

The control of blood flow through a prosthetic valve while minimizing the load on the heart is regarded as one of the performance objectives of these valves. To meet this objective and to assess the potential of a prosthetic heart valve prior to clinical studies, the hydrodynamic performance of these valves is simulated under *in vivo* flow conditions (Baldwin *et al.*, 1997).

Hydrodynamic tests provide information on the real-time performance of prosthetic heart valves (i.e., mechanical, biological, and synthetic heart valves) under steady and pulsatile flow conditions in a controlled environment (Bazan *et al.*, 2016; Wheatley *et al.*, 2000; Fisher *et al.*, 1986). The valve measurements are done under standard conditions, which do not accurately reflect the *in vivo* hemodynamic performance of the valves but do provide a relatively good reflection of the *in vivo* environment (Johnston *et al.*, 1992).

Clinical results of flow measurements and valve reaction under pulsatile flow conditions are difficult to compare with one another due to inherent differences, like the use of anticoagulant therapy and indications for valve implantation (Haaf *et al.*, 2009). For this reason, highly reproducible experiments under *in vitro* conditions are pertinent to the scrutinization of established valves and the development of new prosthetic heart valves.

The ISO 5840:2015 guidelines clearly states that the *in vitro* evaluation of a prosthetic heart valve should include flow characteristics (pulse duplication) and durability testing (fatigue testing). Valvular flow characteristics are assessed using a pulse duplicator system with pulsatile flow to produce pressure and flow waveforms that approximate physiological conditions over the required physiological range. Durability testing aim to evaluate valvular performance over the valve's anticipated lifetime using a fatigue tester. The mechanical valves should be exposed to 600 million cycles (equivalent to 15 years *in vivo*) and the bio-prosthetic heart valves to at least 200 million cycles (equivalent to 5 years) (ISO 5840:2015; Lu *et al.*, 2003).

2.4 PULSE DUPLICATION

2.4.1 The history of pulse duplication

This section will only highlight some of the pioneering work and major contributions made towards the development of pulse duplication systems. Although the earliest method for the *in vitro* testing of heart valves was described in 1513 by Leonard da Vinci, the first pioneering

designs of pulse duplication systems were reported by Davilla in 1956 and Kolff and colleagues in 1959 (Wieting, 1989).

In the 1960's *in vitro* testing became much more quantitative than that of the previous decade. Quantitative pulse duplication studies were first used with the development of the Smeloff-Cutter valve in 1965 (Zilla *et al.*, 2008). In 1966 Wieting introduced his pulse duplication system followed by revisions in 1969 which included the use of anatomically designed testing chambers and the incorporation of a pneumatic power unit (Vitamek) and a mock-circulating system designed by O'Bannon. The Wieting system was used to test various heart valves by making normal and high-speed flow pattern movies and to measure velocity profiles from flow pattern photographs, shear stress, pressure drop, and backflow for the various heart valves (Wieting, 1989). In 1969 a substantial contribution was made by Bellhouse with the description of the fluid mechanics of the natural aortic and mitral valves. This was studied in an aortic chamber with sinuses, and a left ventricular-shaped testing chamber with an expanding "rubber bag" (Bellhouse, 1972).

Various pulse duplications systems were described by Wright in 1970, analysing the flow characteristics of heart valves in a piston-driven ventricular shaped chamber and aortic arch model. In 1971 Orin presented the concept of energy loss across prosthetic heart valves. Hwang and Reul's developed a pulse duplicator in the late 1970s that incorporates a flexible left ventricle bag compressed by a computer-controlled servo-hydraulic system (Wieting, 1989). Yoganathan, Harrison and Corcoran collaborative efforts made a major contribution towards *in-vitro* testing in 1979 (Yoganathan *et al.*, 1979; Cape *et al.*, 1996). Yoganathan continued actively studying heart valves using the latest technology provided by laser-doppler, echo-doppler and colour-doppler echocardiography to analyse the *in vitro* hemodynamic data.

The original hydro-mechanical pulse duplicator evolved in the 1980s to the "Superpump" which is manageable and programmable through a computerized system to provide a very sophisticated heart valve analysis system. In the 1980s the team of Martin, Tindale and Black began reporting on investigations of heart valves (Tindale *et al.*, 1982). Chandran contribute to the investigation by reporting on the effect of valve orientation, effect of blood analogue

fluids on tissue valves and the effect of wedging of aortic valves (Chandran *et al.*, 1989; Chandran *et al.*, 1986).

Since then every aspect/component used in modern day pulse duplication systems became more sophisticated. Today, pulse duplicators are equipped with thin acrylic windows permitting echocardiographic imaging, doppler flow measurements, and particle imaging velocity (PIV) for interrogation of flow field regions that allows for more advanced hydrodynamic testing (Bazan *et al.*, 2011). Although most pulse duplicators in the past were “self-build” systems, today pulse duplicator systems are commercially available of which the systems offered by ViVitro Labs Inc. (ViVitro Superpump M series) and BDC Labs Inc. (HDT-500 pulse duplicator) is probably the most popular.

In conclusion, *in vitro* testing must continue to apply all the latest technological advances to expand our understanding of the functioning of prosthetic heart valves before implantation in humans commence, to aid us on our quest to find the “ideal prosthetic heart valve” (Wieting, 1989).

2.4.2 The purpose and function of the pulse duplicator system

The main purpose of pulse duplication is to realistically assess the performance of a heart valve prosthesis under simulated cardiac conditions in a controlled environment.

The pulse duplicator system functions as a hydraulic model resembling the left heart of a human, connected to a windkessel model of the human systemic circulation (Verdonck, 1992; Fisher *et al.*, 1986; Westerhof *et al.*, 1971). In general, most of the pulse duplicator systems work on the principle that the fluid enters the model from a controllable preload reservoir that represent the lungs via two rigid pulmonary veins. The fluid runs through the mitral valve and reaches the left ventricle. The left ventricle ejects through the aortic valve into the afterload system consisting of an air chamber or windkessel and a hydraulic resistor. The hydraulic function of the arterioles and capillaries are mimicked by the resistor. A constant venous pressure of 5 mmHg is maintained by a venous reservoir. Both the preload lung and

the venous reservoir is equipped with an overflow system, ending in a central buffer reservoir out of which the test fluid is continuously pumped into the lung reservoir.

The left ventricle is mounted in a Perspex housing and is represented as an anatomically shaped silicon sac. The silicon sac is surrounded by water and connected to an external circuit, consisting of Perspex cylindrical reservoirs. The contraction and relaxation of the cardiac chamber is controlled by pressurized air that is delivered to the external circuit.

As the pulse duplicator system is computer controlled, a targeted left ventricular pressure curve is sent to the computer system and a feedback system controls the amount of pressurized air delivered to the system such that the target curve is followed as closely as possible (Verdonck *et al.*, 1997; Verdonck, 1992). The system allows the variation of physiological parameters such as heart rate, stroke volume and pressure levels.

The test fluid used in the system is also adapted so that it simulates the viscosity of blood. As a test fluid, a mixture of 40% glycerine – 60% water is commonly used to simulate the dynamic viscosity of 3.0 mPa.s of blood (Bazan and Ortiz, 2016).

Through the years, the complex function of the left heart and arterial system have been simulated by adapting pulse duplicator systems in several ways thus producing varying valvular test conditions. Some of the benchtop pulse duplicator systems include the “Yoganathan-FDA system”, “Aachen pulse duplicator”, “Sheffield pulse duplicator” and the “ViVitro pulse duplicator”. Flow, pressure and even Doppler measurements made with these systems make it possible to estimate the hydrodynamic performance of artificial heart valves in a controllable *in vitro* environment (Dasi *et al.*, 2007; De Paulis *et al.*, 2005; Grigioni *et al.*, 2004; Milo *et al.*, 2003).

2.4.3 The mechanical components of the pulse duplicator system

The methods used to evaluate the function of prosthetic heart valves under pulsatile flow conditions have become increasingly sophisticated since the work described by Wieting (1989) and Write and Temple (1971).

The pulse duplicator system simulates the systemic circulation, including the left atrium, left ventricle and the large arteries. The ISO 5840:2015 guidelines states that the *in vitro* evaluation of prosthetic heart valves is essentially limited to the aortic position (ISO 5840:2015; Verdonck *et al.*, 1997). The ISO standard also states that a pulse duplicator should come equipped with a valve chamber with relevant dimensions to replicate the haemodynamic characteristics across the valve. The systemic circulation is represented by a reservoir (left atrium), a pump (left ventricle), compliance elements (aorta) and a resistance element (peripheral resistance) (Fisher *et al.*, 1986). The system must be capable of producing pressure and flow waveforms that simulate a range of physiological parameters, from a resting state to exercise.

The majority of test rigs can be divided into four sections (Rajeev *et al.*, 2012):

- i) The pump used to generate pulsatile flows to simulate the function of the heart.
- ii) Two unidirectional valves along with its mounting fixtures (usually one of them is the test valve).
- iii) A set of hydraulic components representing the circulatory system, referred to as the afterload.
- iv) An instrumentation system for data acquisition and analysis.

Emphasis will be placed on the ViVitro pulse duplication system because it was the system used to assess the hydrodynamic performance of prosthetic valves in this study. The ViVitro pulse duplicator system is used by the US Food and Drug Administration and is recognised by regulatory bodies worldwide including Technical Inspection Association (TÜV), British standard Institution (BSI) and the Chinese State Food and Drug Administration (SFDA)(adapted from <http://vivitrolabs.com/product/pulse-duplicator/>).

2.4.3.1 ViVITro pulse duplicator system

The ViVITro left heart model emulates the pressures and flows of the left heart. The pulse duplicator system simulates physiological or other complex flow variations while allowing the user to vary the peripheral resistance and the compliance of the system. Pressure measurements can be collected from the aortic, ventricle and atrial sites via pressure ports and the volumetric flow rate is measured before the aortic valve. Transparent viewpoints allow for multiple viewing angles of the valve including inflow and outflow, perpendicular and parallel to the flow direction (<http://vivitrolabs.com/product/pulse-duplicator/>) (Figure 2.12).

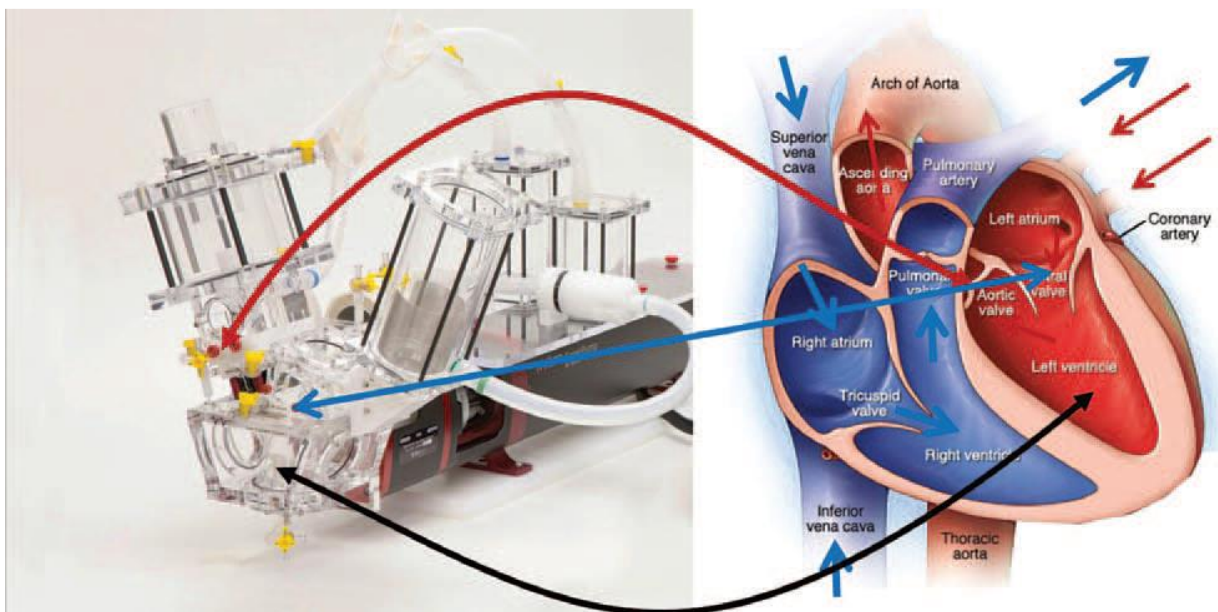


Figure 2.12: The ViVITro system with a schematic representation of the heart (adapted from ViVITrolabs.com)

2.4.3.2 The ViVITro Labs AR series SuperPump

The AR series Superpump consists of a digital amplifier with stroke volume display and preprogrammed waveforms driving a piston-in cylinder pump (Baldwin *et al.*, 1997) (Figure 2.13).



Figure 2.13: The ViVibro Labs AR series SuperPump (adapted from ViVibro.com)

The pump piston is located in a ball screw/servo motor/encoder unit driven by a motor controller which functions by comparing the actual position against the desired position defined by the input waveform. Accurate positioning of the piston resulting in the desired pulsatile flow is achieved by the precision of the ball screw. The encoder ViVigen software is included with the SuperPump series and allows for the generation of custom waveforms which can be uploaded to the controller via the built-in USB port. Furthermore, the SuperPump series include analogue outputs for position, dL/Dt (flow) and the sync pulse which makes the SuperPump adaptable to any custom-made pulse duplication system (adapted from <http://vivitrolabs.com/product/pulse-duplicator/>).

The ViVibro Labs AR series SuperPump include the following features:

- i. Digital precision control of a pump-in-cylinder designed linear actuator used to generate physiological flows.
- ii. Stand-alone capability with five pre-programmed cardiac waveforms created by the user.
- iii. Range of capable rates are 4 to 200 beats per minute.
- iv. Range of stroke volume 0 to 150 ml.
- v. Digital controlled and created waveforms by ViVigen or ViViTest software.
- vi. Control, create, input or store cardiac waveforms at various physiological states and frequencies and other standard waveform generating equipment.

The ViVitro Labs AR SuperPump series was manufactured by an ISO 13485 accredited facility designed to meet both regulatory requirements (ISO 5840 and FDA) or research needs.

2.4.3.3 The valvular chambers of the ViVitro pulse duplicator

The ViVitro pulse duplicator has three valvular chambers; (1) ventricle chamber, (2) atrium chamber and (3) the aortic chamber (Figure 2.3). To perform a hydrodynamic assessment on a prosthetic valve, the valve is mounted in the appropriate aortic or mitral position of the model left ventricle and a companion valve is placed in the remaining position (Baldwin *et al.*, 1997).

The sewing ring around the valve is inserted into a silicon rubber fitting which follows the form of the test chamber. The silicon rubber ensures a completely sealed fitting to reduce leakage between the ventricle and aortic chambers. The chamber of the apparatus is a critical part of the testing rig, as the geometry of the pulse duplicator chambers affect the performance of the valve being studied. This determines the dynamic pressure or flow waveforms produced in the test rig. Cylindrical rigid test conditions have been widely used and only the geometry, close to the valve, has been modelled on physiological data (Leondes, 2001; Fisher *et al.*, 1986).

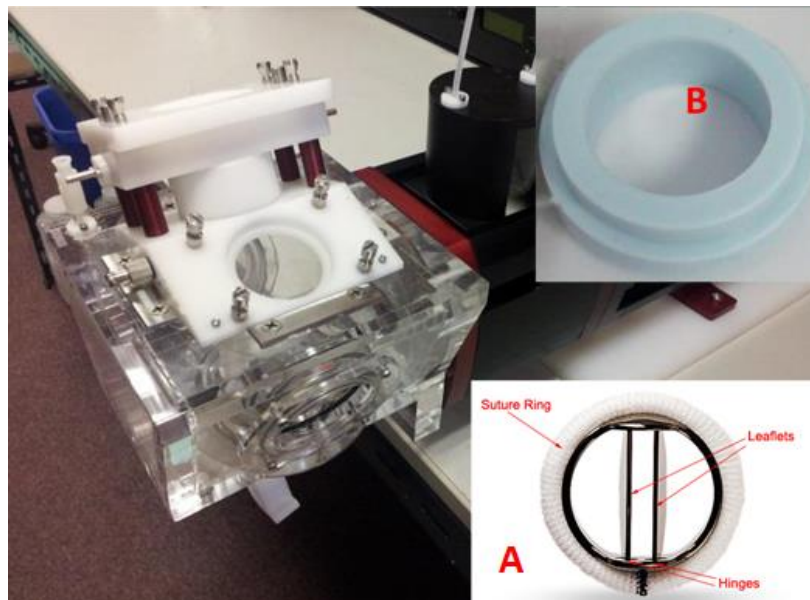


Figure 2.14: Presentation of the chambers insertion in the pulse duplicator. (A) Prosthetic heart valve (B) Second plastic ring to secure valve (C) plastic slot in rig in which prosthetic valve is fixed (adapted from <http://vivitrolabs.com/product/pulse-duplicator/>)

2.4.3.4 Afterload and peripheral resistance

The pressure waveforms can be controlled by adjusting the air pressure in the compliance chambers. The viscoelastic impedance adapter (VIA), situated between the linear actuator and the ventricle, can reduce the initial pressure spike due to the rigid system, and can delay peak flow to replicate physiological flow conditions (Jennings *et al.*, 2001). The peripheral resistance is adjusted to control the aortic pressure and mimic the systemic resistance of the body.

2.4.3.5 ViVitest Data Acquisition System (DAS)

ViVitest is part of the ViVibro Data Acquisition System (DAS) software family (Figure 2.4). In combination with the pulse duplicator system it collects hydrodynamic testing data to meet ISO 5840 requirements. The Superpump is controlled by the ViVitest software while simultaneously measuring pressure and flow data. It monitors, processes, and reports data such as regurgitant fraction, effective orifice area (EOA), and other valve performance indicators. Output files are available in .CSV format for easy analysis in Excel and MatLab (adapted from <http://vivitrolabs.com/product/pulse-duplicator/>).



Figure 2.15: ViVitest Data Acquisition system (DAS) (adapted from <http://vivitrolabs.com/wp-content/uploads/2016/02/Pulse-Duplicator-Brochure-2016-VIVI-MKT-046.pdf>)

2.4.4 Performing pulse duplication analysis

Before testing of a prosthetic heart valve can commence on a pulse duplicator it is important to take the following factors into account (Wright, 1979):

- i. The testing liquid should be appropriate for the prosthesis and the temperature of the liquid should be the same as normal body temperature.
- ii. The flow characteristics of the pulse duplicator should be known, reproducible and almost the same as physiological flow.
- iii. The geometry of flow passages through the pulse duplicator should be relevant to the vessels and chambers of a normal heart.
- iv. The test rig must be capable of testing both the smallest and largest mitral and aortic valve prostheses in clinical use.
- v. The test rig should be orientated to exert gravitational forces similar to those found in a patient.
- vi. Suitable pressure taping points should be selected.

The parameters defined to assess valve performance during pulsatile flow are many and varied. Reul *et al.* (1993) states that measurements should cover the following aspects: (a) pressure difference and leakage in non-pulsatile flow as first indication of acceptability, (b) pressure difference in pulsatile flow under various conditions as a reference for clinical conditions, (c) closure and leakage volumes as a measure for hemodynamic competence, (d) energy losses as a measure of the additional work load for the heart and potential blood damage, (e) detailed evaluation of the downstream velocity field for the assessment of stasis and recirculation areas in the context of potential thrombus depositions, and (6) laminar and turbulent shear stresses as parameters for potential blood damage and platelet activation. Pressure and flow measurements are the primary determinants (Black *et al.*, 1983) of valve performance and is evaluated with respect to the following parameters:

- *Stroke volume*: the volume of fluid flowing through a valve in the forward direction during a cardiac cycle.

- *Regurgitation*: the volume of fluid that flows through a valve in the reverse direction during one cycle. It is the sum of the closure volume and the leakage volume and is expressed as a percentage of the stroke volume.
- *Cardiac output*: the mean flow through a valve per minute and
- *mean systolic pressure difference*: the average value of the pressure difference across the valve during the systolic or forward flow phase (ventricle pressure – aortic pressure).

The pulse duplication environment simulates pulsatile cardiac flow under various clinical conditions by manipulating heart rate, cardiac output, stroke volume and afterload. In accordance with the ISO 5480:2015 guidelines for the hydrodynamic assessment of heart valves the following hydrodynamic parameters should be calculated for any condition (ISO 5480:2015; Kuettinga *et al.*, 2014; Strobe, 2010):

- Effective orifice area (EOA)
- Q_{rms} (during forward flow)
- Trans-valvular pressure gradient
- Regurgitant volumes
- Trans-valvular energy losses

Table 2.1 represents the minimum performance requirements which the *in vitro* test results must meet or exceed given as a function of valve size, valve annulus diameter, and valve position (ISO 5840:2015). The minimum performance requirements correspond to the following pulsatile-flow conditions: bpm of 70 cycles/min, a simulated CO of 5.0 L/min, a mean aortic pressure of 80 mmHg and a systolic duration of 35%.

Table 2.1: The minimal ISO 5840:2015 performance requirements for pulse duplication evaluation

Position	Aorta valve						Mitral valve				
Valve size (TAD, mm)	19	21	23	25	27	29	31	25	27	29	31
EOA (cm ²)	>0.70	>0.85	>1.00	>1.20	>1.40	>1.60	>1.80	>1.20	>1.40	>1.60	>1.80
Regurgitant fraction (%)	<10	<10	<10	<10	<10	<10	<10	<10	<10	<10	<10

[EOA =Effective orifice area in square centimetres; TAD = test valve annulus diameter; mm = millimetre]

2.4.4.1 Calculating pulse duplication hydrodynamic metrics

i) Transvalvular pressure readings (TVP)

The instantaneous pressure gradients can be calculated by taking the difference between the ventricle and aortic chamber, trans-valvular pressure reading (TVP), over several cycles (Haaf *et al.*, 2009). Maximum TVP is calculated as the maximum pressure gradient recorded across the valve from the aortic and ventricular pressure readings (Ramaswamy *et al.*, 2013).

ii) Mean systolic pressure difference

The mean systolic pressure difference is determined by taking the average of the ventricular pressure (P_v) minus aortic pressure (P_{Ao}) determined as

$$\Delta P_{sys} = \frac{1}{N} \sum_1^N P_v - P_{Ao} \quad (\text{ISO 5840:2005})$$

The interval over which the average is calculated and can be split into three different categories.

- P = interval where the TVP is positive
- F = interval where the flow rate is positive
- H = interval starting with 0 TVP and ending with 0 flow

The mean systolic pressure difference is calculated using the P interval as stipulated in ISO 5840:2005.

iii) Closing and leakage volume

The closing volume (V_{CL}) and leakage volume (V_L) equations represent the time integrals of aortic flow during closing and leakage periods, respectively. The closing volume is defined as the regurgitant volume that flows back through the valve during the time interval of valve closure (T_{CL}). The leakage volume is defined as part of regurgitant volume that passes during the rest of the cycle (T_L) and the closed state of the valve through the gap between the occluder and the valve ring (de Paulis *et al.*, 2005). The closing and leakage volumes are calculated based on the following time intervals:

- *Closing*: from the time, the flow rate becomes negative till the instance of valve closure (t_2).
- *Leakage*: from t_2 till the end of the cardiac cycle (t_3).

Total regurgitant volume is simply calculated by the sum of the closing and leakage volumes (Ramaswamy *et al.*, 2013).

iv) Effective orifice area (EOA)

EOA is defined as the part of the primary “theoretically possible” orifice area (POA) being used during systole. The performance index (PI) of a heart valve is defined as the relation of EOA to POA (Haaf *et al.*, 2009).

The aortic root mean square (RMS) forward flow rate (Q_{rms}) provides a useful metric for quantifying the magnitude of forward flow rate as follows (Ramaswamy *et al.*, 2013):

$$Q_{rms} = \sqrt{\frac{\int_{t_1}^{t_2} q_v(t)^2 dt}{t_2 - t_1}} \quad (\text{ISO 5840:2005})$$

The EOA (based on blood properties) can be computed for 3 intervals, P, F, and H from the TVP during each of these periods (Chandran *et al.*, 2007). In this study, the EOA was based using the P interval in line with ISO 5840:2005:

$$EOA = \frac{Q_{rms}}{51.6 \sqrt{\frac{\Delta P}{\rho}}} \quad (\text{ISO 5840:2005})$$

2.4.5 Pros and cons associated with pulse duplication

The use of pulse duplicator systems to assess valve functionality during pulsatile flow, or to investigate valvular mechanics, is relatively well established however both the system and the operation is not without pitfalls (Temple *et al.*, 1964; Fisher *et al.*, 1986).

Even though pulse duplicators, if used correctly per the ISO 5840:2015 guidelines, can produce reproducible data, measure instantaneous flow through the valve and provide good visibility of the valve being tested, they also have disadvantages.

Many sophisticated laboratories have undertaken studies to provide comparative evaluations of valve substitutes but did not provide any insight into the valves' *in vivo* performance. The interpretation of such *in vitro* results must be approached with caution by recognizing their limitations when extrapolated to the *in vivo* situation (Tindale *et al.*, 1982; Black *et al.*, 1983).

The main disadvantages are that the flow patterns in the left ventricle are not modelled and the inertia of the fluid in the rigid tubes can distort pressure waveforms (Fisher *et al.*, 1986). It is known that the rigid tubes do not mimic the tissue compliance, however the ViVitro pulse duplicator includes an aortic and aortic root compliance chamber to simulate the tissue compliance as much as possible. The fluid flow patterns cannot be visually assessed to determine regions of recirculation or high shear stresses.

2.5 ECHOCARDIOGRAPHY

Echocardiography has been widely accepted as a non-invasive technique for *in vivo* visualization, but can also be used for the *in vitro* assessment of prosthetic heart valves (Pibarot *et al.*, 2012; Leefe *et al.*, 1995). Modern day pulse duplicators like the ViVitro pulse duplication system is equipped with thin acrylic windows that permit echocardiography imaging and Doppler flow measurements. These windows are situated on the side or on top of the valve. The top viewing chamber allows taking echocardiographic images directly above the valve (Figure 2.16).

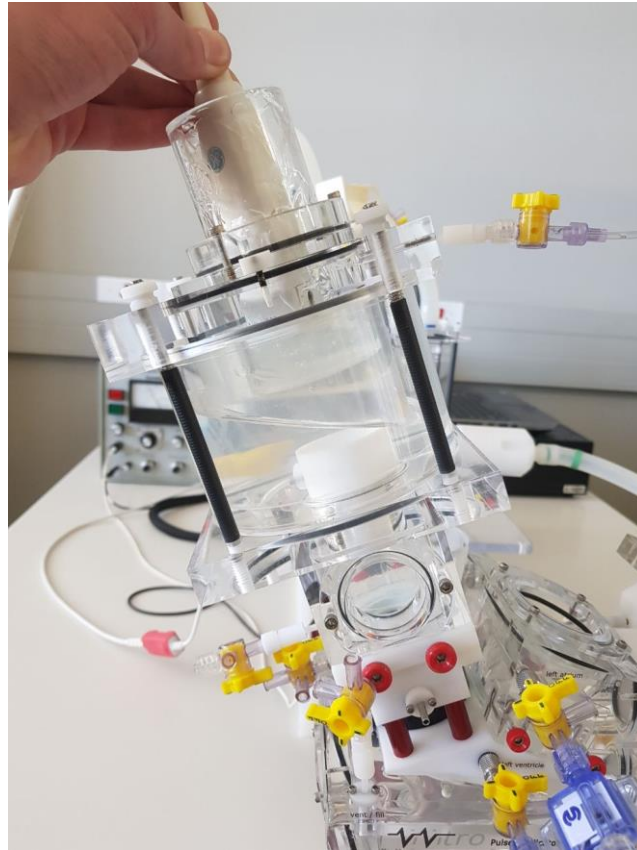


Figure 2.16: Echocardiographic viewing chambers in a ViVitro pulse duplication system

2.5.1 The history of echocardiography

By using an industrial ultrasonic flaw detector, Inge Edler (Director of the Cardiovascular Laboratory, Lund University) and Carl Hellmuth Hertz (physicist) obtained time-varying echoes transcutaneous from within the heart that marked the beginning of a new diagnostic non-invasive technique (Singh and Goyal, 2007; Edler and Lindström, 2004). The first echoes were recorded via M-mode and were from the posterior wall of the left ventricle and from another structure thought to be the anterior wall of the left atrium. The first clinical application of M-mode echocardiography assessed the mitral valve from the shapes of the corresponding waveforms.

The technique was further validated in the late 1960s with the discovery of contrast echocardiography, extending its range of applications. Although two-dimensional echocardiography was first demonstrated in the late 1950s, transesophageal echocardiography only followed in the late 1960s. However, the demonstration of real-time

two-dimensional echocardiography using a linear transducer array by Bom in Rotterdam revolutionized and popularized the use of echocardiography. This was followed by the development of the pulsed Doppler method also in the late 1960s which led to new opportunities for clinical innovation (Mohamed *et al.*, 2010). Technology evolved over many years, and over the last few years a quantum leap was seen in the use of 3D and 4D echocardiographic application.

2.5.2 The purpose and function of echocardiography

Echocardiography has become the primary assessment tool for patients that have prosthetic heart valves. Comprehensive guidelines exist for the evaluation of prosthetic heart valves and has been published by the American Society of Echocardiography (ASE) and the European Association of Echocardiography (EAE)(Zoghbi *et al.*, 2009). Echocardiographic interrogation of prosthetic heart valves must be done from multiple windows and proper alignment of the Doppler beam with flow direction is important (Blauwet *et al.*, 2014).

An echocardiogram is an ultrasonic graphic outline of the heart's physiological movement. The test is non-invasive and provides images of heart valves and chambers using high frequency sound waves. Echocardiography is used to evaluate the pumping action of the heart and is often combined with Doppler ultrasound and colour Doppler to evaluate blood flow across heart valves (Otto, 2004).

Echocardiography involves two-dimensional (2D) ultrasound interrogation of the heart utilizing the brightness mode to image cardiac structures based on their density and location relative to the chest wall (Levine, 2009) by utilizing transthoracic and transoesophageal probes. The computer in the ultrasound machine uses algorithms to reconstruct images of the heart. The depth of the structures is determined by the time it takes the ultrasound to return to the probe. The intensity of the returning signal determines the density and size of the structures with which the ultrasound comes in contact. The probe performs Doppler as well, which measures the frequency shift of the returning ultrasound that determine the speed and direction of moving blood through the heart structures (Dokainish, 2006).

During Doppler ultrasound, the flow velocity in a target control volume of fluid is assessed by the detection of the Doppler shift in ultrasound waves reflected from micro-particles in the fluid, such as blood cells or small seedling particles (Levine, 2009). When directing the ultrasound beams towards a moving target, the transducer determines the frequency shift (Δf) which is the difference between the transmitted frequency of the transducer (f_t) and the received frequency (f_r). The frequency shift is related to the velocity of the moving target (v), transmitted frequency (f_t), and the angle between the direction of the ultrasound beam and the direction of the moving target (Anavekar and Oh, 2009) (Figure 2.17).

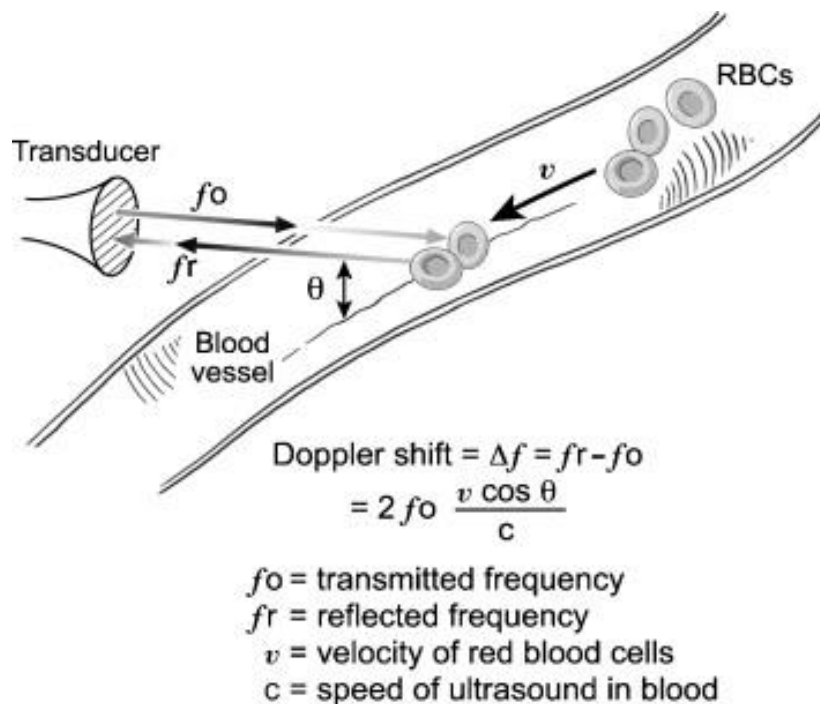


Figure 2.17: The Doppler effect (adapted from Anavekar and Oh, 2009)

Doppler has three modes (Anavekar and Oh, 2009; Levine, 2009):

- Colour Doppler, utilizes different colours (blue and red) to identify forward and back flow from the transducer respectively, to identify flow acceleration qualitatively by showing a mix of colour to represent high velocity of aliased flow.
- Pulsed-wave(PW) Doppler, can localize the site of flow acceleration but is prone to aliasing (Figure 2.18).
- Continuous-wave (CW) Doppler, cannot localize the level of flow acceleration but can identify very high velocities without aliasing (Figure 2.18). For the purposes of this study only continuous wave Doppler was used to assess flow characteristics of the aortic prosthetic heart valves.

Continuous wave Doppler ultrasound measures the shifts in reflected ultrasound frequency proportional to all the velocities detected by the beam. The maximal signal is a measurement of the maximum velocity present. In a prosthetic heart valve, this maximal velocity is the high velocity jet that is flowing through the valve orifice (Stewart *et al.*, 1991). CW Doppler is optimal when performed with a non-imaging transducer with two crystals which have a high signal to noise ratio. CW facilitates high velocities but does not localize the depth of origin of the signal and is used in high velocities on valve stenosis and regurgitation (Otto, 2004).

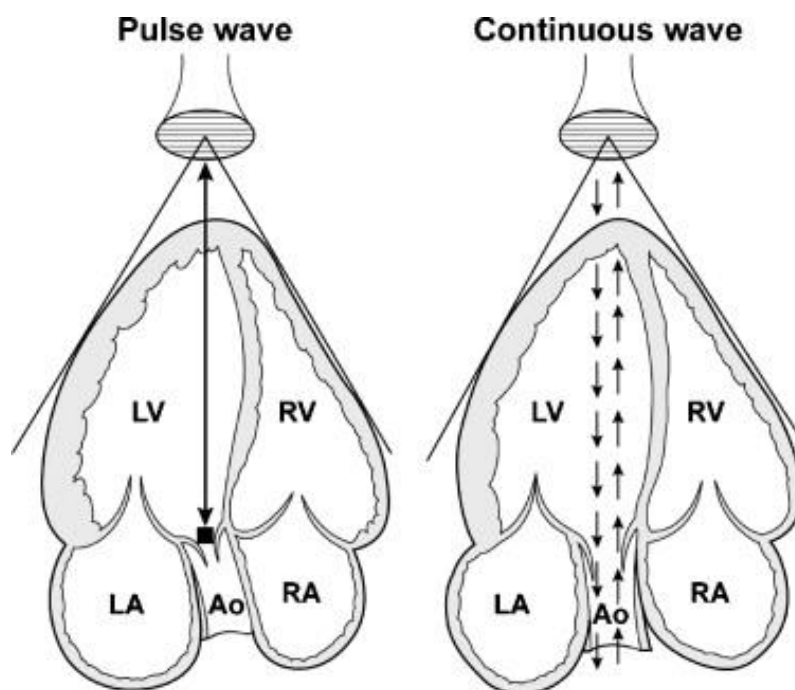


Figure 2.18: Doppler pulsed wave and continuous wave Doppler echocardiography from the apical view (adapted from Anavekar and Oh, 2009) [Ao, aorta; LA, left atrium; LV, left ventricle; RA, right atrium; RV, right ventricle]

A complete echocardiography includes two-dimensional (2D) imaging of the prosthetic valve, evaluation of the leaflet/occlude morphology and mobility, measurement of transprosthetic gradients and effective orifice area (EOA), estimation of the degree of regurgitation, evaluation of the left ventricle (LV) size and systolic function, and calculation of systolic arterial pressure (Pirabot *et al.*, 2009). The quantitative parameters that is included in the assessment of prosthetic heart valves are (Sordelli *et al.*, 2014):

- Trans-prosthetic velocity and pressure gradient

- Trans-prosthetic jet contour and acceleration time
- Doppler velocity index (DVI)
- EOA

As ultrasound is relatively inexpensive and non-invasive in comparison to computed tomography (CT) and magnetic resonance (MR), more and more specialists use ultrasound to assess valvular geometry.

2.5.3 Prosthetic valvular geometry determined by echocardiography

The velocity measurements estimate the transvalvular pressure gradient (TPG) using the Bernoulli equation and calculate the effective orifice area (EOA) of valves using the continuity equation (Durand *et al.*, 1999). This is a relatively accurate approach for the assessment of native and bio-prosthetic heart valves but shows significant variability when used for mechanical valves, due to the complex flow velocity distributions and valve designs (Sordelli *et al.*, 2014).

2.5.3.1 Flow velocity

A flow velocity profile is the spatial uproar of velocities in a cross section at a specific intra-cardiac location. A flat flow velocity profile occurs when all the flow lines are parallel in a laminar flow pattern with the same velocity. When the velocity is higher in the middle and lower at the walls of the vessel then the profile is curved. Peripheral vessels have curved flow-velocities and intra-cardiac flows have flat flow velocity profiles. Flow velocity is equalized by factors such as tampering with the flow stream, acceleration of flow and inlet type geometry (Otto, 2004). Peak velocity should be averaged over 3-5 consecutive beats if the patient is in sinus rhythm or over 5-10 beats if in atrial fibrillation. It should be measured at the top of the dense part of the waveforms only with a well-defined peak.

Flat flow profiles occur in the proximal aorta, pulmonary artery, mitral and tricuspid annuli. In the ascending aorta, the velocity flow along the inside curve of the aortic arch is higher and it is lower along the outer curve, causing the flow profile to become skewed (Otto, 2004).

Flow velocity increases in relation to the degree of narrowing, whether due to a stenotic valve, ventricular septal defect or regurgitant orifice. The velocity through a narrow jet is related quantitatively to the pressure gradient across the narrowing. This is expressed using the Bernoulli equation $\Delta P = 4v^2$, where ΔP is the instantaneous pressure gradient (mmHg) and v the instantaneous velocity (m/s) (Otto, 2004).

The high frequency shifts (velocities) of the Doppler are accurate since the sampling is continuous. Velocity underestimation can occur with either pulsed or CW Doppler techniques and is important when measuring high-velocity jets due to stenosis, regurgitation or intracardiac abnormalities (Otto, 2004).

A) Velocity ratio (VR)

The ratio of peak sub-aortic to peak transaortic velocity gives an approximate guide to valvular orifice behaviour. It is equivalent to a performance index (the ratio of effective orifice area to total valve area). It is useful for serial measurements in the same individual where the diameter of the left ventricular outflow tract is assumed to be constant (Chambers *et al.*, 1994).

B) Velocity time integral (VTI)

The velocity time integral (VTI) or time velocity integral (TVI) is the area measured under the Doppler velocity curve for each heartbeat. The pulse wave is at the level of the valve annulus and parallel to blood flow direction. The TVI is used to calculate the cardiac output (CO) and cardiac index (CI) (Kerut *et al.*, 2007).

The TVI of the LVOT is measured at the same level in the LVOT where the diameter was measured. The VTI at the AV level is determined by CW Doppler in the same view (Apical 5C) through the aortic valve. TVI measurements and SV calculations allow for valvular regurgitant fraction and shunt calculations (Kerut *et al.*, 2007).

2.5.3.2 Valvular gradients

For each prosthetic heart valve, it is important to determine both the mean and peak gradients.

A) Mean gradient

Pressure gradient is calculated from the velocity by using the Bernoulli equation. The gradient is average from the velocity curve and the unit is comparable to the invasive measurements. The accurate pressure gradients are dependent on the precise velocity data that is flow dependent (Baumgartner, 2009). The velocity jet is related to the pressure gradient across the valve according to an unsteady $\frac{1}{2}$ Bernoulli equation:

$$\Delta P = \frac{1}{2}\rho(v_2^2 - v_1^2) + \rho\left(\frac{dv}{dt}\right)dx + R(v) \quad (\text{Otto, 2004})$$

ΔP is pressure gradient across the stenosis, ρ the mass density of blood ($1.06 \times 10^3 \text{ kg/m}^3$), v_2 the velocity in the jet, v_1 the velocity proximal to the stenosis, (dv/dt) the time-varying velocity at each distance along the flow stream and R a constant describing the viscous losses for that fluid and orifice (Otto, 2004).

B) Peak gradient

In contrast to mean gradient, peak gradient (peak-to-peak or peak instantaneous) is a less reliable measurement of valve hemodynamics. This can be attributed to the substantial influence of LV contractility in addition to the influence of trans-valvular flow. The peak pressure gradient is an especially unreliable indicator of hemodynamics in the setting of a prosthetic AV, where high velocities are commonly observed immediately after valve opening (Bach, 2010).

2.5.3.3 Effective orifice area (EOA)

EOA is the minimal cross-sectional area of the flow jet, the cross-sectional area of the vena contracta, downstream of a native or bio-prosthetic aortic heart valve. The EOA is the standard parameter used for clinical assessment of aortic valve stenosis severity. It can be determined either with the Doppler echocardiography by using the continuity equation or

from catheterization by applying the Gorlin formula. EOA determined by Doppler or by catheter may vary with increasing flow rate (Garcia *et al.*, 2004).

The continuity equation should be used if the left ventricle is significantly impaired or if the peak trans-aortic velocity is high (> 3m/s) and it is not certain whether it is because of relative obstruction or high flow.

$$EOA = CSA * \frac{VTI_1}{VTI_2} \quad (\text{Chambers } et al., 1994)$$

The use of the product of CSA and VTI_1 has been validated for artificial heart valves. The continuity equation can be simplified by assuming similar waveform shape above and below the valve:

$$EOA = CSA * \frac{v_1}{v_2} \quad (\text{Chambers } et al., 1994)$$

where v_1 is the sub-aortic peak velocity and v_2 is the aortic velocity. This form of the equation is simpler to apply and is in general use but tends to underestimate at orifice areas above 1cm^2 . CSA is calculated from the left ventricular outflow tract diameter (d) assuming a circular cross-section:

$$CSA = \frac{\pi d^2}{4} \quad (\text{Chambers } et al., 1994)$$

The diameter of the left ventricular outflow tract should be averaged from three parasternal long axis frames frozen in early systole (transthoracic echocardiography). Care must be taken to open out this region until the dimension looks maximal. The measurement should be made from the leading edge of the septum to the leading edge of the anterior mitral leaflet echocardiograph. The measurement should be made if there is severe left ventricular hypertrophy or bowing of the anterior mitral leaflet. It should be performed with a coexistent mitral prosthesis only if the blooming from the sewing ring of the mitral valve is trivial (Chambers *et al.*, 1994).

The continuity equation is limited by its wide confidence intervals (Ci). For normal functioning bi-leaflet valves the difference between measured and calculated orifice area has a 95% Ci of

around -0.5 to $+0.5$ cm^2 , with errors arising mainly in the measurement of sub-aortic diameter and sub-aortic velocity. In practice, the effective orifice area should be regarded as a semi-quantitative guide rather than a precise measurement of function (Chambers *et al.*, 1994).

2.5.4 Echocardiography and pulse duplication

Because valve opening behaviour and patterns of regurgitation and closure vary widely among valves of different designs, echocardiographic experience gained with one type of valve cannot readily be extrapolated to another.

Therefore, the focus of this dissertation is to compare the pulse duplication findings between the tested valves to the echocardiography derived findings when performing pulse duplication.

CHAPTER 3

METHODOLOGY

The objectives for this research study were two-fold. The first objective was to perform a comparison of the results of prosthetic heart valve testing using pulse duplication and echocardiography together on a pulse duplicator. Secondly, to determine the overall performance of various prosthetic heart valves using pulse duplication.

3.1 STUDY LOCATION AND MATERIAL

Comprehensive pulse duplication and echocardiographic analysis were performed on three (3) commercial valves, the Glycar valve and the ViVitro reference valve using the ViVitro pulse duplicator (ViVitro Laboratories Incorporated, British Columbia, Canada) within the department of Cardiothoracic Surgery, Faculty of Health Sciences, University of the Free State (UFS), Bloemfontein, South Africa. Data acquisition and interpretation was done with the help of a mechanical engineer.

The echocardiography analysis was done with the help of an anaesthesiologist, cardiology technologist and a paediatric cardiologist, all from the Faculty of Health Sciences, UFS, Bloemfontein, South Africa.

Pulse duplication analysis and echocardiography was performed and compared on the following prosthetic heart valves:

- i) Commercial available valves:*
 - 21 mm Carbomedics bi-leaflet (Sorin Medical)
 - 21 mm Medtronic-Hall tilting disk valve (Medtronic Medical)
 - 19 mm Perimount tissue valve (Edwards-Life Sciences Corporation)

- ii) Other*
 - 21 mm Glycar valve
 - 21 mm ViVitro non-tilting disc valve (ViVitro Labs Inc.) (reference valve)

The 19 mm Perimount tissue valve was used because the valve was donated, thus limiting project costs.

3.2 STUDY DESIGN AND LAYOUT

The study design was a prospective analytical study. The study layout is summarized in Figure 3.1. A hydrodynamic evaluation was performed on each of the five (5) prosthetic heart valves using pulse duplication and echocardiography. All the valves were inserted in the aortic position in the pulse duplicator and echocardiographic measurements was performed through the viewing chambers of the pulse duplicator. The study concludes with a comparison between the acquired pulse duplication and echocardiographic data.

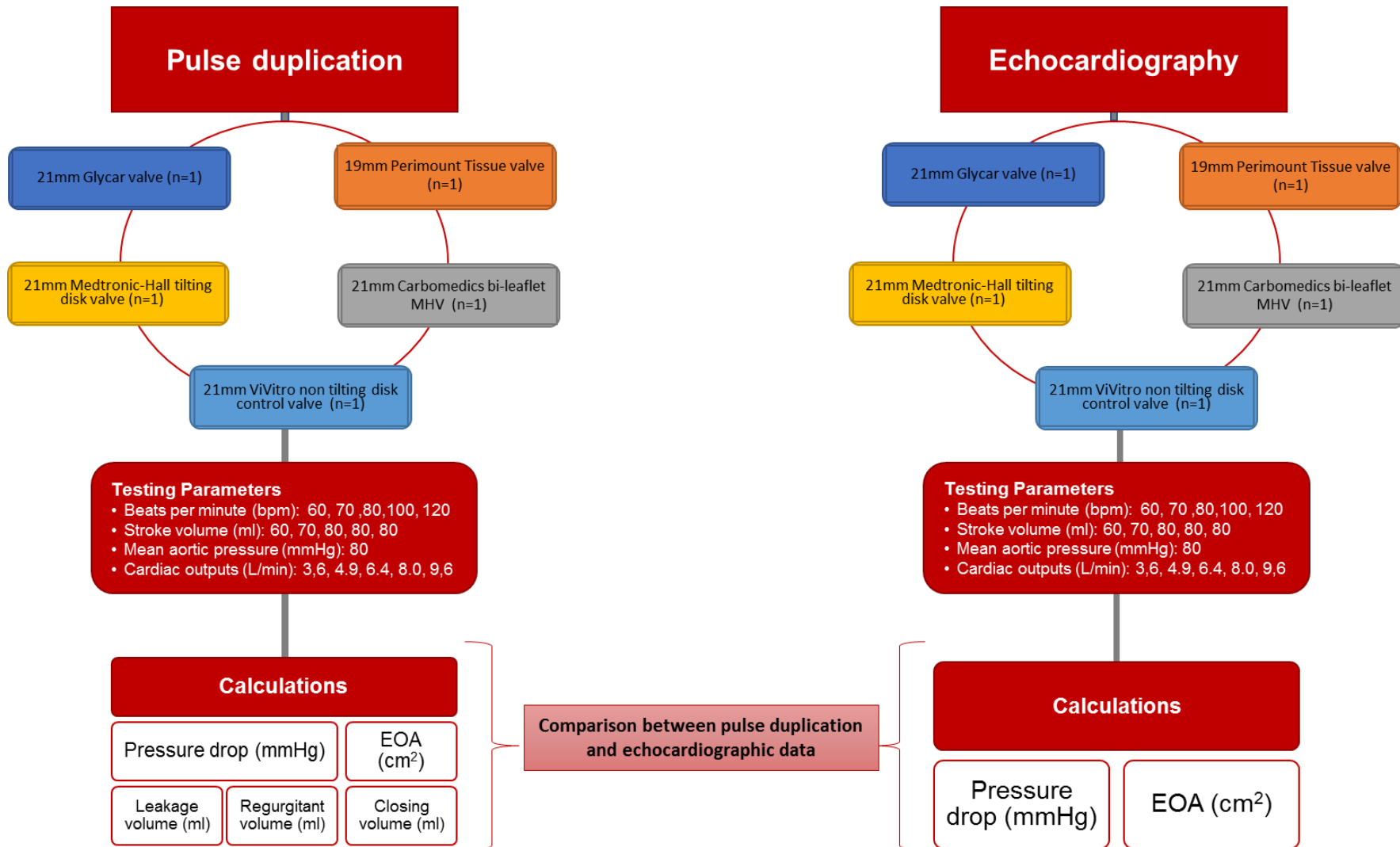


Figure 3.1: The *in vitro* evaluation of the flow dynamics of five prosthetic heart valves using pulse duplication and echocardiography.

3.3 HYDRODYNAMIC EVALUATION OF PROSTHETIC HEART VALVES

3.3.1 Pulse duplication

The pulse duplicator used for hydrodynamic testing simulates cardiac conditions to provide detailed information on flow characteristics and cardiac performance. The test chambers simulate the geometry of the left ventricle and the aorta to simulate realistic physiological flows. Each valve was tested under five different physiological test conditions.

3.3.1.1 Pulse duplicator apparatus and testing method

The ViVibro pulse duplicator system (ViVibro Labs Inc., British Columbia, Canada) in combination with the ViVitest data acquisition system (ViVibro labs Inc.) were used to assess the hydrodynamic performance and flow characteristics of the valves (Figure 3.2). This system is used for the evaluation of cardiovascular implants and is validated according to the ISO 5840:2005 guidelines and requirements.

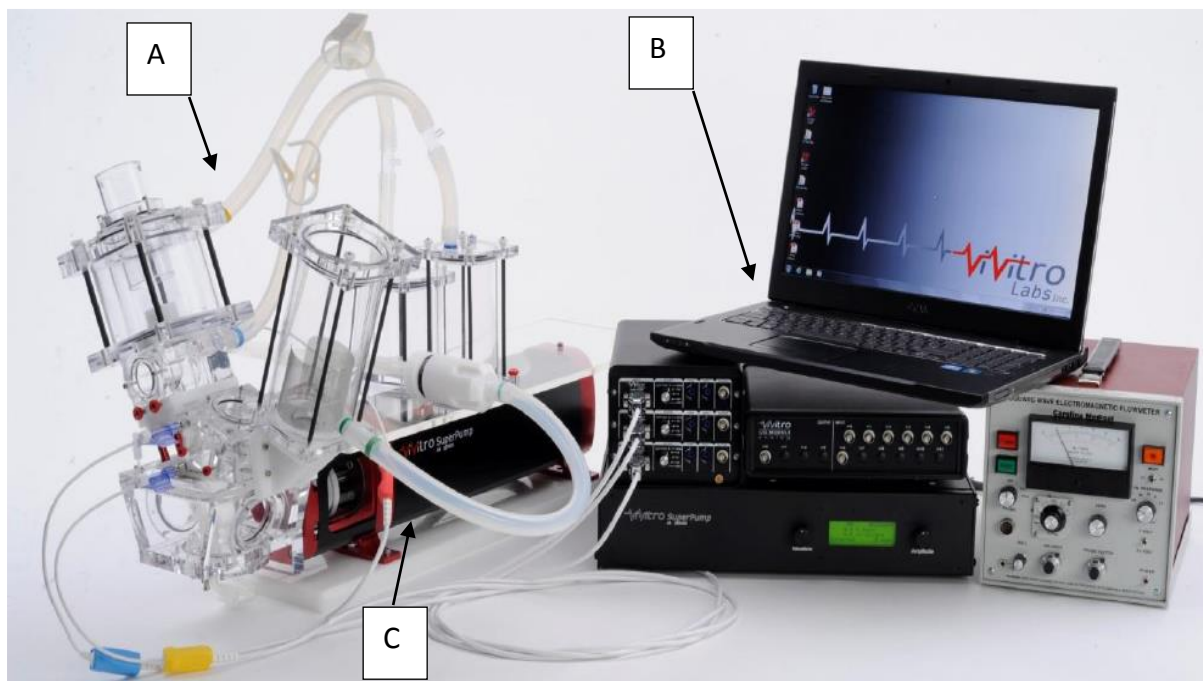


Figure 3.2: ViVibro pulse duplicator and ViVitest data acquisition system. (A) ViVibro pulse duplicator system (B) ViVitest data acquisition system (C) ViVibro Superpump(adapted from: <http://vivitrolabs.com/product/pulse-duplicator/>)

The system mimics a pneumatically actuated, left heart model that includes; a mitral valve, aortic valve, left atrium, left ventricle, aorta with systemic resistance, aortic compliance and aortic root compliance chambers. Ventricular pressure is generated via the ViVITro SuperPump.

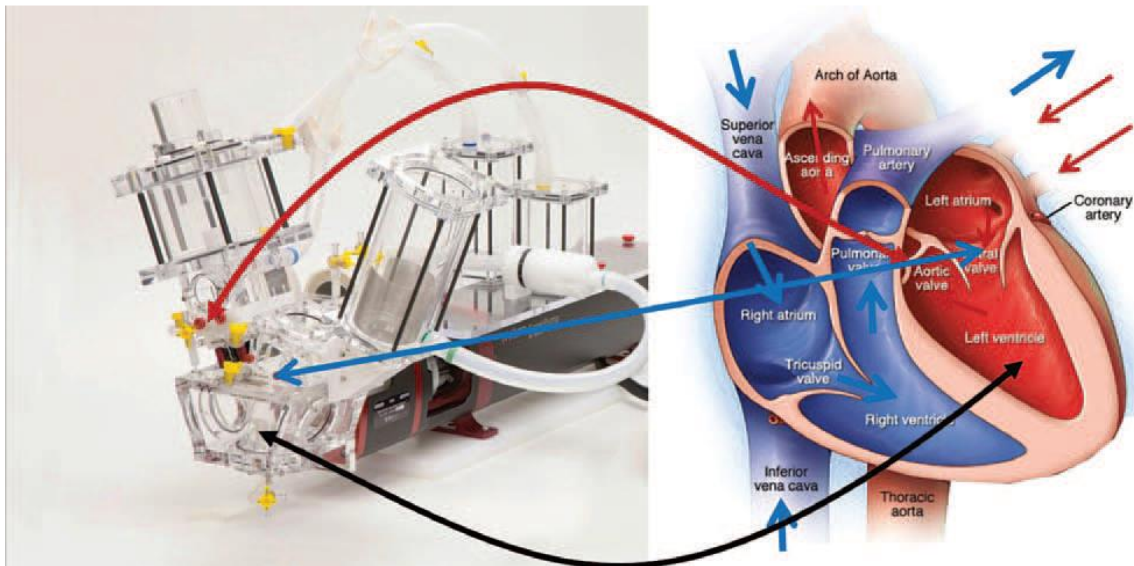


Figure 3.3: The ViVITro Pulse duplication system mimicking the human heart (adapted from <http://vivitrolabs.com/wp-content/uploads/2016/02/Pulse-Duplicator-Brochure-2016-VIVI-MKT-046.pdf>)

Summarized pulse duplication testing procedure

The test method was performed according to the standard operating procedure published in the ViVITro operating manual (ViVITro.com). The five (5) prosthetic heart valves were all evaluated in the aortic position. To eliminate regurgitation and possible para-valvular leaks the valves were secured in the aortic position using a compression container and sealing ring.

The pulse duplicator was calibrated by a ViVITro technician prior to use, which included the SuperPump, electromagnetic flow meter and pressure transducers. The electromagnetic flow meter was calibrated by an oscillating column of fluid in the aortic chamber by means of the pump, according to the ViVITro user manual. The recording instrumentation was switched on at least 30 minutes prior to testing to allow the flow meter and pressure transducers to stabilise. The zero position was set immediately prior to testing of the flow and pressure signals to minimise drift.

Pressure transducers are situated at the outflow tract distal to the aortic valve and in the ventricle chamber to measure the mean pressure gradients. The volumetric flow rate was recorded by an ultrasonic flow meter situated between the ventricle and the prosthetic valve. A blood analogue (ISO 5840:2015) of 45% by weight aqueous glycerine solution was added to the saline solution to create a viscosity of 3.5 centipoise (cps). The mean arterial pressure (MAP) was maintained at 80 mmHg and the stroke volume, pump beats (beats per minute) and cardiac output were varied according to Table 3.1.

According to Table 3.1, the stroke volume and beats per minute (BPM) was set using the programmable waveform generator and the mean arterial pressure was kept at 80mmHg by adjusting the afterload. The capturing of 10 cycles was performed when the flow conditions reached a stable point at the desired testing flow condition. During the 10 cycles, the pulse duplicator takes 256 measurements per cycle that was referred to as a sample. The start of a measurement was at the beginning of systole (beginning of the forward flow pump phase). The flow/pressure/volume graphs as illustrated in Figure 3.10 were then generated.

Table 3.1: Physiological testing conditions used during pulse duplication

Test Condition	Mean Aortic Pressure (mmHg)	Beats per minute	Stroke volume (ml)	Cardiac output (L/min)
1. Resting state	80	60	60	3.6
2. Low cardiac output	80	70	70	4.9
3. High cardiac output	80	80	80	6.4
4. Exercise	80	100	80	8.0
5. Maximum effort	80	120	80	9.6

(mmHg = millimetre mercury; ml = millilitre; L/min = litre per minute)

As outlined by ISO 5840:2015 arterial pressure, ventricular pressure and aortic pressure were measured at specific points throughout the cycle. The following flow and pressure data were recorded and calculated by the ViVitest data acquisition system:

- Pressure drop (Δp) (mmHg)
- Effective Orifice Area (EOA) (cm²)
- Regurgitant Fraction (RF) (%)

- Volumetric flow rate (ml/s)
- Closing volume (ml)
- Leakage volume (ml/s)

3.3.1.2 Calculation of pulse duplication parameters

i) Pressure drop (ΔP)

In order to calculate the average pressure drop, the positive pressure interval, where the ventricle pressure is higher than the aortic pressure, is determined. The average pressure was then calculated over the positive pressure interval. To determine the pressure drop across the valve the following were employed (Figure 3.5 to Figure 3.7).

The cardiac cycle is represented by the pressure generated in the ventricle (Figure 3.54) and the aorta (Figure 3.5) and the difference between the two pressure graphs (ventricle – aortic pressure) was generated to produce Figure 3.6 from the 256 sample values obtained per cycle. Using the graph in Figure 3.6, the point at which the trans-aortic pressure became positive was used as the starting point (point 1 in the graph) and ended as soon as the pressure dropped below zero (point 2). This was employed in all the 25 tests (5 valves at 5 test conditions) in this study.

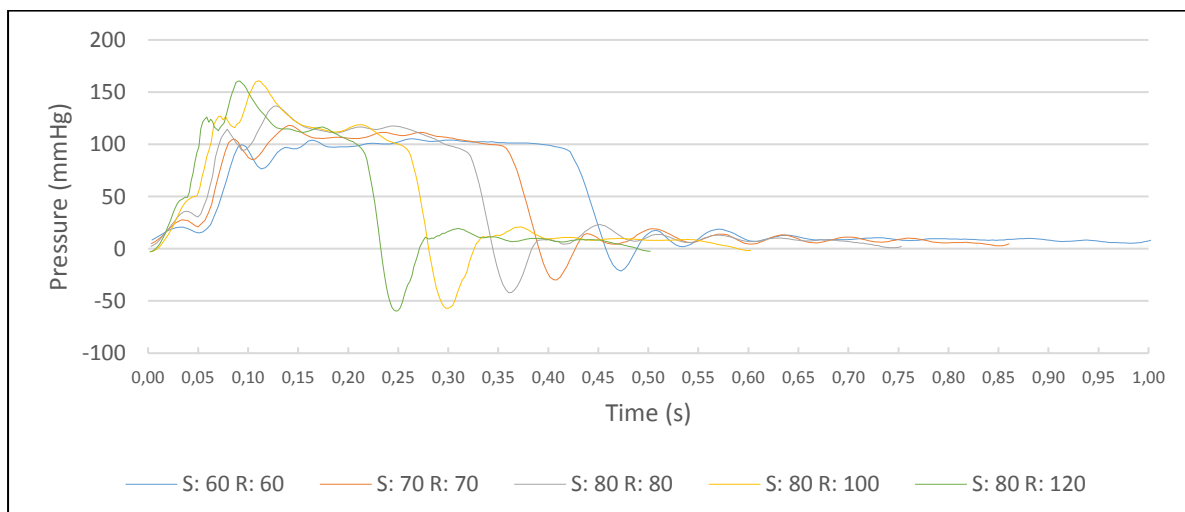


Figure 3.4: The ventricle pressure measured for the bi-leaflet valve over time during a cardiac cycle under the five test conditions [S:60 R:60 = CO of 3.6 L/min; S70: R70 = CO of 4.9 L/min; S80: R80 = CO of 6.4 L/min; S80:R100 = CO of 8.0 L/min; S:80: R120 = CO 9.6 L/min]

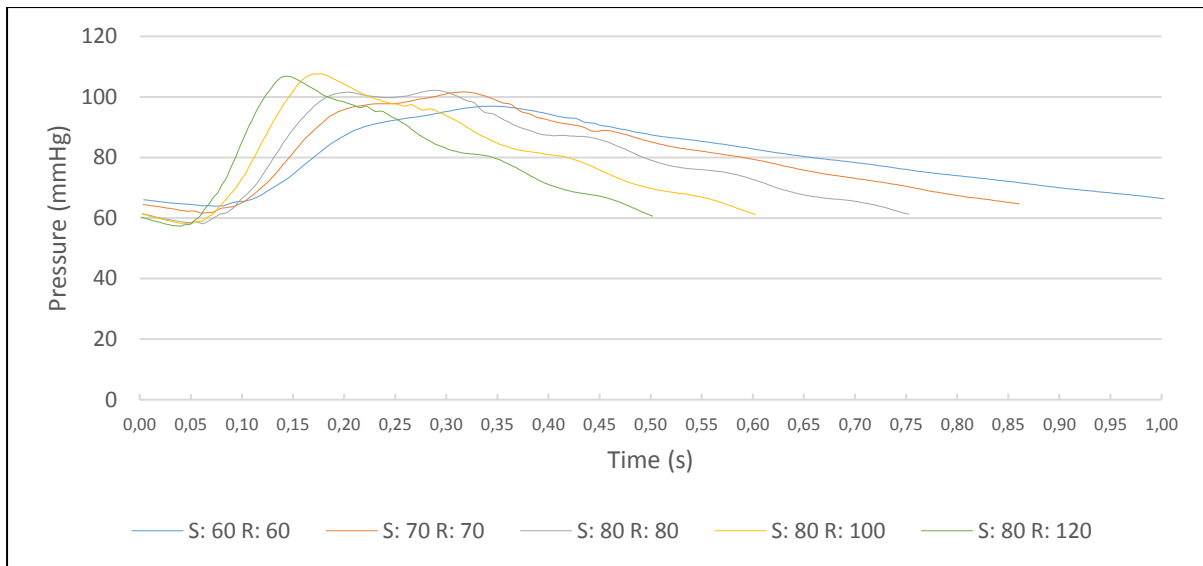


Figure 3.5: The aortic pressure measured for the bi-leaflet valve over time during a cardiac cycle under the five test conditions [S:60 R:60 = CO of 3.6 L/min; S70: R70 = CO of 4.9 L/min; S80: R80 = CO of 6.4 L/min; S80:R100 = CO of 8.0 L/min; S:80: R120 = CO 9.6 L/min]

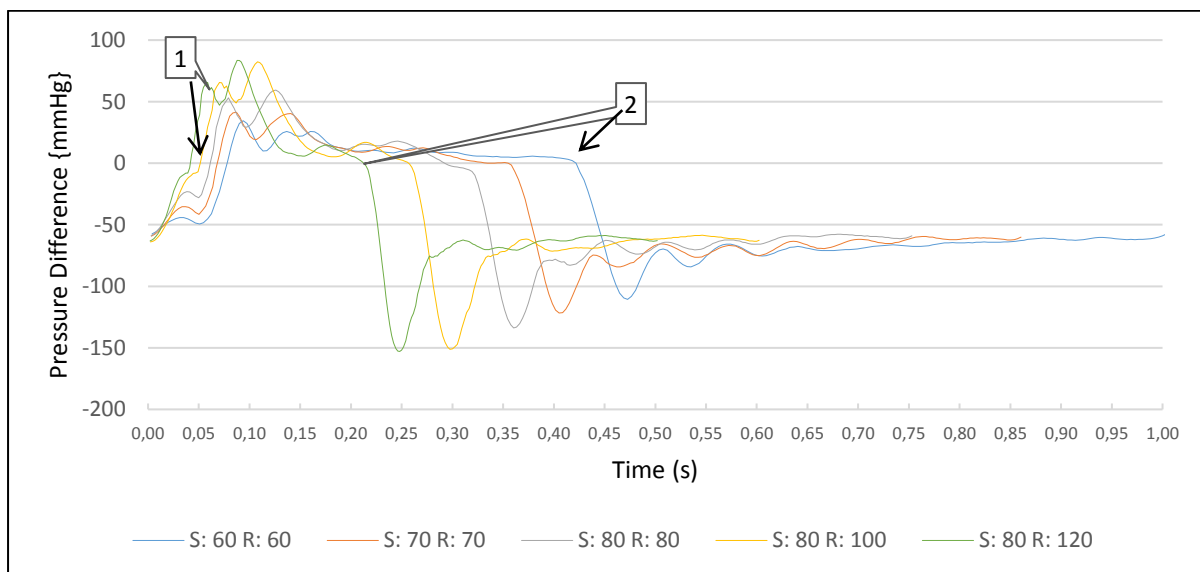


Figure 3.6: The pressure difference between the pressure generated across the valve (Figure 3.5) and the pressure generated in the aorta. The pressure gradient or drop is determined between points 1 and 2. [S:60 R:60 = CO of 3.6 L/min; S70: R70 = CO of 4.9 L/min; S80: R80 = CO of 6.4 L/min; S80:R100 = CO of 8.0 L/min; S:80: R120 = CO 9.6 L/min]

ii) Effective Orifice Area (EOA)

The effective orifice area (EOA) was calculated in accordance with ISO 5840 guidelines (ISO 5840:2015). The EOA is a measure of how easily fluid can flow through the valve based on the flow rate and pressure drop across the valve. The Q_{rms} and average pressure drop are used to determine the EOA.

$$EOA(cm^2) = \frac{Q_{rms}}{51.6 \sqrt{\frac{\Delta p}{\rho}}}$$

Where:

- Q_{rms} (ml/s)** The root mean square of the volumetric flow rate during the positive transvalvular pressure period.
- Δp [mmHg]** The mean systolic pressure difference during the positive transvalvular pressure drop period.
- ρ [g/cm³]** The fluid density.

The Q_{rms} was determined according to the ISO 5840 guidelines (ISO 5840:2015). The Q_{rms} and pressure gradient was measured during the interval shown in Figure 3.7. The time interval starts as soon as the pressure gradient becomes positive during the upstroke and ends when the pressure gradient becomes negative at the down stroke. This period is shown when line 2 is above line 1 in Figure 3.7.

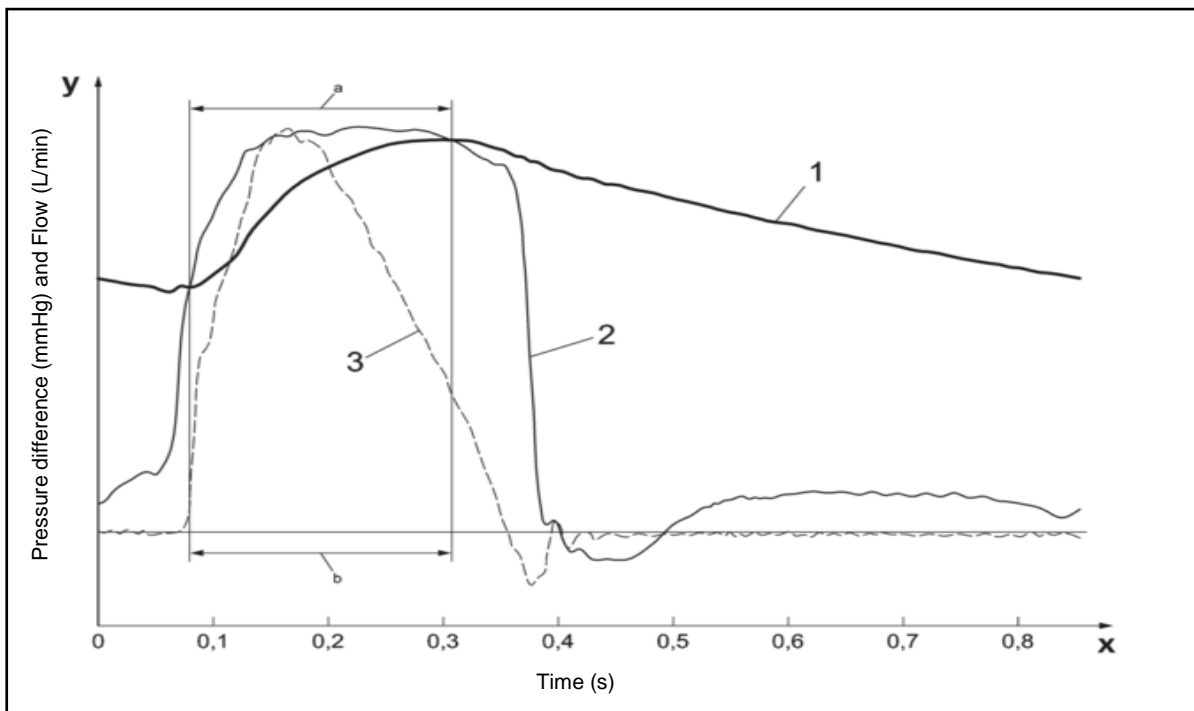


Figure 3.7: Schematic representation of the positive pressure period of an aortic forward flow interval. X-axis represents time in seconds, Y-axis the pressure difference in mmHg and flow in L/min. Line 1 represents the aortic pressure, and Line 2 represents the pressure generated in the left ventricle and Line 3 the Aortic flow rate (adapted from ISO 5840:2015 Part 1)

The Q_{rms} is calculated according the equation below and is defined as(ISO 5840:2005):

$$Q_{rms} = \sqrt{\frac{\int_{t_1}^{t_2} q_v(t)^2 dt}{t_2 - t_1}}$$

Where:

Q_{rms} (ml/s) The root mean square forward flow during the positive differential pressure period in ml/s.

$q_v(t)$ The instantaneous volumetric flow at time t.

t1 The time at the start of the positive differential pressure period.

t2 The time at the end of the positive differential pressure period.

iii) Regurgitant fraction (RF)

The regurgitant fraction was determined according to the ISO 5840:2015 guidelines, which details the differentiation between closure and leakage volume. The sum of regurgitation was analysed in total volume and in percent of the total stroke volume (percentage regurgitation). An example of the volumetric flow rate vs time across the valve over the cardiac cycle is shown in Figure 3.8, where arrow 1 indicates the closing volume and arrow 2 indicates the leakage volume.

In order to calculate the closing volume, the total volume of fluid during is calculated by calculating the area under the graph in region 1 and 2 in Figure 3.8. The volume is determined by

$$Volume = \int_{t_1}^{t_2} Q dt$$

where Q is the volumetric flow rate and t_1 and t_2 are the intervals for either volume 1 or volume 2 (Figure 3.8). The point of differentiation between the closing and leakage volume is when the volumetric flow rate gradient transitions from a positive gradient to a negative gradient after a negative flow rate has occurred. Closing volume is the total volume from the zero flow to the transition point, and the leakage volume is the total volume from the transition point to the end of the cycle.

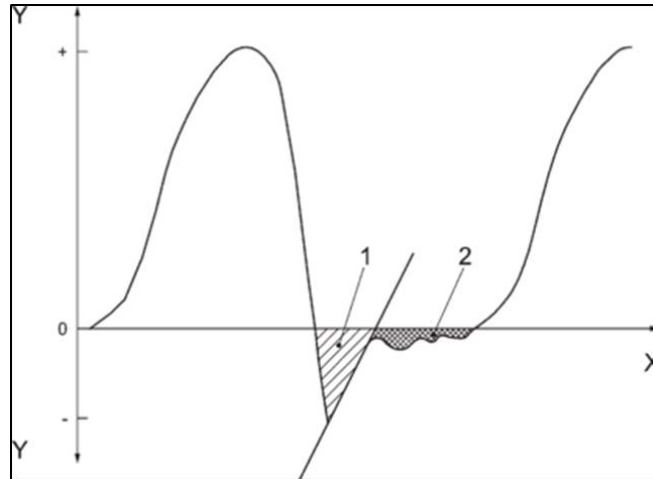


Figure 3.8: The flow wave form and regurgitant volumes for one cycle, with the volumetric change rate (Y-axis) in relation to time (X-axis). Using this graph, the regurgitant fraction is calculated. The closing volume (1) and the leakage volume (2) is determined once the volumetric rate drops below the zero-reference point (Adapted from Kuettinga *et al.*, 2014, ISO 5840:2015 Part 1)

3.3.2 Echocardiography

With the use of high pitched sound waves the echocardiogram creates images providing diagnostic information about the heart's chambers, valves, walls and blood vessels (flow) attached to the heart.

The ViVitro pulse duplication system is equipped with thin acrylic windows that permit echocardiography imaging and Doppler flow measurements during pulse duplication. Each valve was tested under five different physiological conditions (Table 3.1) and simultaneously the valvular characteristics of each valve was captured using echocardiography.

3.3.2.1 Echocardiography apparatus and testing method

Echocardiography was performed by a cardiac technologist in consultation with a paediatric cardiologist and cardiothoracic surgeon (Figure 3.9). The ViVid Q (General Electric, GE) echocardiographic system was used and all images were digitally captured and processed using the EchoPAC software package. An S10 transducer was used and conductivity was ensured by the use of ultrasound-gel (Kendon Medical Supplies Pty. Ltd., Johannesburg, South Africa).

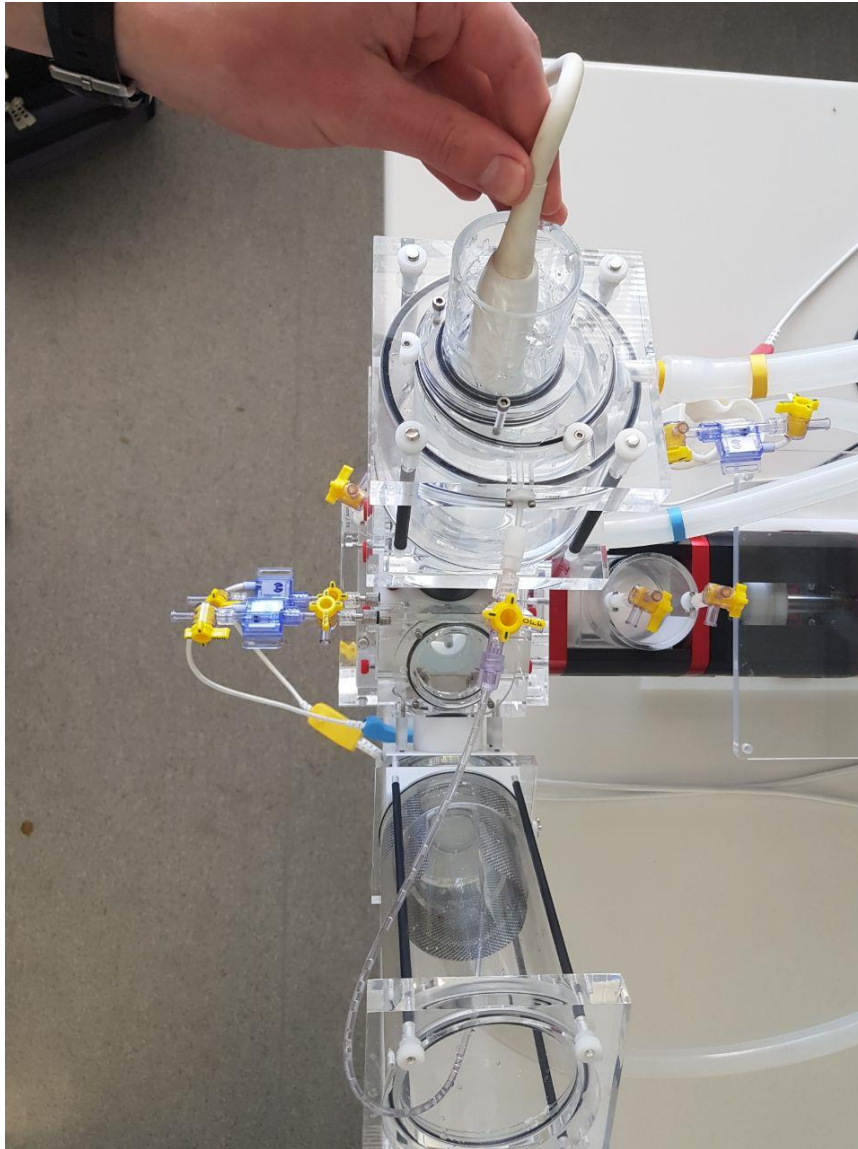


Figure 3.9: Echocardiography performed during pulse duplication

Summarized testing procedure

The flow characteristics of the five (5) prosthetic heart valves were performed consecutively while performing the pulse duplication analysis. All valves were secured in the aortic position.

The echocardiographic viewing chamber is situated perpendicular to the valve. The S10 transducer was fixed at 11cm between the valve and the tip of the transducer at an angle of 90 degrees to the valve. The imaging depth of the GE ViVid Q echocardiography machine was set at 15-16 cm. The blood analogue used contained glycerol that improved image quality.

Two-dimensional echocardiography was applied to position the m-line correctly for doppler tracings for the determination of left ventricular dimensions and volumes. Conventional Doppler (continuous wave) and colour Doppler techniques were used for the assessment of the prosthetic valves.

Doppler values were recorded and an average for 5 sequential beats was calculated. All doppler and 2D measurements were repeated 5 times during the same echocardiographic examination and the results averaged.

The following flow and hemodynamic parameters were recorded for each prosthetic valve tested:

- Maximum velocity (Vmax) (m/s)
- Mean velocity (Vmean) (m/s)
- Maximum pressure (Pmax) (mmHg)
- Mean pressure (Pmean) (mmHg)
- Envelope time (Env. Ti) (ms)
- Velocity time integral (VTI) (cm)
- Effective Orifice Area (EOA) (cm²)

3.3.2.2 Calculation of Doppler echocardiography parameters

i. Peak and mean pressure gradient

The simplified Bernoulli equation ($\Delta P = 4v^2$) was used to calculate the transaortic peak and mean gradients from transaortic velocities. This equation accepts that the velocity proximal to the valve is lower than 1 m/s and can be ignored, while transvalvular flow is at least 4 times the proximal flow. The peak gradient was calculated from peak velocity ($\Delta P_{max} = 4v^2_{max}$). The mean gradient was calculated by integrating the gradient over the entire systole ($\Delta P_{mean} = \Sigma 4v^2 / N$). When the proximal velocity is >1.5 m/s, or the aortic velocity is <3 m/s, the proximal velocity should be included in the Bernoulli equation ($\Delta P_{max} = 4(v^2_{max} - v^2_{proximal})$). All commercially available ultrasound machines provide the peak and mean gradients after manual tracing of transaortic CW Doppler spectrum. Transaortic jet velocities

as well as pressure gradient are flow-dependent measures of aortic stenosis severity. During low cardiac output states (e.g. severe left ventricular systolic dysfunction), transaortic velocities and gradients may be relatively low despite the presence of severe aortic stenosis (Baumgartner, 2009).

ii. The continuity equation

The continuity equation states that the flow in the first area must equal the flow in a second area if there are no shunts in-between the two areas. In other words, the flow through the left ventricular outflow tract (LVOT) equals the flow through the (stenotic) aortic valve. The aortic valve area was calculated using the continuity equation after other three variables (cross-sectional area of LVOT and velocity time integrals (VTI) in LVOT and across the aortic valve) are obtained by Doppler echocardiography (Baumgartner, 2009).

The flow through the LVOT (i.e. stroke volume at the level of LVOT), was calculated by multiplying cross-sectional area by the VTI of the LVOT. Cross-sectional area of LVOT was calculated as follow: $CSA (LVOT) = \pi (LVOT \text{ diameter}/2)^2$.

In doing so, it was easy to calculate the aortic valve area (AVA) by dividing the LV stroke volume by the AV VTI:

$$AVA [cm^2] = (LVOT \text{ CSA} \times LVOT \text{ VTI}) / AV \text{ VTI}$$

(Baumgartner, 2009).

CHAPTER 4

RESULTS & DISCUSSION

4.1 INTRODUCTION

In this chapter the hydrodynamic results of five (5) prosthetic heart valves, measured by pulse duplication and echocardiography will be presented, followed by a comparison between the prosthetic valve pulse duplication results and the echocardiography results.

The heart valves that displayed comparative parameters between echocardiography and pulse duplication were analysed further and the data presented.

4.2 PULSE DUPLICATION RESULTS OF THE FIVE (5) PROSTHETIC HEART VALVES

The pulse duplication hydrodynamic test results for all five (5) prosthetic heart valves at each test condition is given in Table 4.1.

Table 4.1: Hydrodynamic pulse duplicator and echocardiographic results for the prosthetic heart valves per test condition

		Pulse Duplication: 60 BPM 60 SV					Pulse Duplication: 70 BPM 70 SV					Pulse Duplication: 80 BPM 80 SV					Pulse Duplication: 100 BPM 80 SV					Pulse Duplication: 120 BPM 80 SV				
		Glycar	Tissue	Bileaflet	Tilting	Vivitro	Glycar	Tissue	Bileaflet	Tilting	Vivitro	Glycar	Tissue	Bileaflet	Tilting	Vivitro	Glycar	Tissue	Bileaflet	Tilting	Vivitro	Glycar	Tissue	Bileaflet	Tilting	Vivitro
Pulse Duplication	Pressure Drop	17.150	8.242	6.650	4.692	11.001	22.567	13.922	14.168	18.632	25.043	29.686	22.115	24.478	27.684	44.214	34.908	29.105	36.514	37.534	64.657	45.605	32.586	48.181	53.111	82.655
	EOA	1.267	1.740	2.002	1.084	1.348	1.486	1.690	1.779	1.518	1.120	1.686	1.694	1.640	1.711	1.029	1.861	1.731	1.573	1.766	0.989	1.885	1.884	1.572	1.777	0.987
	Leakage Volume	2.209	14.599	0.015	2.638	0.226	3.525	17.087	0.066	7.286	0.230	3.706	13.206	0.628	3.483	0.153	3.286	12.250	1.608	4.810	0.731	4.113	9.686	1.994	5.332	3.083
	Closing Volume	3.694	0.560	0.416	0.606	0.397	4.846	0.717	0.624	1.856	1.281	4.989	0.686	0.789	1.862	1.729	6.889	0.852	0.890	2.590	2.988	5.520	5.384	0.739	2.322	2.573
	Regurgitation	9.84%	25.27%	0.72%	5.41%	1.04%	11.96%	25.44%	0.99%	13.06%	2.16%	10.87%	17.36%	1.77%	6.68%	2.35%	12.72%	16.38%	3.12%	9.25%	4.65%	12.04%	18.84%	3.42%	9.57%	7.07%
		Echo: 60 BPM 60 SV					Echo: 70 BPM 70 SV					Echo: 80 BPM 80 SV					Echo: 100 BPM 80 SV					Echo: 120 BPM 80 SV				
		Glycar	Tissue	Bileaflet	Tilting	Vivitro	Glycar	Tissue	Bileaflet	Tilting	Vivitro	Glycar	Tissue	Bileaflet	Tilting	Vivitro	Glycar	Tissue	Bileaflet	Tilting	Vivitro	Glycar	Tissue	Bileaflet	Tilting	Vivitro
Echo	EOA	0.52	0.85	0.82	0.60	0.74	0.41	0.76	0.72	0.47	0.83	0.53	0.79	0.74	0.49	0.95	0.54	0.91	0.74	0.54	0.65	0.39	1.03	0.85	0.56	0.74
	Vmax	1.85	2.49	2.58	1.31	3.27	2.31	3.22	3.93	2.44	4.59	2.71	4.60	4.98	3.53	6.12	3.88	5.16	5.85	4.95	4.60	4.52	6.18	6.69	5.65	6.18
	Vmean	0.89	1.32	1.40	0.84	1.52	1.15	1.74	2.15	1.49	2.16	1.40	2.35	2.63	1.97	3.06	2.16	2.53	3.17	2.77	2.68	2.51	2.96	3.96	3.25	3.52
	Pmax	13.66	24.79	22.67	6.84	42.81	21.34	41.38	61.84	23.89	84.45	29.46	84.52	99.36	49.91	150.02	60.16	106.46	137.14	97.98	84.78	81.76	152.96	179.39	127.95	152.80
	Pmean	4.46	9.30	10.46	3.30	14.39	7.38	16.30	24.93	10.93	28.58	10.59	30.02	37.40	20.06	54.17	25.05	36.56	55.14	39.98	36.73	32.00	53.58	83.25	54.74	65.40
	ENV TI	349.20	387.40	352.80	425.80	293.60	307.60	335.60	270.60	281.20	268.40	287.00	332.60	266.20	248.40	247.50	223.20	275.20	205.40	207.20	194.40	173.00	235.20	172.80	186.20	167.80
	VTI	31.04	51.11	49.46	35.72	44.52	35.48	58.54	58.04	41.66	57.98	40.02	78.28	69.80	49.04	75.70	48.18	69.58	65.32	57.08	51.98	43.44	69.46	68.32	60.26	58.94

BPM = beats per minute, SV = stroke volume, Bi-leaflet = mechanical Bi-leaflet valve, tilting = Medtronic-Hall tilting disk valve, EOA = effective orifice area, Echo = Echocardiography, V_{max} = maximum velocity, V_{mean} = mean velocity, P_{max} = Maximum pressure drop, P_{mean} = mean pressure drop, ENV TI = valve envelope time corresponding to the ejection time, VTI = velocity time integral

The following graphs represent the data reflected in Table 4.1 for each of the valves corresponding to each of the investigated parameters.

4.2.1 Pressure drop

The pressure drop for each valve at each test condition is shown in Figure 4.1. The Glycar valve had the largest pressure drop across the valve at the lowest CO (3.6 L/min) of 17.15 mmHg vs. ViVitro (11.0 mmHg), bi-leaflet (6.65 mmHg), tilting disk (4.69 mmHg) and tissue valve (8.24 mmHg). However, the pressure drop increased steadily and at a slower rate than the other four valves, resulting in a superior performance of the Glycar valve. The maximum pressure drop for the Glycar valve was lower at a CO of 9.6 L/min (45.61 mmHg) compared to the ViVitro (82.65 mmHg), bi-leaflet (48.18 mmHg) and tilting disk (53.11 mmHg) valves. The ViVitro valve had the greatest pressure drop across the valve except at a low CO of 3.6 L/min where the Glycar valve had a slightly larger pressure drop. The tissue valve performance was the best overall for all the CO's.

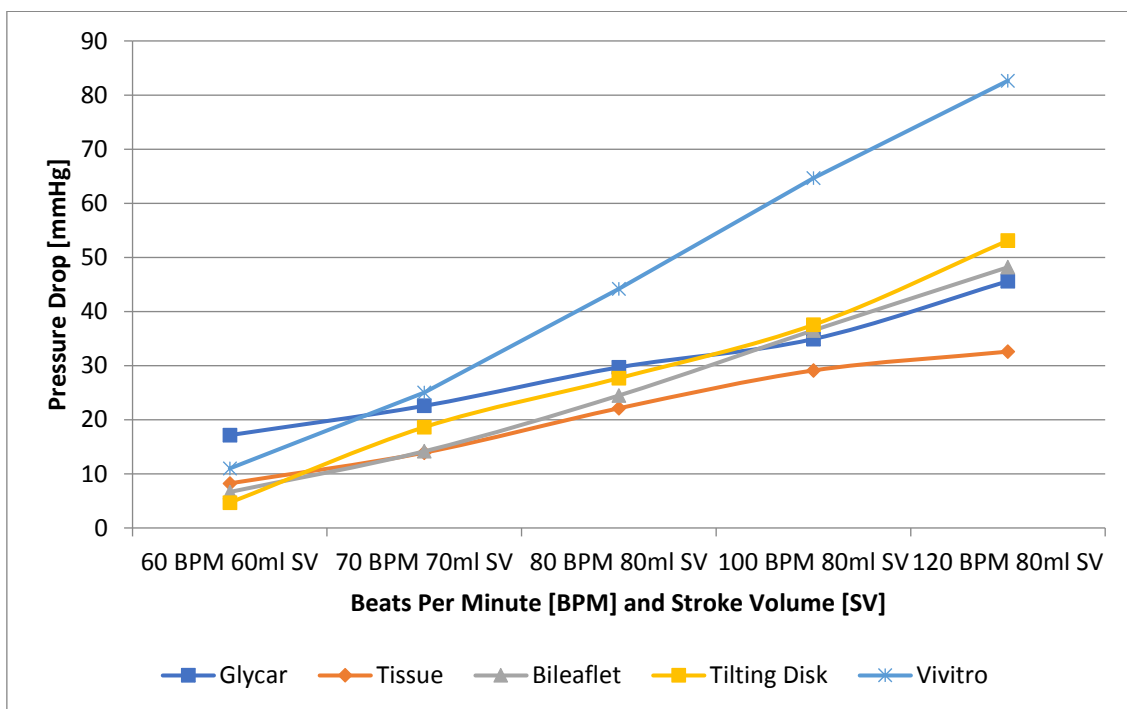


Figure 4.1: Pressure drop for each prosthetic valve per test condition [60 BPM 60ml SV = CO of 3.6 L/min; 70 BPM 70 ml SV = CO of 4.9 L/min; 80 BPM 80ml SV = CO of 6.4 L/min; 100 BPM 80 ml SV = CO of 8.0 L/min; 120 BPM 80 ml SV = CO of 9.6 L/min] (mmHg = millimetre mercury, BPM = beats per minute, SV = stroke volume)

4.2.2 Effective orifice area (EOA)

The EOA was calculated for each of the five valves and plotted against the different test conditions (Figure 4.2). The tissue valve was a 19 mm valve because the valve was sponsored.

The EOA of the ViVitro valve was lower than that of the other valves at 0.99 cm². The Glycar and tissue valve had the highest EOA of 1.885 cm² and 1.884 cm² respectively at a peak CO of 9.6 L/min, followed by the tilting disk and bi-leaflet valves at 1.77 and 1.57 cm² respectively.

The bi-leaflet valve had the highest EOA at 2.002 cm² (CO 3.6 L/min), however the EOA deteriorated as the CO increased to a low of 1.572 cm² at a CO of 9.6L/min.

All the valves performed well above the EOA requirement (0.85 for a 21mm valve) as stated in the ISO 5840:2015 standard.

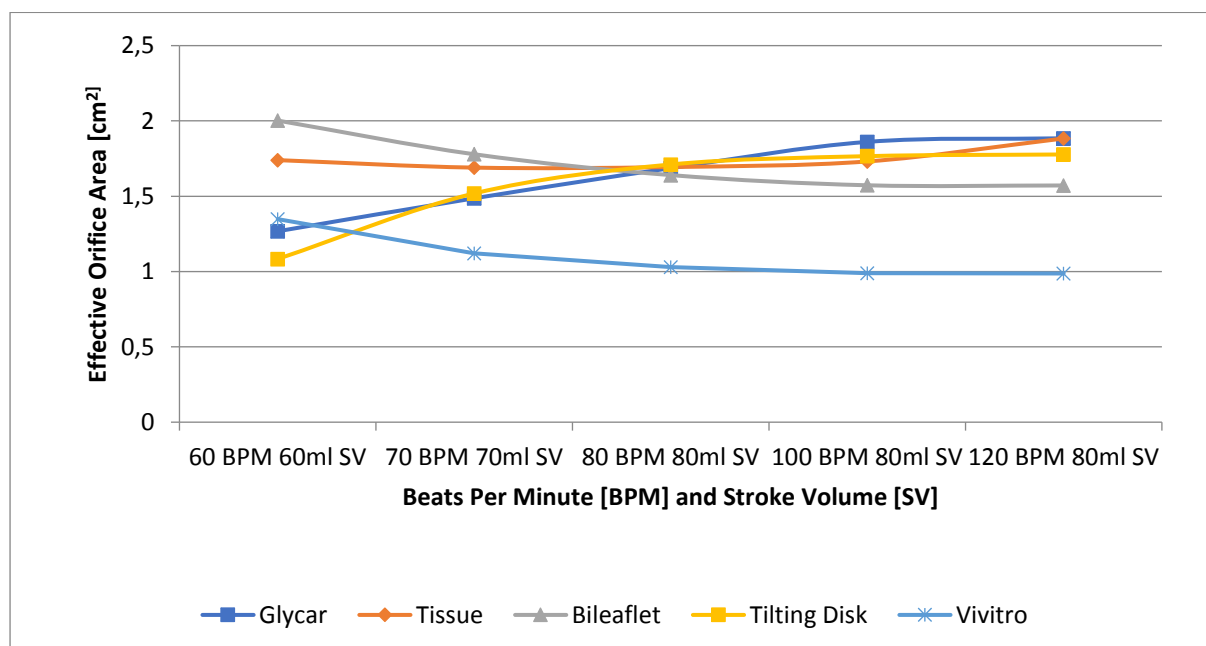


Figure 4.2: Pulse duplication: EOA and BPM:SV comparison between prosthetic heart valves per test condition [60 BPM 60ml SV = CO of 3.6 L/min; 70 BPM 70 ml SV = CO of 4.9 L/min; 80 BPM 80ml SV = CO of 6.4 L/min; 100 BPM 80 ml SV = CO of 8.0 L/min; 120 BPM 80 ml SV = CO of 9.6 L/min](cm² = square centimetre, BPM = beats per minute, SV = stroke volume)

4.2.3 Regurgitation fraction (RF)

The regurgitation fraction (RF), shown in Figure 4.3 is the combination of the closing and leakage volume as a percentage of the SV. The tissue valve had the largest RF for all test conditions, ranging from 16.3% (CO 8.0 L/min) to 25.6% (4.9 L/min). The bi-leaflet valve had the lowest RF (0.72% - 3.42%) followed by the ViVitro valve (1.04% - 7.07%), the tilting disk valve (5.41% -13.06%) and the Glycar valve (9.84% - 12.72%).

The RF is a combination of the closing volume and the leakage volume during the closed phase of a valve. As the closing mechanism of each of the valves may influence the RF, the individual volumes of the closing and leakage volumes were analysed independently (Figure 4.4-4.5).

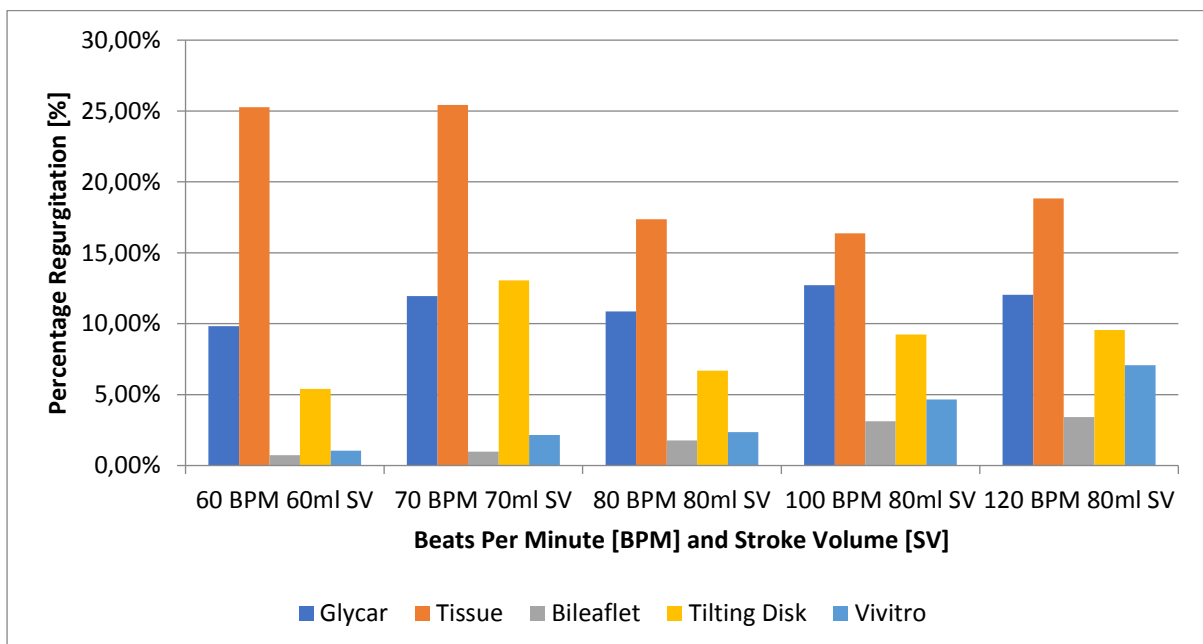


Figure 4.3: Pulse duplication percentage regurgitation comparison between prosthetic valves per test condition[60 BPM 60ml SV = CO of 3.6 L/min; 70 BPM 70 ml SV = CO of 4.9 L/min; 80 BPM 80ml SV = CO of 6.4 L/min; 100 BPM 80 ml SV = CO of 8.0 L/min; 120 BPM 80 ml SV = CO of 9.6 L/min](BPM = beats per minute, ml = millilitre, SV = stroke volume)

4.2.4 Closing volume

The closing volumes for each valve during each test condition is shown in Figure 4.4. The closing mechanics of the Glycar valve differs from the other valves, resulting in a significantly higher closing volume ranging from a minimum of 3.69 mL at a CO of 3.6 L/min, to a maximum of 6.89 mL at a CO of 8 L/min. The tissue valve had acceptable closing volumes during all testing conditions of 0.56 – 0.85 ml, however a sharp increase in the closing volume was measured as the CO was increased from 8 L/min (0.85 ml) to 9.6 L/min (5.84 ml).

The bi-leaflet valve closing volume ranged from 0.42 – 0.89 ml, the tilting disk valve 0.61 – 2.59 ml and the ViVitro valve 0.39 – 2.99 ml.

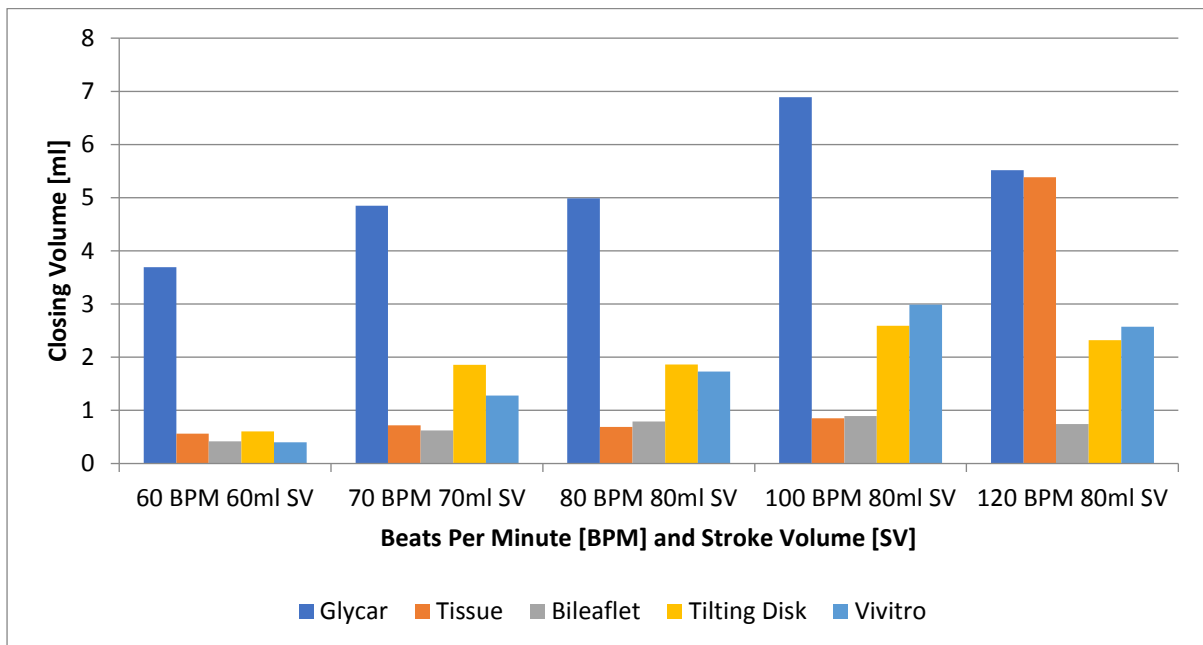


Figure 4.4: Pulse duplication closing volume comparison between prosthetic valves per test condition [60 BPM 60ml SV = CO of 3.6 L/min; 70 BPM 70 ml SV = CO of 4.9 L/min; 80 BPM 80ml SV = CO of 6.4 L/min; 100 BPM 80 ml SV = CO of 8.0 L/min; 120 BPM 80 ml SV = CO of 9.6 L/min](ml = millilitre, BPM = beats per minute, ml = millilitre, SV = stroke volume)

4.2.5 Leakage volume

The leakage volume per beat for each valve at each test condition is shown in Figure 4.5. The leakage volume of the tissue valve was responsible for the excessive RF measured during each of the test conditions ranging from 9.6 ml (CO 9.6 L/min) to 17 ml (CO 4.9 L/min). The Glycar valve had a lower leakage volume (2-4 ml) than its closing volume (3.6-5.5 ml), as well as having a lower leakage volume than the tissue and tilting disk valves (2.7-7.3 ml). The ViVitro and bi-leaflet valves had minor amounts of leakage at 0.15–3.08 ml and 0.015 to 1.99 ml respectively, which increased slightly at larger CO, however the leakage volume remained minimal.

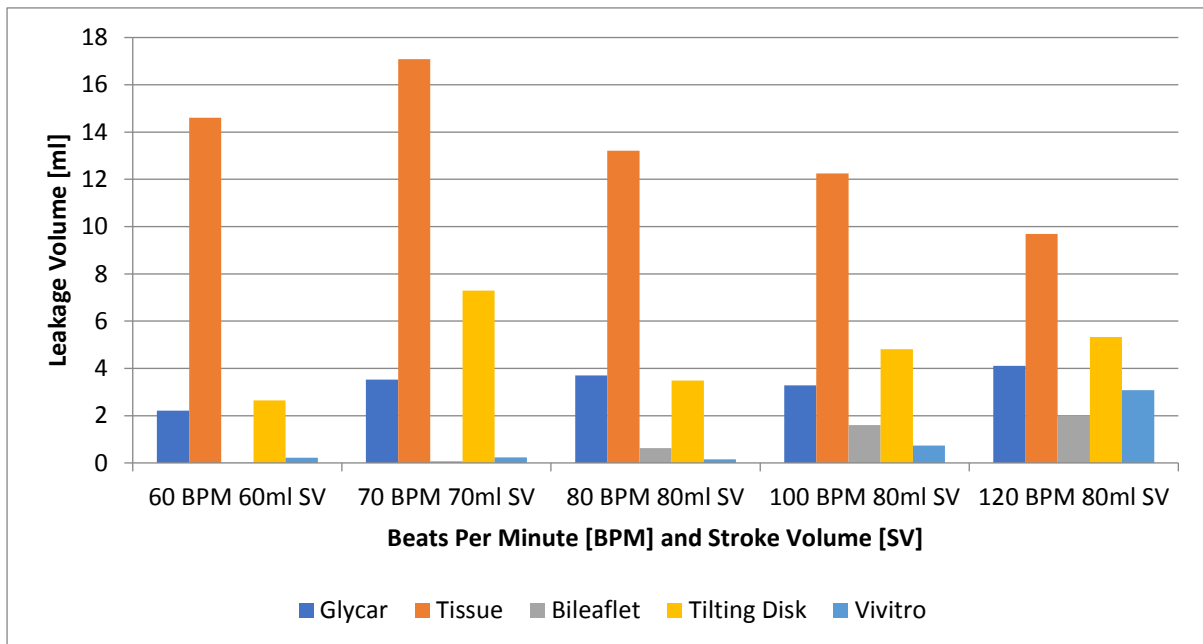


Figure 4.5: Pulse duplication leakage volume comparison between prosthetic valves per test condition [60 BPM 60ml SV = CO of 3.6 L/min; 70 BPM 70 ml SV = CO of 4.9 L/min; 80 BPM 80ml SV = CO of 6.4 L/min; 100 BPM 80 ml SV = CO of 8.0 L/min; 120 BPM 80 ml SV = CO of 9.6 L/min](ml/s = millilitre per second, BPM = beats per minute, ml = millilitre, SV = stroke volume)

4.3 ECHOCARDIOGRAPHIC RESULTS OF THE FIVE (5) PROSTHETIC HEART VALVES

The testing conditions for the echocardiography tests were performed at the same test conditions as the pulse duplication and the results recorded simultaneously on the pulse duplicator. The EOA and mean pressure difference provide the performance of the valve with echocardiography.

4.3.1 Pressure drop

The pressure drop determined from echocardiography is shown in Figure 4.6. All valves apart from the ViVitro valve show a consistent increase in the pressure drop for a corresponding increase in CO. The pressure drop decreased at a CO of 8 L/min for the ViVitro valve with recovery at 9.6 L/min. The Glycar valve had the lowest overall pressure drop for a CO from 4.9 L/min (4.46 mmHg) to 9.6 L/min (32 mmHg).

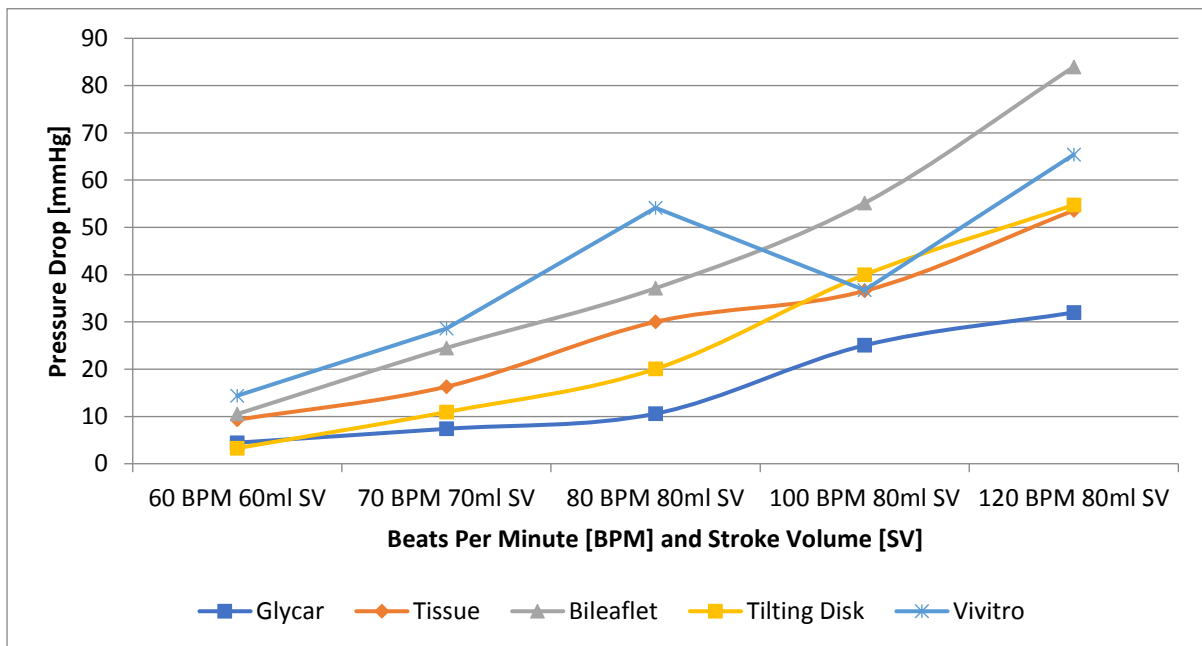


Figure 4.6: Echocardiography measured pressure drop comparison between prosthetic valves per test condition [60 BPM 60ml SV = CO of 3.6 L/min; 70 BPM 70 ml SV = CO of 4.9 L/min; 80 BPM 80ml SV = CO of 6.4 L/min; 100 BPM 80 ml SV = CO of 8.0 L/min; 120 BPM 80 ml SV = CO of 9.6 L/min](mmHg = millimetre mercury, BPM = beats per minute, SV = stroke volume)

4.3.2 Percentage difference: pressure drop

The percentage difference between the pulse duplication and echocardiography pressure drop is shown in Figure 4.7. A positive value in Figure 4.7 indicates that the pulse duplication value is greater than the echocardiography value. The tissue and bi-leaflet valves' pressure drop measured echocardiographically differs from the pulse duplicator between 11.4% and 42.26% throughout the testing conditions and showed the highest consistency. The tilting disk, bi-leaflet and Glycar valves exhibit large fluctuations when comparing the pulse duplication and echocardiography pressure drop, resulting in minimal correlation between the two measurements.

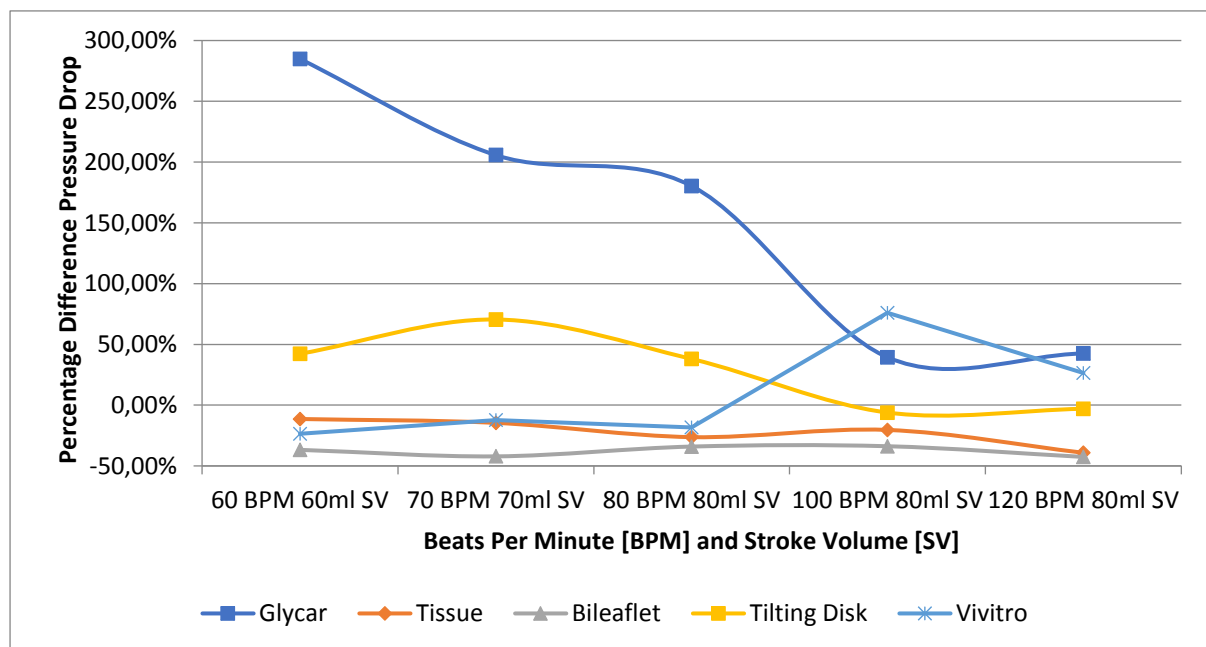


Figure 4.7: Echocardiography percentage pressure drop comparison between prosthetic valves per test condition[60 BPM 60ml SV = CO of 3.6 L/min; 70 BPM 70 ml SV = CO of 4.9 L/min; 80 BPM 80ml SV = CO of 6.4 L/min; 100 BPM 80 ml SV = CO of 8.0 L/min; 120 BPM 80 ml SV = CO of 9.6 L/min](BPM = beats per minute, SV = stroke volume, ml = millilitre)

The pressure drop for the bi-leaflet and tissue valve for both pulse duplication and echocardiography is shown in Figure 4.8. There is a correlation between the pulse duplicator and echocardiography results, however the values do not match exactly. The largest error recorded for both valves is 42.26%, with the echo over-estimating the pulse duplicator pressure drop. Therefore, the pulse duplicator pressure performance of the valve was better than that measured echocardiographically on the pulse duplicator.

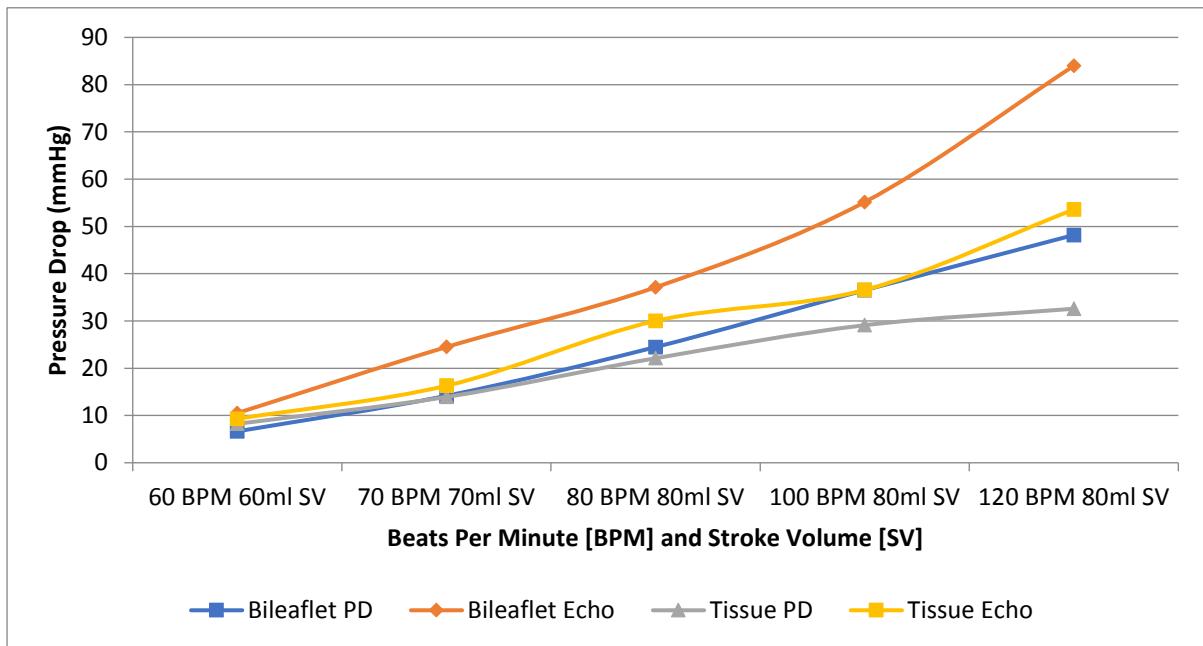


Figure 4.8: Echocardiography vs. pulse duplication pressure drop for bi-leaflet and tissue valve per test condition [60 BPM 60ml SV = CO of 3.6 L/min; 70 BPM 70 ml SV = CO of 4.9 L/min; 80 BPM 80ml SV = CO of 6.4 L/min; 100 BPM 80 ml SV = CO of 8.0 L/min; 120 BPM 80 ml SV = CO of 9.6 L/min] (mmHg = millimetre mercury, BPM = beats per minute, ml = millilitre, SV = stroke volume)

4.3.3 Effective orifice area (EOA)

The EOA measured echocardiographically for each of the five valves is shown in Figure 4.9. The bi-leaflet and Glycar valves EOA showed better consistency across the CO range than the ViVitro, tissue and tilting disk valves. The ViVitro valve EOA dropped drastically at a CO of 8 L/min, similar to the sudden pressure drop of the ViVitro valve.

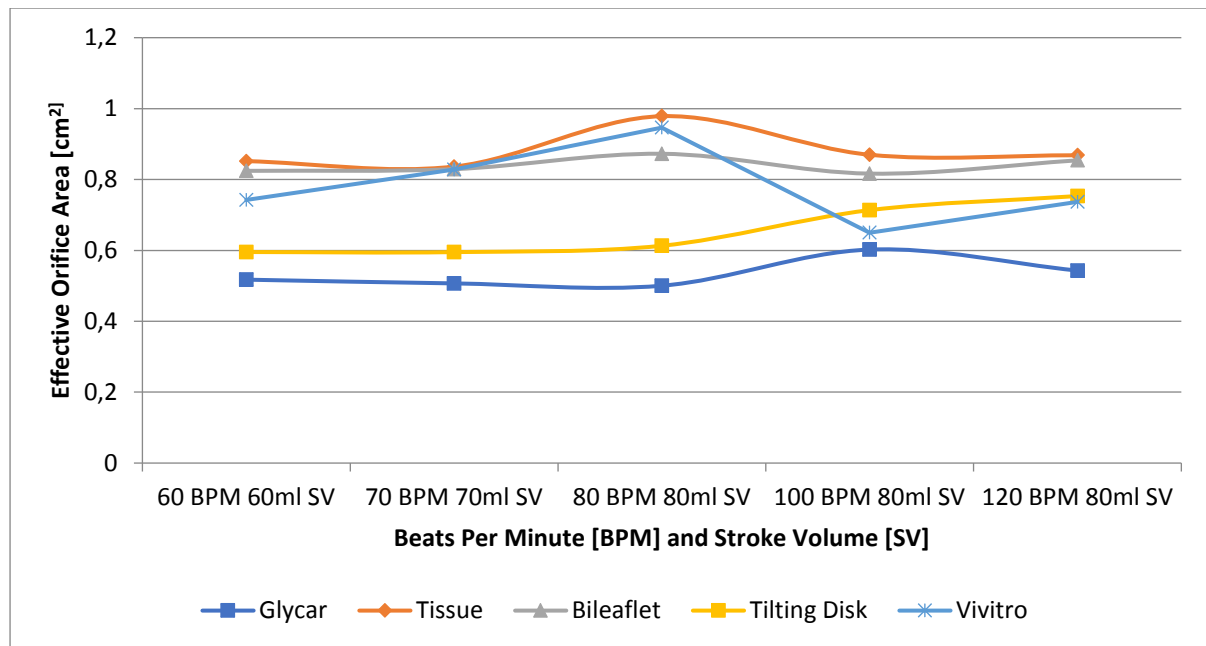


Figure 4.9: Echocardiography EOA comparison between prosthetic valves per test condition [60 BPM 60ml SV = CO of 3.6 L/min; 70 BPM 70 ml SV = CO of 4.9 L/min; 80 BPM 80ml SV = CO of 6.4 L/min; 100 BPM 80 ml SV = CO of 8.0 L/min; 120 BPM 80 ml SV = CO of 9.6 L/min](cm²millimetre square centimetre, BPM = beats per minute, SV = stroke volume)

4.3.4 Percentage difference of EOA

The percentage difference of the EOA between the pulse duplicator and echocardiography is given in Figure 4.10. All valves exhibit minimal correlation between the pulse duplication and echocardiography, with the difference ranging from 8.75% to 247.1% for all valves over all five CO conditions. The EOA percentage difference of the tissue valve ranges from 73.1% to 116.9%, whilst the bi-leaflet ranges from 84.0% to 142.9%. The EOA error is much larger than the pressure drop error for the tissue and bi-leaflet valves.

According to the data no definite correlation occurs between the echocardiography and the pulse duplicator data for the EOA. There is a correlation of the pressure drop between the pulse duplicator and echocardiography for the tissue and bi-leaflet valve.

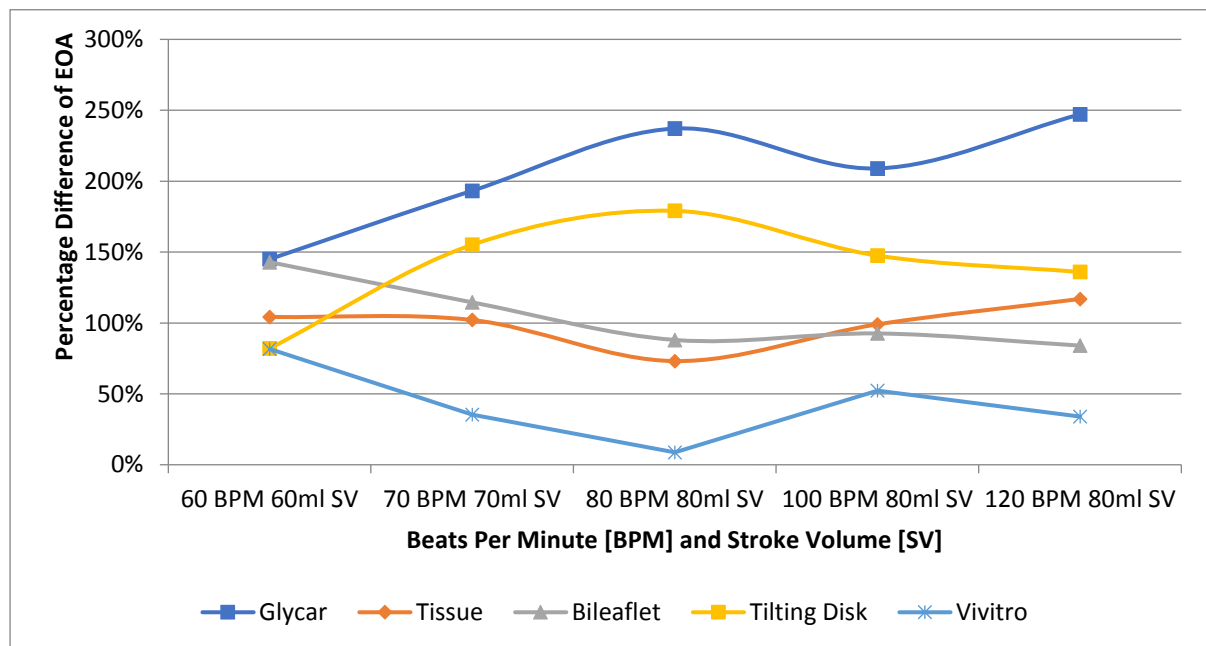


Figure 4.10: Echocardiography percentage difference in EOA comparison between prosthetic valves per test condition [60 BPM 60ml SV = CO of 3.6 L/min; 70 BPM 70 ml SV = CO of 4.9 L/min; 80 BPM 80ml SV = CO of 6.4 L/min; 100 BPM 80 ml SV = CO of 8.0 L/min; 120 BPM 80 ml SV = CO of 9.6 L/min](BPM = beats per minute, SV = stroke volume)

4.4 DISCUSSION

4.4.1 Introduction

In this study, the pulse duplication data of five (5) valves were compared during five (5) test conditions. Pulse duplication data is rarely available in the literature and direct comparisons are therefore limited. In order to establish a pulse duplication program at our institution, the ViVitro valve supplied with the pulse duplicator as a reference valve was compared to three commercial valves, namely a bileaflet mechanical valve (Carbomedics bi-leaflet, Sorin medical), a tilting disc mechanical valve (Medtronic-Hall, Medtronic medical), and a tissue valve (Perimount, Edwards medical). Additionally, pulse duplication data of a re-engineered poppet valve (Glycar) was obtained. The data was analysed to obtain comparative data between the commercial valves. All of the data was analysed according to FDA and ISO standards.

This study looked at comparative data between echocardiography and pulse duplication data in the bench testing setting in order to evaluate the possible application in *in vivo* studies. This may have an application in valve evaluation and design situations where comparative data is available to extrapolate the performance of the valve *in vitro* to the performance of the valve *in vivo*. We therefore attempted to find a relationship between pulse duplication generated data and the findings of the echocardiography data.

4.4.2 Pulse duplication

4.4.2.1 Pressure Drop

The ViVitro valve exhibited the highest pressure drop across the valve. However, the ViVitro valve is not designed for implantation in humans but rather to test the pulse duplicator setup and is therefore used as a reference valve. The valve has a flat, un-aerodynamic disc occluder that result in higher energy loss across the valve, and therefore a higher pressure drop.

The mechanical bi-leaflet had a very high pressure drop at a CO of 3.6 L/min of 6.65 mmHg with a high of 48.18 mmHg and could be due to the geometric orifice size of the valve. The

21mm bi-leaflet valve has a cross-section diameter of 16.7mm across the widest diameter and 14.66mm in length from hinge to hinge (Figure 4.11).

Results found by Haaf *et al.* (2009) on a 20mm St. Jude Medical bi-leaflet valve had a pressure drop of 16.7 mmHg at 60 BPM and 73 ml SV. This is larger than the bi-leaflet valve used in this study with a pressure drop of 6.65mmHg and 14.16mmHg at 60 BPM 60 ml SV and 70 BPM 70 ml SV respectively. The difference could be due to a completely rigid setup used by Haaf *et al.* (2009) whereas the ViVitro pulse duplicator has compliance chambers to better mimic physiological conditions. Haaf *et al.* (2009) also showed a pressure drop of 17.9mmHg for a 20mm Hall-Kaster Tilting Disk Medtronic-Hall, compared to 4.69mmHg and 18.63mmHg at 60 BPM 60 ml SV and 70 BPM 70 ml SV respectively in this study.

Reul *et al.* (1993) performed pulse duplication on four different bi-leaflet valves with an annulus diameter of 27mm. All four valves had a pressure drop of less than 2mmHg at the lowest cardiac outputs, which may be attributed to the significantly larger valve.

The tissue valve outperformed all the other valves when referring to the pressure drop. As the CO increased the subsequent increase in the pressure drop was the lowest of all the valves and at a maximum CO of 9.6 L/min the pressure drop was only 32 mmHg (well below the other valves).



Figure 4.11: Bi-leaflet valve internal diameter measurement

The pressure drop across the Glycar valve was the largest at a CO of 3.6 L/min, however as the CO increased the increase of the pressure drop was lower compared to the bi-leaflet and tilting disk valves but greater than the tissue valve.

4.4.2.2 Effective orifice area (EOA)

The EOA provides an indication of the ease of a valve to allow fluid to flow through a valve by relating the root mean square of the flow rate with the pressure drop. Therefore, a larger EOA represents a better functioning valve and therefore a better valve design.

The EOA for the tissue, Glycar and tilting disk valves all increased with an increase in CO, showing much different behaviour to the performance of the bi-leaflet and ViVitro valves where the EOA decreased. The EOA tends to stabilise between a CO of 8L/min to 9.6L/min for all valves apart from the tissue valve where the valve has an increase in EOA.

It is interesting to note that even with an increase in pressure drop, the EOA still increased for the Glycar, tissue and tilting disk valves. By looking at the formula for the EOA, the EOA is influenced by the flow through the valve and the pressure drop. As the EOA increased for the Glycar, tissue and tilting disk valves, the ability of the fluid to flow through the valve was superior to the increase in the pressure drop. This is opposite what occurs in the bi-leaflet and ViVitro valves, where the much smaller diameter of the bi-leaflet valve, and the flat plate shape of the ViVitro valve, influence the fluid flow ability and pressure drop.

$$EOA = \frac{Q_{rms}}{51.6 \sqrt{\frac{\Delta P}{\rho}}} S \quad (\text{ISO 5840:2005})$$

However, even the ViVitro valve that have, in comparison to the other valves, a very poor performance, all of the tested valves performed well above the ISO 5840:2015 cut-off of 0.85 cm² for a 21-mm mechanical prosthetic heart valve as required for FDA and CE registration.

Haaf *et al.* (2009) reported on the EOA of prosthetic valves, however the values were obtained observationally by determining the orifice area of the valve at peak systole visually and not according to the current ISO and FDA requirements. The EOA was not reported by Reul *et al.* (1993).

4.4.2.3 Regurgitation fraction (RF)

The Glycar valve had a high RF and this can be ascribed to the poppet design of the valve. The closing volume of the valve (ranging from 3.7 mL to 6.9 mL) was the highest of all the valves but the leakage volume was very low, therefore resulting in a relatively high RF. There was also no direct relationship between the closing volume and the CO. The Glycar valve functions as a type of poppet, where the fluid that does not fully flow around the poppet during systole sits beneath the poppet as the flow rate becomes zero, and eventually flows back down at the start of diastole with the poppet. This behaviour was noted and confirmed through particle imaging velocimetry tests (Davis *et al.*, 2016 unpublished data), where the poppet moved with the same velocity as the fluid around it during closing. Once the poppet is seated on the housing the valve has minimal leakage.

The tissue valve on the other hand had a high RF due to a high leakage volume. As the CO increased the closing volume also increased contributing to the high RF at a high CO. As part of the tissue valve design a regurgitation of up to 10% is allowed. The large value of the tissue valve leakage volume was due to a paravalvular leak. Attempts were made to limit the expected leakage volume by creating a specific fitting to house the tissue valve, however the leakage volume still remained much larger than the closing volume due to excessive movement of the tissue valve inside the fitting, creating gaps for paravalvular leaks.

The RF of the bi-leaflet and ViVitro valve was extremely small due to the efficient sealing of the leaflets with the valve housing, resulting in extremely low leakage volumes. The thin leaflets of the bi-leaflet valve form a firm seal between the leaflets and the housing, where the spring-loaded plate of the ViVitro valve forms a quick and efficient seal, vastly improving on the leakage volume. The valve closing action is rapid and early during the first phase of valve closure resulting in very low closing volumes.

Haaf *et al.* (2009) reported the highest volume regurgitation on the Hall-Kaster Tilting Disk valve at 10.2ml and 8.5ml for the St. Jude bi-leaflet valve. The bi-leaflet valve had a total regurgitation volume of 0.4 and 0.69ml at 60 BPM 60 SV and 70 BPM 70 SV respectively, where the tilting disk valve had a total regurgitation volume of 3.2ml and 9.1ml at 60 BPM 60 SV and 70 BPM 70 SV, respectively.

Reul *et al.* (1993) showed that the RF varied greatly from a low CO to a high CO, ranging from 24% to 7.5% for CO from 3L/min to 8L/min. This observation is counter to that found in this study, where the RF increased for the bi-leaflet and ViVitro valves, and showed an increasing tendency for the Glycar and tilting disk valves, except for the RF at 70 BPM 70 SV.

4.4.3 Echocardiography

4.4.3.1 Pressure Drop

The echocardiographic results for the pressure drop showed a consistent rise for a corresponding increase in the CO, similar to that of the pulse duplicator, apart from the ViVitro valve at 8 L/min. However, by examining the percentage difference between the pulse duplicator and echocardiographic pressure drop (Figure 4.7) the Glycar, tilting disk and ViVitro valve showed no comparison. The difference in pressure drop between the pulse duplication and echocardiography varied by a minimum of 11.4% and a maximum of 42.26% in line with literature (Arabia *et al.*, 1989; Stewart *et al.*, 1991).

A further examination of the difference between the pulse duplicator and echocardiography was performed between the tissue and the bi-leaflet valves, with the results shown in Figure 4.8. There is an almost linear increase in the pressure difference between the echocardiography and pulse duplication results for the pressure drop. The correlation between pulse duplication and echocardiography is promising for the comparison of only specific valve data measured *in vivo*.

An evaluation of echocardiography and pulse duplication results of heart valves were performed by Johnston *et al.* (1992). However, the echocardiography was not performed on the pulse duplicator, but instead on resting patients. Johnston *et al.* (1992) reported a good correlation between the results obtained using pulse duplication and those obtained using echocardiography on patients.

4.4.3.2 Effective orifice area (EOA)

The results for the EOA measurements using echocardiography revealed relatively flat EOA values apart for the ViVitro valve, as also seen in the pulse duplication results. However, the magnitude of the EOA values are not equivalent. This is verified by examining the percentage difference of the pulse duplication and echocardiography for the EOA. The average difference between the pulse duplication and echocardiography EOA value for the tissue valve is approximately around 100% and showed the most consistency for all of the valves.

A potential reason for the inaccuracy of the echocardiography results in a pulse duplicator could be due to the setup with the continuous wave setting. The continuous wave projects the ultrasound in a line down the centre of the tube, through the centre of the valve as shown in Figure 4.12. For the tissue valve and bi-leaflet valve, it is possible for the continuous wave to go right through the centre of the valve, but without going through the valve itself. This is not possible for the ViVitro, tilting disk and Glycar valve.

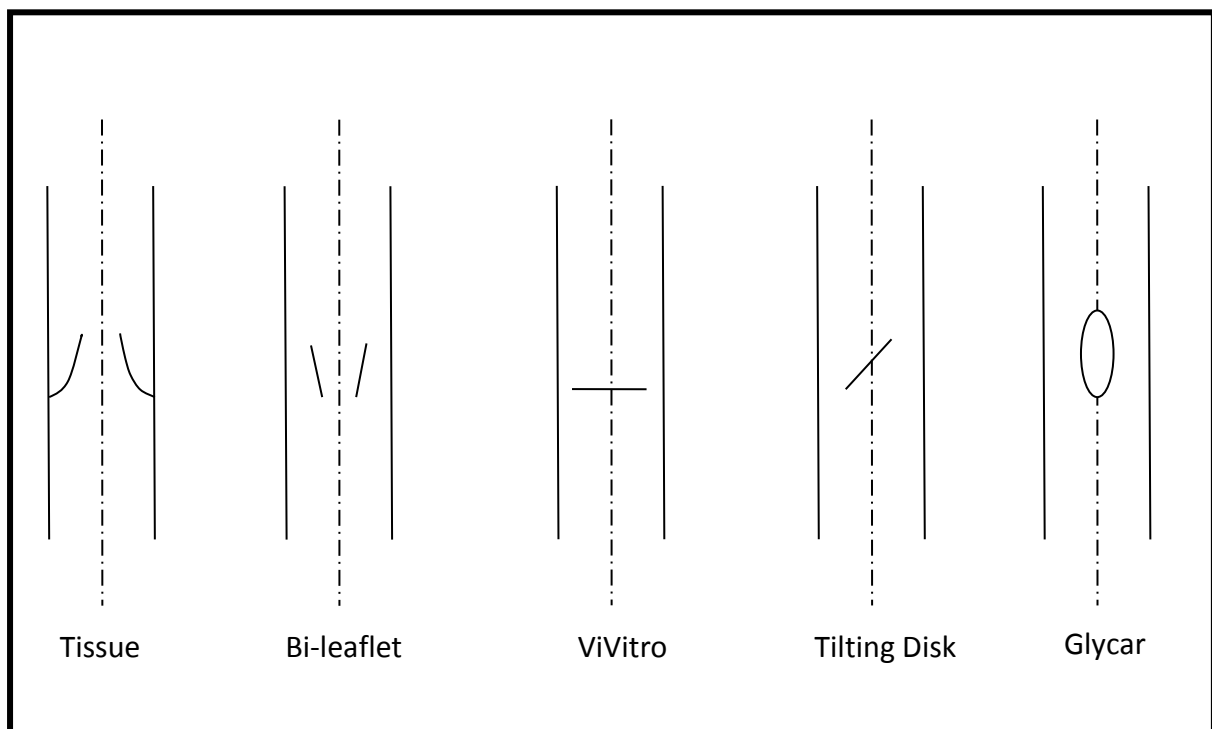


Figure 4.12 Echocardiographic continuous wave propagation through the five valves

CHAPTER 5

CONCLUSION

Heart valve surgery and valvular heart disease still pose a significant threat to patients worldwide. Pulse duplication is widely accepted as a valid method to determine the performance of heart valves during their development. Few specialised centres exist to perform pulse duplication tests accurately in accordance to the required ISO and FDA standards for cardiovascular implants. Real-time patient data of prosthetic heart valves is however not obtained with pulse duplication but with echocardiography. Modern day pulse duplicators come equipped with viewing chambers that can allow for echocardiographic measurements. The purpose of this study was to perform pulse duplication and echocardiography simultaneously on five (5) different prosthetic heart valves using a commercial ViVitro pulse duplicator.

The pulse duplication results show that all five (5) valves meet the ISO standard for the minimum EOA value of 0.85 for 21mm prosthetic aortic valves. The EOA relates the ability of fluid to flow through the valve by relating the volumetric flow rate to the pressure drop. The pressure drop is not an ISO requirement individually, as the pressure drop is included in the EOA calculation. The bi-leaflet, tilting disk and ViVitro valve all met the RF requirement of 10% for 21mm aortic valves, apart from the tilting disk at a CO of 4.9L/min. The RF of the Glycar valve was slightly larger (9.84% to 12.72%) than the minimum required 10% apart from at the lowest CO where the RF was 9.84%. The leakage volume for the Glycar valve was minimal, and the closing volume largely contributed to the RF. A possible reason for the higher closing volume was due to the function of the Glycar valve, which acts like a type of plunger, where the fluid beneath the poppet flows back into the ventricle at the start of diastole.

The tissue valve had significantly higher RF (16.38% to 25.44%) attributed to the leakage volume. The leakage volume was due to expected para-valvular leaks, to which new fittings

to house the tissue valve were made to address the leakage. The echocardiography pressure drop results were comparable with the pulse duplication data for the bi-leaflet and tissue valve only. The results differed between 11.4% and 42.26%, which is in line with published literature where the reported difference is no more than 50%. The EOA results from the echocardiography were not comparable to the pulse duplication data for any valve. We speculate that the shape of the valve influences the echocardiographic results, as the tilting disk, Glycar and ViVitro valves all have an obstruction in the continuous wave line when performing echocardiographic measurements.

To conclude, there is no absolute comparison between pulse duplication and echocardiographic measurements performed simultaneously on the same pulse duplicator. A comparison could only be made for the pressure drop of the bi-leaflet and tissue valve.

5.1 Limitations

Current limitations of the study are para-valvular leaks and operator dependant echocardiographic results. The leakage volume of the tissue valve was much higher than the other four valves. As the pulse duplicator has a silicon rubber clamped between the housing of the pulse duplicator, a fitting was manufactured to allow the tissue valve to fit into the silicon rubber. However, the leakage volume was still significant and a new design must be considered to reduce the para-valvular leak. The echocardiographic results were also highly user dependant, based on the angle of the transducer and distance from the valve. The test was setup to minimise the user dependant errors.

5.2 Recommendations

Further studies would be to redesign the echocardiographic viewing chambers to allow for measurements to be extracted perpendicular to the flow using pulse and continuous wave echocardiography. This could allow for measurements to be performed without any obstructions from the valve, however errors may be introduced with selecting measurement points for the pulse wave echocardiography and would require further investigation.

CHAPTER 6

REFERENCES

- ACC/AHA 2006 Guidelines for the Management of Patients With Valvular Heart Disease: Executive Summary: A Report of the American College of Cardiology/American Heart Association Task Force on Practice Guidelines (Writing Committee to Revise the 1998 Guidelines for the Management of Patients With Valvular Heart Disease): Developed in Collaboration With the Cardiovascular Angiography and Interventions and the Society of Thoracic Society of Cardiovascular Anaesthesiologists: Endorsed by the Society Cardiovascular Angiography and Interventions and the Society of Thoracic Surgeons. 2006. *Circulation*, 114: 450-537.
- Anavekar NS, Oh JK. 2009. Doppler echocardiography: A contemporary review. *Journal of Cardiology*, 54:347-358.
- Antunes MJ. 2015. Requiem for a good mechanical heart valve: Farewell to the Medtronic hall valve. *The Journal of Thoracic and Cardiovascular Surgery*, 149:1492-1494.
- Antunes MJ, Wessels A, Sadowski RG, Schutz JG, Vanderdonck KM, Oliveira JM. 1988. Medtronic-Hall valve replacement in a third-world population group: a review of the performance of 1000 prostheses. *Journal of Thoracic Cardiovascular Surgery*, 95:980-993.
- Arabia FA, Talbot TL, Stewart SFC, Nast EF, Clark RE. 1989. A computerized physiological pulse duplicator for *in vitro* hydrodynamic and ultrasonic studies of prosthetic heart valves. *Biomedical Instrumental and Technology*, 23:205-215.
- Babuška I, Banerjee U, Osborn E. 2004. Generalized Finite Element Methods: Main Ideas, Results, and Perspective. *International Journal of Computational Methods*, 1(1):67-103.

- Bach DS. 2003. Choice of prosthetic heart valve: update for the next generation. *Journal of the American College of Cardiology*, 42(10):1717-1719.
- Bach DS. 2010. Echo/Doppler evaluation of hemodynamics after aortic valve replacement: Principles of interrogation and evaluation of high gradients. *Journal of America College of Cardiollogy*,3:296-304.
- Baldwin TJ, Campbell A, Luck C, Ogilvie W, Sauter J. 1997. Fluid dynamics of the Carbomedics kinetic bi-leaflet prosthetic heart valve. *European Journal of Cardiothoracic Surgery*, 11:287-292.
- Baumgartner H, Hung J, Bermejo J, Chambers JB, Evangelista A, Griffin BP, Lung B, Otto CM, Pellikka PA, Quiñones M. 2009. Echocardiographic assessment of valve stenosis: EAE/ASE recommendations for clinical practice. *European Journal of Echocardiography*,10(1):1-25.
- Barannyk O, Karri Sand Oshkaio P. 2013. *In Vitro* Study of the Influence of the Aortic Root Geometry on Flow Characteristics of a Prosthetic Heart Valve. *The American Society of Mechanical Engineers*, 4:14-18.
- Barnard CN, Schrire V, Goosen CC. 1963. Total aortic replacement. *Lancet*, 2:856.
- Bazan O, Ortiz JP. 2016. Duration of asystole and diastole for hydrodynamic testing of prosthetic heart valves: comparison between ISO 5840 standards and in vivo studies. *Brazilian Journal of Cardiovascular Surgery*, 31(2):151-157.
- Bazan O, Ortiz JP. 2011a. Experimental validation of a cardiac simulator for *in vitro* evaluation of prosthetic heart valves. *Brazilian Journal of Cardiovascular Surgery*,31(2):197-204.
- Bazan O, Ortiz JP. 2011b. Design conception and experimental setup for *in vitro* evaluation of mitral prosthetic valves. *Brazilian Journal of Cardiovascular Surgery*, 26(2):1-9.

- Bazan O, Ortiz JP. 2011c. Design and construction of a new pulse duplicator system for *in vitro* evaluation of prosthetic heart valves – conception of an experimental setup in mitral position. *Brazilian Congress of Mechanical Engineering*, pp253-257.
- Bazan O, Ortiz JP. 2016. Experimental validation of a cardiac simulator for *in vitro* evaluation of prosthetic heart valves. *Brazilian Journal of Cardiovascular Surgery*,31(2): 151–157.
- Black MM, Drury PJ, Tindale WB. 1983. Twenty-five years of heart valve substitutes: a review. *The Royal Society of Medicine*, 76:667-680.
- Bellhouse BJ. 1972. Fluid mechanics of heart valves. *Cardiovascular Fluid Dynamics*, 6:261-285.
- Bernal JM, Rabassa JM, Gutierrez-Garcia F, Morales C, Nistal JF, Revuelta JM. 1998. The Carbomedics valve: experience with 1049 implants. *The Annals of Thoracic Surgery*, 65(1):137-143.
- Blauwet LA, Fletcher AM. 2014. Echocardiographic assessment of prosthetic heart valves. *Division of Cardiovascular Diseases*, 57:100-110.
- Buntz B. 2012. TAVR, still the next big thing in cardiology. *Medical Device and Diagnostic Industry*,59:253-263.
- Butany J, Fayet C, Ahluwalia MS, Blit P, Ahn C, Munroe C, Israel N, Cusimano RJ, Leask RL. 2003. Biological replacement heart valves identification and evaluation. *Cardiovascular Pathology*, 12:119-139.
- Butchart EG, Li HH, Payne N, Buchan K, Grunkemeier GL. 2001. Twenty years' experience with the Medtronic-Hall valve. *Journal of Thoracic Cardiovascular Surgery*,121:1090-1100.

- Cape EG, Sung HW, Yoganathan AP. 1996. Hemodynamic assessment of Carbomedics bi-leaflet heart valves by ultrasound: studies in the aortic and mitral position. *Ultrasound in Medicine*, 22(4):421-430.
- Chambers J, Fraser A, Lawford P, Nihoyannopoulos P, Simpson I. 1994. Echocardiography assessment of artificial heart valves: British Society of Echocardiography position paper. *British Heart Journal*, 71:6-14.
- Chambers J, Cross J, Deverall P, Sowton E. 1993. Echocardiographic description of the Carbomedics bi-leaflet prosthetic heart valve. *American College of Cardiology*, 21(2):398-405.
- Chandran KB. 2010. Role of computational simulations in heart valve dynamics and design of valvular prosthesis. *Cardiovascular Engineering and Technology*, 1(1):18-38.
- Chandran KB, Cabell GN, Khalighi B, Chen CJ. 1983. Laser anemometry measurements of pulsatile flow past aortic-valve prosthesis. *Journal of Biomechanics*, 16:865-873.
- Chandran KB, Fatemi R, Hiratzka LF, Harris C. 1986. Effect of wedging on the flow characteristics past tilting disc aortic valve prosthesis. *Journal of Biomechanics*, 19(3):181-186.
- Chandran KB, Schoepfoerster R, Dellsperger KC. 1989. Effect of prosthetic mitral valve geometry and orientation on flow dynamics in a model human left ventricle. *Journal of Biomechanics*, 22(1):51-57, 59-65.
- Chandran KB, Yoganathan AP, Rittgers SE. 2007. *Biofluid Mechanics: The Human Circulation*. 1st edition. CRC Press, Taylor & Francis Group; pp. 277–314.
- Cleland J and Molly PJ. 1973. Thrombo-embolic complications of the cloth-covered Starr-Edwards prostheses No.2300 aortic and No 6300 mitral. *Thorax*, 28: 41-47.

- Cox JL, Meyers K, Gharib M, Quijano RC. 2005. Tubular heart valves: A new tissue prosthesis design – Preclinical evaluation of the 3F aortic bioprosthesis. *Journal of Thoracic Cardiovascular Surgery*, 130:250-257.
- Cribier A. 2012. Development of transcatheter aortic valve implantation (TAVI): 20-year-old odyssey. *Archives of Cardiovascular Diseases*, 105(3):146-152.
- Dangas GD, Weitz JI, Giustino G, Makkar R, Mehran R. 2016. Prosthetic heart valve prosthesis. *Journal of the American College of Cardiology*, 68(24):958.
- Dasi LP, Simon HA, Sucosky P, Yoganathan AP. 2009. Fluid mechanics of artificial heart valves. *Clinical Expo Pharmacology and Physiology*, 36(2):225-237.
- Dasi LP, Simon GL, Sotiropoulos F, Yoganathan AP. 2007. Vorticity dynamics of a bi-leaflet mechanical heart valve in an axisymmetric aorta. *Physics and Fluids*, 19:105-117.
- Davis K, Jordaan CJ, Thompson-Jooste L, Botes L, Frater RWM, Smit FE. 2016. Comparing the hemodynamics of a re-engineered poppet valve to a Bi-leaflet aorta valve. Department of Cardiothoracic Surgery, University of the Free state, Bloemfontein (unpublished data).
- De Gaetano F, Serrani M, Bagnoli P, Brubert J, Stasiak J, Moggridge GD, Costantino ML. 2015. Fluid dynamic characterization of a polymeric heart valve prototype (Poli-Valve) tested under continuous and pulsatile flow conditions. *International Journal of Artificial Organs*, 38(11):600–606.
- De Paulis R, Schmitz C, Scaffa R, Nardi P, Chiariello L. 2005. *In vitro* evaluation of aortic valve prosthesis in a novel valved conduit with pseudosinuses of Valsalva. *The Journal of Thoracic and Cardiovascular Surgery*, 130:1016-1021.
- Dokainish H. 2006. Echocardiography. *Journal of American College of Cardiology*, 48:2053-2069.

- Durand LG, Carcia D, Sakr F, Sava H, Cimon R, Pibarot P, Fenster A, Dumesnil JG. 1999. A new flow model for Doppler ultrasound study of prosthetic heart valves. *The Journal of Heart Valve Disease*, 8:85-95.
- Dumont K, Vierendeels J, Kaminsky R, van Nooten G, Verdonck P, Bluestein D. 2007. Comparison of the hemodynamic and thrombogenic performance of two bi-leaflet mechanical heart valves using a CFD/FSI model. *Journal of Biomechanical Engineering*, 129(4):558-565.
- Edler I, Lindström K. 2004. The history of echocardiography. *Ultrasound Medical Biology*, 3:1565-1644.
- Falkovich G. 2011. Fluid Mechanics, a short course for physicists. 1st Edition. Cambridge University Press, pp.11-17.
- Fisher J, Jack GR, Wheatley DJ. 1986. Design of a function test apparatus for prosthetic heart valves. Initial results in the mitral position. *Clinical Physics and Physiology*, 7(1):63-73.
- Frater RWM, Salomon NW, Rainer WG, Cosgrove DM, Wickham E. 1992. The Carpentier-Edwards pericardial aortic valve: intermediate results. *Annals of Thoracic Surgery*, 53:764-771.
- Frater RWM. The UCT aortic valve used without anti-coagulants. *New York Surgical Clinics*, 1969.
- Fung YC. 1997. Biomechanics: Circulation. 2nd Edition, Springer-Verlag New York, pp.577.
- Goa G, Wu Y, Grunkemeier GL, Furnary AP, Starr A. 2004. Durability of pericardial versus aortic valves. *Journal of American College of Cardiology*, 44(2):384-388.

- Garcia D, Pibator P, Landry C. 2004. Estimation of aortic valve effective orifice area by Doppler echocardiography: effects of valve inflow shape and flow rate. *Journal of American Society*, 17:756-765.
- Gravlee GP, Davis RF, Stammers AH, Underleider RM. 2008. *Cardiopulmonary Bypass, Principles and Practice*. 3rd Edition. Lippencott Williams & Wilkins, a Wolters Kluwer business, pp. 686-689.
- Grigioni M, Daniele C, D'Avenio G, Mordivenio G, Morbiducci U, Del Gaudio C, Abbate M, Dimeo D. 2004. Innovative technologies for the assessment of cardiovascular devices: State of the art techniques for artificial heart valve testing. *Expert Revised Medical Devices Review*, 1:81-93.
- Grunkemeier GL, Anderson WN. 1998. Clinical evaluation and analysis of heart valve substitutes. *The Journal of Heart Valve Disease*, 7(2):163-169.
- Ghanbari H, Viatge H, Kidane AG, Burriesci G, Tavakoli M, Seifalian AM. 2009. Polymeric heart valves: new materials, emerging hopes. *Trends Biotechnology*, 27:359-367.
- Gott VL, Alejo DE, Cameron DE. 2003. Mechanical heart valves : 50 years of evolution. *Annals of Thoracic Surgery*, 76:S2230-2239.
- Jennings ML, Butterfield M, Walker PG, Watterson KG, Fisher J. 2001. The influence of ventricular input impedance on the hydrodynamic performance of bio-prosthetic aortic roots *invitro*. *The Journal of Heart Valve Disease*, 20:269-275.
- Hakki A, Iskandrian A, Bemis C, Kimbiris D, Segal B, Brice C. 1981. A simplified valve formula for the calculation of stenotic cardiac valve areas. *Circulation*, 63(5):1050-1055.
- Harkin DE, Curtis LE. 1967. Heart surgery – Legend and a long look. *The American Journal of Cardiology*, 19(3):393-400.

Haaf P, Steiner M, Attmann T, Pfister G, Cremer J, Lutter G. 2009. A novel pulse duplicator system: evaluation of different valve prostheses. *Thoracic Cardiovascular Surgery*, 57(1):10-17.

<https://www.ncbi.nlm.nih.gov/pmc/articles/PMC3839173/> [Visited 24September 2017].

ISO 5840 Cardiovascular implants- Cardiac valve prostheses. International Standards Organisation, 1989:12(01). Also available as British Standard BS Cardiovascular implants – Part 1, Methods of test for heart valve substitutes and requirements for their packaging and labelling. *British standards Institution*, 1990.

Johnston RT, Weerasena NA, Butterfield M, Fisher J, Spyt TJ. 1992. Carbomedics and St Jude Medical bi-leaflet valves: an *in vitro* and *in vivo* comparison. *European Journal of Cardiothoracic Surgery*, 6:267-271.

Karaci AR, Aydemir NA, Harmandar B, Sasmazel A, Saritas T, Tuncel Z, Yekeler I. 2012. Surgical Treatment of Infective Valve Endocarditis in Children with Congenital Heart Disease. *Journal of Cardiothoracic Surgery*, 27:93-98.

Kerut EK, McIlwain EF, Plotnick GD. 2007. Echocardiography examination and echocardiography anatomy. *American Journal of Cardiology*, 100(8):1271-1273.

Korossis SA, Fisher J, Ingham E. 2000. Cardiac valve replacement: a bioengineering approach. *Biomedical Material and Engineering*, 10:83-124.

Knirsch W, Nadal D. 2011. Infective endocarditis in congenital heart disease. *European Journal of Pediatrics*, 170(9):1111-1127.

Kuan YH, Dasi LP, Yoganathan A, Leo HL. 2011. Recent Advances in Polymeric Heart Valves Research. *International Journal of Biomaterials Research and Engineering*, 1(1):1-17.

- Kuettinga M, Sedaghatb A, Utzenratha M, Sinningb JM, Schmitza C, Roggenkampa J, Werner N, Schmitz-Rodea T, Steinseifer U. 2014. *In vitro* assessment of the influence of aortic annulus ovality on the hydrodynamic performance of self-expanding trans-catheter heart valve prosthesis. *Journal of Biomechanics*, 47:957-965.
- Leefe SE, Gentle CR. 1995. A review of the *in vitro* evaluation of conduit mounted cardiac valve prostheses. *Medical Engineering and Physics*, 17:497-506.
- Leo HL, Simon HA, Dasi LP, Yoganathan AP. 2006. Effect of hinge gap width on the microflow structures in 27mm bi-leaflet mechanical heart valves. *Journal of Heart Valve Disease*, 15:800-808.
- Leondes C. 2001. Cardiovascular techniques. *Biomechanical Systems Technology and Applications*. 2nd Edition. World Scientific Publishing Inc. pp 11.
- Levine GN. 2009. *Cardiology Secrets: Questions will be asked*. 4th edition. Elsevier Saunders, p54.
- Lichtenstein SV, Cheung A, Ye J, Thompson CR, Carere RG, Pasupati S. 2006. Transapical minimal invasive aortic valve implantation in humans: Initial clinical experience. *Circulation*, 114:591-596.
- Lillehei CW, Nakib A, Kaster RL. 1989. The origin and development of three new mechanical valve designs: toroidal disc, pivoting disc and rigid bi-leaflet cardiac prosthesis. *Annals of Thoracic Surgery*, 48:S35-36.
- Livanova Sorin, Carbomedics valves. <http://www.livanova.sorin.com/file/view-1370.action> [Accessed 15 September 2015].
- Lu PC., Liu J., Xi B., Li S., Wu J., Hwang N.H.C. 2003. On accelerated fatigue testing of prosthetic heart valves. In: Hwang N.H.C., Woo S.L.Y. (eds) *Frontiers in Biomedical Engineering. Topics in Biomedical Engineering International Book Series*. Springer, pp. 185-196.

- Macmanus Q, Grunkemeier G, Lambert L, Starr A. 1978. Non-cloth covered caged ball prosthesis. *Journal of Thoracic Cardiovascular Surgery*, 76:788-794.
- Matthews AM. 1998. The development of the Starr-Edwards heart valve. *Texas Heart Institute Journal*, 25:282-293.
- Marijon E, Mirabel M, Celermajer DS, Jouven X. 2012. Rheumatic heart disease. *Lancet*, 379:953-64.
- Milo S, Rambod E, Gutfinger C, Gharib M. 2003. Mitral mechanical heart valves: *in vitro* studies of their closure, vortex and micro bubble formation with possible medical implications. *European Journal of Cardiothoracic Surgery*, 24:364-370.
- Mohamed AA, Arifi A, Omran A. 2010. The basics of echocardiography. *Journal of the Saudi Heart Association*, 22:71-76.
- Mol A, Smits AI, Bouten CV, Baaijens FP. 2009. Tissue engineering of heart valves: advances and current challenges. *Expert Revised Medical Devices*, 6(3):259-275.
- Otto CM. 2004. Textbook of clinical Echocardiography. 5th Edition. Saunders: Elsevier, p9.
- Pibarot P, Dumesnil JG. 2009. Prosthetic heart valves. Selection of the optimal prosthesis and long-term management. *Circulation*, 119 :1034-1048.
- Pibarot P, Dumesnil JG. 2012. Doppler echocardiography evaluation of prosthetic valve function. *Heart*, 78:69-77.
- Pick AW, White A, Ford GC, Wilson AC. 1997. Clinical and haemodynamic performance of the 19mm Carpentier-Edwards pericardial bioprosthesis in the small aortic root. *Asia Pacific Heart Journal*, 6(1):11-15.

- Pipilis AG, Efstratiadis T, Kyrtatos P, Mallios K. 2007. Thirty-seven-year follow-up of a 'less known' aortic valve prosthesis. *European Heart Journal*,15:1813.
- Pratt GH. 1952.The Role of Anticoagulant Therapy in Surgery. *Surgical Clinics of North America*, 32(2):369-386.
- Rajamannan NM. 2011. Calcific aortic valve disease: Cellular origins of valve calcification. *Arteriosclerosis and Thrombosis of Vascular Biology*, 31:2777-2778.
- Rajeev A, Sujesh S, Sivakumaran N, Vayalappil C. 2012. A linear after-load model for a cardiovascular pulse duplicator. *Association for Computing Machinery*, 8(2):493-497.
- Ramaswamy, S, Gottlieb, D, Engelmayr Jr GC, Aikawa E, Schmidt DE, Gaitan-Leon DM, Sales VL, Mayer Jr JE, Sacks MS. 2010. The role of organ level conditioning on the promotion of engineered heart valve tissue development *in-vitro* using mesenchymal stem cells. *Biomaterials*, 31:1114-1125.
- Ramaswamy S, Salinas M, Carrol R, Landaburo K, Ryans X, Crespo C, Rivero A, Al-Mousily F, DeGroff C, Bleiweis M, Yamaguchi H. 2013.Protocol for relative hydrodynamic assessment of tri-leaflet polymer valves. *Journal of Visualised Experiments*, 80:1-11.
- Rao GHR. 2016.Flow velocity, fluid dynamics and vascular pathophysiology. *The Scientific pages of Heart*, 1:(1)1-8.
- Reul H, Van Son JAM, Steinseifer U, Schmitz B, Schmidt A, Schmitz C. 1993. *In vitro* comparison of bi-leaflet aortic valve prosthesis. *Journal of Thoracic Cardiovascular Surgery*, 9:412-420.
- Schrire V, Beck W, Hewitson RP, Barnard CN. 1970.Immediate and long-term results of aortic valve replacement with University of Cape Town aortic valve prosthesis. *British Heart Journal*, 32:255-263.

Sierad LN, Simionescu A, Albers C, Chen J, Maivelett J, Tedder ME, Liao J, Simionescu DT. 2010. Design and testing of a pulsatile conditioning system for dynamic endothelialisation of polyphenol-stabilized tissue engineered heart valves. *Cardiovascular Eng. Technology*, 1(2):138-153.

Singh S, Goyal A. 2007. The origin of echocardiography: A tribute to Inge Edler. *Texan Heart Institute Journal*, 34(4): 431-438.

Sordelli C, Severino S, Ascione L, Coppolino P, Caso P. 2014. Echocardiographic assessment of heart valve prosthesis. *Journal of Cardiovascular Echography*, 24(3):103-113.

Spinner EM. The history of heart valves: An industry perspective. *Frontiers of Engineering*. 2015;19:55-63.

Starr Edwards heart valve, The national museum of American History. http://americanhistory.si.edu/collections/search/object/nmah_1726277 [Accessed 24 June 2012].

Stewart SF, Burté F, Clark RE. 1991. *In vitro* quantification of regurgitant jet flow by colour Doppler ultrasound and conservation of momentum. *ASAIO Trans*, 37(3):454-455.

Strope ER. Design considerations for the *In Vitro* testing of cardiovascular prosthesis. 2010; <https://dynateklabs.com/design-considerations-for-the-in-vitro-testing-of-cardiovascular-prosthesis/> [Accessed July 2017].

Temple LJ, Serafin R, Calvert NG, Drabble JM. 1964. Principles of fluid mechanics applied to some situations in the human circulation and particular to the testing of valves in a pulse duplicator. *Human Circulation*, 9:261-267.

- Tindale WB, Black MM, Martin TRP. 1982. *In vitro* evaluation of prosthetic heart valves: anomalies and limitations. *Clinical Physics and Physiology Measures*, 3(2):115.
- Tropea C, Yarin AL, Foss JF. 2007. Handbook of experimental fluid mechanics. 1st Edition. Springer, pp. 661-676.
- Verdonck P. 1992. Relevancy of a computer controlled *in-vitro* model of cardiac mechanics in physiological circumstances. IEEE, *Computers in Cardiology*, Durham, North Carolina, USA. 11-14 October, pp592-594.
- Verdonk PR, Van Nooten GJ, Belleghem Y. 1997. Pulse duplicator hydrodynamics of for different bi-leaflet valves in the mitral position. *The International Society of Cardiovascular Surgery*, 5(6):593.
- ViVitro Laboratories, Pulse duplicator. <http://vivitrolabs.com/product/pulse-duplicator> [Accessed 25 March 2011].
- ViVitro Laboratories. <http://vivitrolabs.com/wp-content/uploads/2016/02/Pulse-Duplicator-Brochure-2016-VIVI-MKT-046.pdf> [Accessed 16 May 2011].
- Westerhof N, Elzinga G, Sipkema P. 1971. An artificial arterial system for pumping hearts. *Journal of Applications and Physiology*, 31(5):776-781.
- Wheatley DJ, Raco L, Bernacca GM. 2000. Polyurethane: material for the next generation of heart valve prosthesis? *European Journal of Cardiothoracic Surgery*, 17:440-448.
- Wieting DW. 1989. *In Vitro* Testing of Heart Valves: Evolution Over the Past 25 Years. *The Society of Thoracic Surgeons*, 48: S12-13.
- Wright JTM, Temple LJ. 1971. An improved method for determining the flow characteristics of prosthetic mitral heart valves. *Thorax*, 26:81.

Wright JTM.1979. Handbook of Tissue heart valves: Hydrodynamic evaluation of tissue valve. 1st Edition. Butterworth & Co Ltd, pp. 29-88.

Yin W, Krukenkamp B, Saltman A, Gaudette G, Suresh K, Bernal O, Jesty J, Bluestein D. 2006. Thrombogenic performance of a St. Jude bi-leaflet mechanical heart valve in a sheep model. *ASAIO Journal*, 52:28-33.

Yoganathan AP, He Z, Jones CS. 2004.Fluid mechanics of heart valves. *Annual Revised of BiomedicalEngineering*,6:331-362.

Yoganathan AP, Chandran KB, Sotiropoulos F. 2005. Flow in prosthetic heart valves: State of the art and future directions. *Annals of Biomedical Engineering*, 12:1689-1694.

Yoganathan AP, Corcoran WH, Harrison EC. 1979.Pressure drop accros prosthetic aortic heart valves under steady and pulsatile flow *in-vitro* measurements. *Journal of Biomechanics*, 12(2):153-164.

Zilla P, Brink J, Human P, Bezuidenhout D. 2008.Prosthetic heart valves: Catering for the few. *Biomaterials*, 29:385–406.

Zoghbi WA, Chambers JB, Dumesnil JG, Foster E, Gottdiener JS, Grayburn PA, Khandheria BK, Levine RA, Marx GR, Miller FA Jr, Nakatani S, Quiñones MA, Rakowski H, Rodriguez LL, Swaminathan M, Waggoner AD, Weissman NJ, Zabalgoitia M. 2009.Recommendations for evaluation of prosthetic valves with echocardiography and Doppler ultrasound: A report from the American Society of Echocardiography's Guidelines and Standards Committee and the Task Force on Prosthetic Valves, developed in conjunction with the American College of Cardiology Cardiovascular Imaging Committee, Cardiac Imaging Committee of the American Heart Association, the European Association of Echocardiography, a registered branch of the European Society of Cardiology, the Japanese Society of Echocardiography and the Canadian Society of Echocardiography, endorsed by the American College of Cardiology Foundation, American Heart Association, European Association of Echocardiography, a registered branch of the

European Society of Cardiology, the Japanese Society of Echocardiography, and Canadian Society of Echocardiography. *Journal of American Society of Echocardiography*, 22(9):975-1014.